

AN INVESTIGATION OF NUCLEAR EXCURSIONS TO  
DETERMINE THE SELF-SHUTDOWN EFFECTS IN  
THERMAL, HETEROGENEOUS, HIGHLY ENRICHED,  
LIQUID-MODERATED REACTORS

by

JOHN ROBERT FAGAN

B.S., University of Nebraska, 1957

-----

A MASTER'S THESIS

submitted in partial fulfillment of the  
requirements for the degree

MASTER OF SCIENCE

Department of Nuclear Engineering

KANSAS STATE UNIVERSITY  
Manhattan, Kansas

1962

L.D.  
2668  
T4  
1962  
F25  
C-2

TABLE OF CONTENTS

Documents

1.0	INTRODUCTION.....	1
2.0	THEORY.....	13
2.1	Derivation of Equations.....	13
2.2	Analytical Solutions.....	16
2.2.1	Temperature Distributions.....	23
2.2.2	Surface Heat Flow.....	26
2.3	Reactivity Effects Due to Temperature Coefficient and Fuel Expansion.....	28
2.4	Reactivity Effects Due to Steam Formation.....	30
3.0	RESULTS AND DISCUSSION.....	37
3.1	Temperature Distributions and Surface Heat Flow.....	37
3.2	Reactivity Effects.....	47
3.3	Conclusions.....	59
3.4	Further Investigation.....	64
	ACKNOWLEDGEMENT.....	66
	LITERATURE CITED.....	67
	APPENDICES.....	71
	APPENDIX A: Derivation of Solutions for the Temperature Distribution in the Fuel and Moderator of a Unit Cell.....	72
	APPENDIX B: Description and Explanation of the IBM-650 Computer Program Used for Fitting Empirically Experimental Data with the Sum of Several Terms of Exponential Form.....	88
	APPENDIX C: Description and Explanation of the IBM-650 Computer Program for Fitting Empirically Experimental Data with an Even Fourier Series.....	96

APPENDIX D:	Description and Explanation of the IBM-650 Computer Program Used to Calculate Temper- ature Distributions.....	103
APPENDIX E:	Description and Explanation of the IBM-650 Computer Program Used to Calculate the Surface Heat Flow.....	113

## Nomenclature of Terms Not Defined in Text

$k_{\text{eff}}$	Effective multiplication factor.
$\epsilon$	Fast fission factor.
$p$	Resonance escape probability.
$\eta$	Neutrons born per thermal absorption in fuel.
$f$	Thermal utilization.
$B^2$	Buckling, $\text{cm}^{-2}$ .
$L$	Thermal diffusion length, cm.
$\kappa$	$1/L$ , $\text{cm}^{-1}$ .
$\tau$	Fermi age, $\text{cm}^2$ .
$v$	Neutron velocity, cm/sec.
$q_{00}$	Heat generation rate in center of fuel at start of pulse, $\text{btu/hrft}^3$ .
$\tau$	Reciprocal period of power rise, $\text{sec}^{-1}$ .
$A_j, \lambda_j$	Parameters for empirical fit of heat generation rate, $\text{btu/hrft}^3$ and $\text{sec}^{-1}$ respectively.
$B_i, \beta_i$	Parameters for empirical fit of fuel plate surface boundary condition, $^{\circ}\text{F}$ and $\text{sec}^{-1}$ respectively.
$L, L_1$	Thickness of fuel and moderator, respectively in slab geometry, cm.
$R, R_1$	Thickness of fuel and moderator, respectively in cylindrical geometry, cm.
$x$	Distance in fuel from the center of unit cell, slab geometry, cm.
$x_1$	Distance in moderator from outside of unit cell, slab geometry, cm.
$r$	Distance in fuel and moderator from center of unit cell, cylindrical geometry, cm.
$i, j, n$	Summation indices.

f,m            Subscripts denoting fuel and moderator, respectively.

p,s            No. of terms in heat generation rate and interface  
boundary condition approximations.

## 1.0 INTRODUCTION

The concept of reactor safety is extremely important in the engineering application of nuclear power systems. The United States Atomic Energy Commission has therefore authorized an extensive study in this area. This investigation uses experimental data resulting from that study to attempt to define the mechanisms of reactor shutdown.

The safety of a nuclear reactor system is usually considered in terms of its void and temperature coefficients of reactivity. If one designs a reactor in such a manner as to make both of these coefficients negative, the system will tend to stabilize itself if some external perturbation is placed on the system. This is due to the fact that when the excess reactivity,  $k_{\text{eff}} - 1$ , of a system is increased, the power tends to rise, thereby increasing the temperature of the system, and this in turn causes a decrease in reactivity. In the case of a liquid moderated system, voids may be introduced which will further decrease the reactivity.

If one considers the bare reactor age-diffusion criticality equation, 
$$k_{\text{eff}} = \frac{\xi p \eta f e^{-B^2 \tau}}{1 + L^2 B^2}$$
, it is possible to see how these effects manifest themselves in the nuclear constants (22). In the case of the void coefficient, the significant effect is on the Fermi age,  $\tau$ . Since part of the moderator is removed, the age increases, thus decreasing the fast non-leakage factor,  $e^{-B^2 \tau}$ . In the case of the temperature coefficient there are several effects that must be considered. First, the moderator expands because of the positive coefficient of expansion of the liquid.

This results in a decrease in the density of the moderator, and if the reactor is under-moderated the fast non-leakage factor and  $p$  will decrease. Thus it is evident that one safety criteria is that the core should always be slightly under-moderated even though this will increase the critical mass. Second, the fuel elements expand, expelling more of the moderator from the core causing  $k_{eff}$  to decrease; however, simultaneously, the effective size of the core increases, causing a decrease in the buckling,  $B^2$ , of the system. This decrease in buckling has both a positive and a negative effect upon reactivity or  $k_{eff}$ . The increase in size increases the non-leakage factor for both fast and thermal leakage,  $e^{-B^2\tau}$  and  $1/(1 + L^2B^2)$ , respectively. The removal of moderator increases  $\tau$  reducing reactivity as described in the void coefficient discussion. All of the effects described above with the exception of the buckling, must be considered to be of a delayed nature.

Another group of effects exists which affect the reactivity immediately and these effects are therefore classified as prompt (41). The first of these prompt effects is Doppler broadening (38). Because of the increased kinetic energy of  $U^{238}$  target nuclei with increased temperature, the width of resonance absorption is increased, but the height of the peak is decreased (22), because the total area beneath the resonance curve remains constant. If the resonance absorption cross sections are large, so that essentially all neutrons with energies in the resonance region are captured, the widening of the region will result in a decrease in the resonance escape probability,  $p$ , and thus the reactivity decreases as the temperature rises. A second prompt effect is caused by hardening of the thermal neutron spectrum as the moderator temperature



risers. The result of this hardened spectrum is that the average thermal-neutron velocity increases,  $\underline{L}^2$  increases and the thermal non-leakage factor,  $\frac{1}{1 + L^2 B^2}$ , decreases. One would expect that the neutrons per absorption would also be affected by this spectral change but assuming the normal  $1/v$  dependence for all cross sections, this effect cancels since the terms comprising this effect are composed of the ratios of cross sections. One final effect which is neither part of the temperature coefficient nor the void coefficient must be considered. This is the formation of radiolytic gases.

The reasons that one is inclined to speak of prompt and delayed coefficients of reactivity is that for power bursts of low reactivity and correspondingly long periods, the delayed effects may play a great part in the shut-down mechanism. However, if one supposes a burst with a very short period then it is obvious that these delayed effects will not have had time to act. What constitutes a "short time" can be answered by determining the heat transfer time constant of the fuel elements. This, in part, is the subject of the proposed investigation. Iriarte (27) reported heat transfer time constants for infinitely long cylindrical  $UO_2$  fuel elements surrounded by a helium film which served as a thermal bond and which were clad with zirconium, stainless steel or aluminum. While the data presented by Iriarte are not applicable to the SPERT-I or TRIGA Reactors, the techniques may be useful in determining the relative importance of the delayed effects.

Before considering further the scope of this project it is informative to investigate the prior work in the field. During the early summer of 1954 a series of experiments were made on the BORAX-I Reactor to investigate the ability of the reactor, when operated in the subcooled (non-boiling)



condition, to protect itself against the results of sudden, artificially induced increases in reactivity. Inasmuch as this set of experiments completed the program for the BORAX-I Reactor, the final runaway experiment was intentionally made under conditions which led to destruction of the reactor. In the final experiment, a control rod worth four per cent  $k_{eff}$  was ejected from the reactor core, inducing an exponential power increase which had a period of 2.6 milliseconds. This final experiment resulted in a melting of most of the fuel plates and failure of the reactor tank. Fuel plate fragments were scattered for a distance of 200 to 300 feet (8). This set of experiments, along with the earlier operation of the BORAX-I, (7), established two important safety axioms for water moderated reactors. First, for any given system there is a reactivity insertion beyond which the reactor cannot react fast enough to shut itself down before damage is done, and second, water moderated reactors can be designed to have a high degree of inherent self-protection against the effects of sudden large reactivity increases. A less critical fact that resulted from these tests was that if the transients are started at boiling conditions (such as in a boiling water reactor), the maximum power and fuel-plate temperature reached are less than if the transient is started with the reactor in a subcooled condition. This is as would be expected if void formation due to boiling were the shut-down mechanism, since for the subcooled system the reactor could actually achieve a stable positive period before any negative reactivity would result. This, along with the observation of large quantities of steam and water being expelled from the system, led to the conclusion that it was the void formation which was shutting the reactor down. With this background in mind, the Atomic Energy Commission set out on an intensified program

to determine empirically the safe upper operating limits on each class of reactors including the pressurized and unpressurized, boiling and non-boiling thermal reactors, both heterogeneous and homogeneous, and fast-reactor systems (23). This program initiated the SPERT (Special Power Excursion Reactor Tests) and KEWB (Kinetic Experiments on Water Boilers) programs. SPERT is the heterogeneous reactor test facility and KEWB is the design for the same type of tests on a homogeneous reactor test facility. In 1956, W. B. Nyer, et. al. (39), reported the results of the initial transient test on the SPERT-I facility and concluded that the SPERT-I (43) reactor demonstrated qualitatively the results of the BORAX-I experiments although SPERT-I was more stable after the initial power burst. Factors which could contribute to this difference in behavior were the known differences in the fuel assembly construction, the possible differences in the effective void coefficients, and/or the differences in the reflector-tank environment. Another important point discovered at this time was that there was a unique relationship between the peak power and the transient period. The data were fitted rather well by two straight lines on a plot of log reciprocal period versus peak power. The slopes of these lines were approximately 0.8 and 1.7 for the lower and upper regions respectively. The point of intersection occurred at  $\Delta k = 0.74\%$ , or about prompt critical. In June of 1957, R. W. Miller reported on some interesting work in analyzing the reactivity behavior during SPERT-I transients (34). Miller pointed out that it was not necessary to remove all of the initially inserted reactivity to limit a power excursion. This is a result of the delayed neutrons, which for a very short period excursion, do not contribute to the flux during the rise in power. Thus, for short excursions the reactivity

compensation at maximum power need only be  $\Delta k(1-\beta)-\beta$ .  $\Delta k$  is the initial change in  $k_{\text{eff}}$  and  $\beta$  is the delayed neutron fraction. The total  $\Delta k$  must be accounted for in very long period transients. In the case of intermediate period transients the compensated reactivity was calculated as a function of the reciprocal period by numerical solution of the reactor kinetics equations using the experimentally determined power traces. Later in 1957, G. O. Bright, et. al., suggested a model for reactor burst behavior (2), based on the earlier work of Klaus Fuchs at Los Alamos (21). This model postulated a shutdown effect proportional to the energy release. However, the model provided no method for the shutdown energy to be removed and allowed for no time-delays between the energy release and the appearance of the shutdown effect. Much later this model was further modified by S. G. Forbes (13) who let the shutdown effect be proportional to the energy release raised to some power,  $n$ , and allowed for some arbitrary delay time. In this analysis the model was tested against some experimental transients from SPERT-I and values of  $n$  from 1.5 to 2 were successively used. The results also showed that the delay time was significant in matching the data; however no exact value of the delay time was determined. The overall effect of these works is to convince one that the primary shutdown mechanisms are intimately tied up with the energy release although no real information on the exact phenomena can be found. In 1958, Griffing and Deverall (10) coupled the energy shut-down model with the reactor kinetics equation including six delay groups and again showed that the energy model could describe qualitatively the power traces obtained in the SPERT-I transients even long after the initial burst. This work used a mathematical structure of the shut-down equation considered much earlier (1951)

by Chernick (4) for no delay groups and in 1956 by Margulies (31) with one delay group.

In December of 1958, Deverall and Griffing (9) reported the first attempts at trying to relate the shutdown reactivity with the thermodynamic characteristics of the SPERT-I system. In this report the change in reactivity for transients with long periods was related to the temperature rise in the moderator alone although the fact was recognized that the fuel element temperature rise should also be considered. Considering only the moderator temperature rise, they found reactivity compensations at peak power that were roughly one-half of those reported by Miller (34). Since they felt that the data with which they were working were only accurate to within a factor of two, they did not pursue the investigation further. In January of 1958, Horning of Ramo-Woolridge reported on a model for transients in SPERT-I (18). This report develops a general model, taking into account the void formation and the thermal expansion. However, no real attempt was made to interpret these constants in terms of the distribution of energy in the fuel and moderator or the nuclear and thermodynamic constants of the system. Another report, bound under the same cover, by H. C. Corben (26) treats the problem of oscillations found after the burst as the power approaches some steady state level. Although the mechanism responsible for the oscillations need not be the same as the shut-down mechanism, there is certainly the possibility that they are one and the same. A third report by G. Birkhoff (26) treats the problem of void formation from the point of view of the growth of bubbles. The "Bubble Void" is probably the dominant shutdown effect in a certain type of excursion such as in the initial BORAX-I experiments. The analytic representation of this effect is the least known and thus is being widely

sought. An extensive study of bubble formation including a critical review of the literature, an evaluation of the merits of purely theoretical approaches to the development of a void model, and an investigation of the possible formulation of the nucleate boiling void was reported by the Vitro Engineering Company in May of 1959 (28).

Although an exact definition of bubble formation may not be within the scope of this investigation, the determination of the heat flow into the moderator and the transient temperature distribution in the moderator should shed some light on even this difficult problem.

In July of 1958, J. C. Haire (25) reported the results of a great number of the SPERT-I transients. This report presented data on the reactor power, fuel plate surface temperatures and pressures as a function of time during the transients. These are the data that will be used extensively in the initial phases of the investigation proposed herein.

During late 1958 and 1959, several models were proposed to investigate and explain the inherent shutdown characteristics of the SPERT-I reactor. The "Conduction Boiling" model suggested by S. G. Forbes (14) is certainly credible in that it takes into account the flow of heat into the moderator in a much more exact manner than any of the earlier investigations. This model was quite successful in predicting the power, energy release and temperature at the time of peak power as a function of the reciprocal period. However the model still represents the shutdown mechanism in terms of empirical parameters. Also the non-boiling shutdown effects are not taken into account. The "Clipped Exponential" model suggested by R. W. Miller (35) made some very useful assumptions on the shape of the reactor power burst to ease the analytical solution of kinetics equations. While this model produced some useful criteria in the understanding of self-shutdown



it again made use of lumped parameters which were not easily interpreted in terms of the thermodynamic and nuclear characteristics of the system. E. T. Clark (5,6) as early as 1956 had postulated a prompt fission product having a large absorption cross section for thermal neutrons as an explanation of the self-shutdown of power excursions observed in the SPERT-I Reactor. Later evidence (42) seems to indicate that this model is less likely to be valid than the more conventional models.

Also in 1958, General Atomic introduced their TRIGA Reactor with zirconium hydride moderator which demonstrated a larger prompt shutdown mechanism than either the BORAX-I or the SPERT-I (41). In this case the reactor was designed to have a shutdown mechanism which would act by hardening the thermal neutron energy spectrum thus increasing the thermal leakage to cause shutdown. The reason for choosing this effect was that they felt that it would act more quickly and thus provide a safer reactor than the accepted moderator expansion and expulsion mechanisms. The spectrum effect, so important in the TRIGA Reactors must also act to some extent in SPERT-I. The amount of this effect has apparently never been determined.

P. French, in 1959, (18) reported an attempted solution of the transient heat conduction equation in the fuel and moderator to determine the temperature distribution. However, this work appears to be in error in that he forced a separation of variables solution on the equations whereas the spatial and time dependence cannot be expressed as a simple product except after sufficiently long times so that the transient term has disappeared. H. L. McMurtry (32) reported the temperature distribution in a fuel plate, cladding and moderator with exponentially rising power for pure conduction. This is an excellent piece of work but the mathematical

model turns out to be more difficult than is either warranted or necessary for the analysis of the SPERT-I data. The McMurry report makes mention of earlier work by H. Greenspan (24) on the same problem with similar results. Several investigators, Kattwinkel (29), Kirchenmayer (30), Stein (40), Epel (11), Arpacı and Clark (1), Ermakov and Ivanov (12), report analytical solutions to the transient heat conduction equation. However, none of them were working on the problem with reference to the SPERT-I investigations and their results are not directly applicable to the use of the SPERT-I experimental measurements. As a result the temperature distribution in the fuel and moderator during a transient is not well known to date.

In July of 1959, Forbes, et. al. (16), summarized the work done up to that time. They showed that by fitting empirically the "Conduction Boiling" model to the SPERT-I data and including the effect of moderator and fuel element expansion they could fit the experimental compensated reactivity at peak power versus reciprocal period curves for values of the reciprocal period greater than 5 seconds<sup>-1</sup>. They also showed that for values of the reciprocal period greater than 20 seconds<sup>-1</sup>, the steam void contribution to reactivity was considerable. For the longer period region they postulated an additional shutdown effect from radiolytic gases.

This, of course, lends considerable credence to the "Boiling Conduction" model, however it does have one glaring shortcoming. To extend it to another reactor requires at least one transient burst experiment to determine the parameters. However, if the fundamental mechanism were understood exclusively in terms of the basic nuclear, thermodynamic and hydrodynamic characteristics of the system, one could confidently predict the limits of safe operations for different reactor systems.



The satisfactory application of the "Boiling Conduction" model led to two sets of experiments designed to test that model and the postulated radiolytic gas effect. The first set of experiments (20) showed with reasonable certainty that radiolytic gas formation was not a primary contributor to self-shutdown in the SPERT-I Reactor. The second set of experiments (19) consisted of coating all of the fuel plates with approximately five mils of insulation, Lithocote LC-34, and of performing transient tests on the reactor. Some of the tests were run with transients of such magnitude that boiling would occur in the bare core and not in the insulated core. The remaining tests involved transients in which there would be boiling in both cores, and the differences in heat transfer rates were expected to be reflected as changes in the reactor behavior. Power burst shapes for transients of the same period in both the bare and insulated cores were essentially the same. In view of the identical reactor behavior for the bare and insulated tests, it would appear that the core insulation produced no appreciable effects on the shutdown mechanism. Since it seems reasonable to assume that any shutdown effect due to boiling would be effected by the core insulation, boiling would not seem to play any part in the self-shutdown mechanism. However, if the heat transfer rate was small enough there would be negligible temperature drop across the insulation and thus the effect on boiling might be unchanged by the insulation. This experiment shows clearly the need for detailed calculation of the temperature distributions in the fuel and moderator during the transients. One final report should be cited in this summary. In April of 1960, Miller (36) reported on some photographic investigations of boiling during transients

in SPERT-I. These results clearly indicated that boiling was an important agent in the initial reactor self-shutdown whenever the fuel plate temperature was sufficiently high.

## 2.0 THEORY

### 2.1 Derivation of Equations

The direct approach to determining the self-shutdown effects must include the determination of the temperature distributions in the fuel elements and moderator throughout the core during a transient. This problem can be accomplished by investigating the exact temperature distribution in a center element only and relating all effects to this center element. The exact solution of the multi-region, transient heat conduction equations even for a single fuel element, making use of only the power versus time data from the SPERT-I transients, is exceedingly difficult as pointed out in the work by McMurtry (32). However, if use is made of the available fuel plate surface temperature data as well as the power data during a transient, the problem is reduced to two single region problems. Although the solutions are much simplified over the two region problem, they are still complicated and therefore have been programmed for the Kansas State University IBM 650 computer.

The methods for determining the steady state temperature distribution throughout a unit cell of thermal, heterogeneous liquid-moderated reactor are discussed in Nuclear Engineering (41) by C. F. Bonilla and in Nuclear Reactor Physics (37) by R. L. Murray. It will be considered sufficient for this work to outline the differences that must be accounted for in transient operation.

The partial differential equation for conductive heat transfer applicable in the fuel and moderator of a nuclear power reactor during

a transient but before boiling is established is

$$\nabla^2 \theta(x,t) + \frac{q(x,t)}{k} = 1/\alpha \frac{\partial \theta(x,t)}{\partial t} \quad (1)$$

where  $\nabla^2$  is the Laplacian operator (44),  $\theta$  is the temperature rise above the initial temperature  $[T(x,t)-T_0]$ ,  $x$  is the position variable,  $k$  is the mean thermal conductivity,  $\alpha$  is the mean thermal diffusivity,  $t$  is the time variable and  $q$  is the volumetric heat generation rate. This equation in slab and cylindrical geometries is directly applicable to the analysis of transient behavior in a reactor following a change in reactivity. The derivation of solutions to this equation in the fuel and moderator during power transients will be shown in detail for slab geometry (Appendix A) and the important elements of the solution in cylindrical geometry will be tabulated in Section 2.2.1.

In any nuclear reactor there are heating effects due directly to fission fragments and to the attenuation of other nuclear particles. Within the fuel element, fission heating far overrides the other attenuation effects. Therefore, the heat generation rate,  $q_f(x,t)$ , in the fuel elements is proportional to the thermal neutron flux. The neutron flux during a transient can be expressed as a simple product of the spatial and the time dependencies. Thus the heat generation rate is also separable in space and time as shown in equation (2).

$$q_f(x,t) = f_f(x) g_f(t) \quad (2)$$

The spatial dependence,  $f_f(x)$ , can be obtained easily from the steady state analysis (40) and is given in equation (3).

$$f_f(x) = q_{\infty} \cosh \kappa x \quad (3)$$

Here  $q_{oo}$  is the heat generation rate at the center of the fuel,  $\kappa$  is the inverse thermal neutron diffusion length and  $x$  is the distance from the center of the fuel.

The time dependence,  $g_f(t)$ , of the neutron flux and thus the heat generation rate is expressed as the sum of exponentials, thus

$$g_f(t) = \sum_{j=1}^s a_j e^{\lambda_j t} \quad (4)$$

Substituting equations (3) and (4) into equation (2), an expression for  $q_f(x,t)$  is obtained; that is

$$q_f(x,t) = \sum_{j=1}^s q_{oo} \cosh(\kappa x) a_j e^{\lambda_j t} \quad (5)$$

Substituting equation (5) into equation (1) yields the differential equations which must be solved to obtain the temperature distribution in the fuel, that is

$$\nabla^2 \theta_f(x,t) + \sum_{j=1}^s \frac{q_{oo} \cosh(\kappa x) a_j e^{\lambda_j t}}{k} = 1/\alpha \frac{\partial \theta_f(x,t)}{\partial t} \quad (6)$$

Now from investigation of the heat generation rate,  $q_m(k,t)$  in the moderator, it is noted that there is no heating due to fission, but there is heating due to nuclear particles which stream out of the fuel and are attenuated in the moderator. The moderator heating is approximately 5 to 7% (3) of the recoverable energy from fission and is sufficiently uniform in space to be so considered. Therefore,  $q_m(x,t)$  in the moderator is independent of the spatial variable but still is time dependent as shown in equation (7).

$$q_m(x,t) = \sum_{j=1}^s F a_j e^{\lambda_j t} \quad (7)$$

The heating effects in the moderator are proportional to the neutron flux in the fuel; thus  $F$  is the fraction of the recoverable energy released in the fuel which is dissipated in the moderator.

Substitution of equation (7) into equation (1) yields the differential equation to be solved for the temperature distribution in the moderator, that is

$$\nabla^2 \theta_m(x,t) + \sum_{j=1}^s \frac{F a_j e^{\lambda_j t}}{k} = 1/\alpha \frac{\partial \theta_m(x,t)}{\partial t} \quad (8)$$

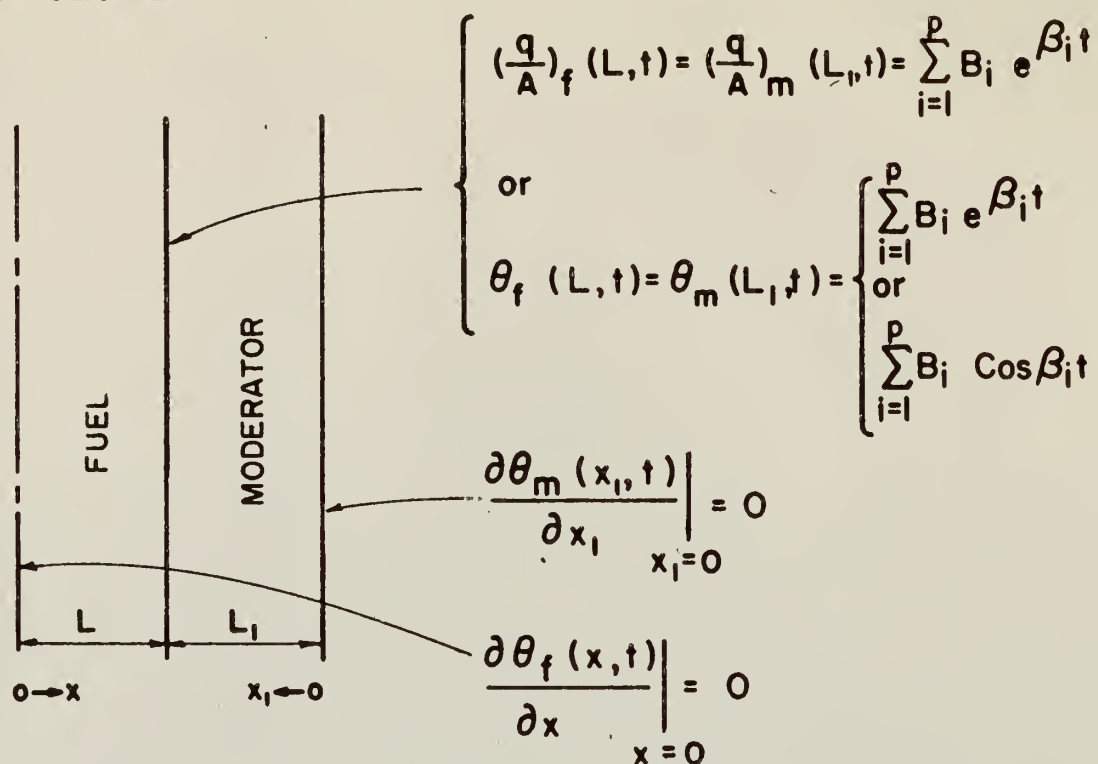
Equations (6) and (8) form the general set which must be solved to obtain the temperature distribution in a unit cell of the reactor during a transient. The geometry of the unit cell in which these equations must be applied is shown in Figure 1. The simultaneous solution of these equations is extremely difficult. The availability of the fuel element surface temperature as a function of time during the transients greatly simplifies this situation. The problem is reduced to solving the equations independently in the fuel and moderator, using the experimentally measured temperatures at the interface as a boundary condition for both equations. The other boundary condition necessary in each case is a zero heat flow condition at the center of the unit cell for the fuel regions and at the boundary of the unit cell for the moderator.

## 2.2 Analytical Solutions

The time dependent thermal diffusion equations in the fuel and moderator can be solved for the temperature distribution assuming that conduction is the primary mode of heat transfer. The equation will hold for all time in the fuel plate. In an attempt to represent as well as



## SLAB GEOMETRY



## CYLINDRICAL GEOMETRY

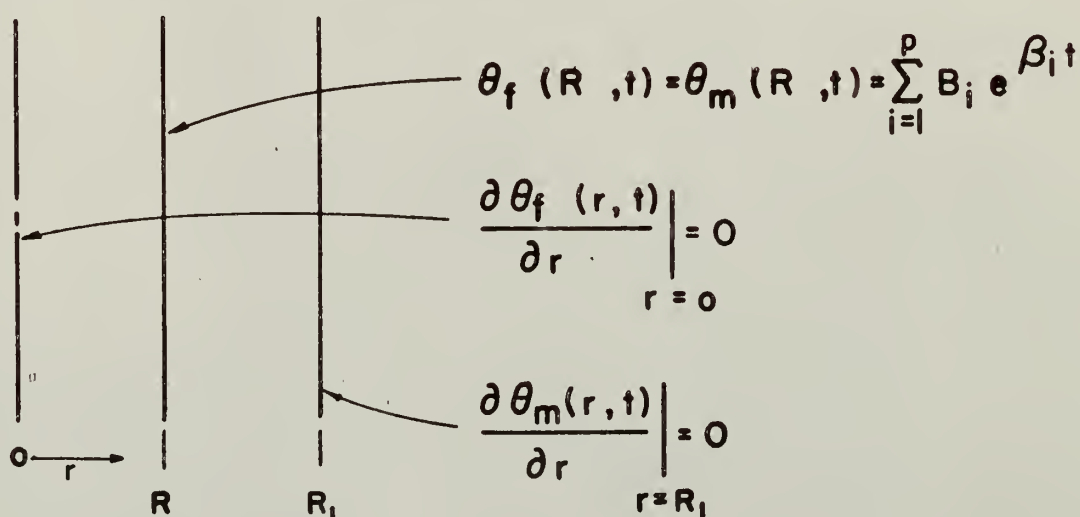


Figure 1. Geometry and boundary conditions in the unit cell used to determine the temperature distributions.



possible the experimental data which is used as input to this problem and to allow some flexibility in the application of these equations, the differential equations were solved subject to several forms of representation of the boundary conditions and the forcing functions. In one case the problem was solved in cylindrical geometry.

In slab geometry the one-dimensional solutions to the transient heat transfer equation, in which the time dependence of heat generation rate and the fuel element surface temperature are represented empirically as  $\sum_{j=1}^s A_j e^{\lambda_j t}$  and  $\sum_{i=1}^p B_i e^{\beta_i t}$  respectively, are derived in Appendix A and are given here as

$$\theta_f(x,t) = \sum_{i=1}^p \frac{B_i \cosh(\sqrt{\frac{\beta_i}{\alpha}} x) e^{\beta_i t}}{\cosh \sqrt{\frac{\beta_i}{\alpha}} L} - \sum_{n=1,3,5,\dots}^{\infty} \frac{\cos(\frac{n\pi x}{2L}) e^{\frac{n^2 \pi^2 \alpha}{4L^2} t}}{(L^2 / n\pi\alpha) \sin \frac{n\pi}{2}}$$

$$\times \left\{ \sum_{i=1}^p \frac{B_i}{\frac{n^2 \pi^2 \alpha}{4L^2} + \beta_i} + \sum_{j=1}^s \frac{q_{oo} \alpha A_j \cosh(\kappa L)}{k \left( \frac{n^2 \pi^2 \alpha}{4L^2} + \lambda_j \right) \left( \frac{n^2 \pi^2 \alpha}{4L^2} + \alpha \kappa^2 \right)} \right\} \quad (9)$$

$$- \sum_{j=1}^s \frac{A_j q_{oo} \alpha e^{\lambda_j t}}{k(\alpha \kappa^2 - \lambda_j)} \left\{ \cosh \kappa x - \frac{\cosh(\kappa L) \cosh(\sqrt{\frac{\lambda_j}{\alpha}} x)}{\cosh \sqrt{\frac{\lambda_j}{\alpha}} L} \right\}$$

and

$$\theta_m(x,t) = \sum_{i=1}^p \frac{B_i \cosh(\sqrt{\frac{\beta_i}{\alpha}} x) e^{\beta_i t}}{\cosh \sqrt{\frac{\beta_i}{\alpha}} L} - \sum_{n=1,3,5,\dots}^{\infty} \frac{\cos \frac{n\pi x}{L} e^{\frac{-n^2 \pi^2 \alpha}{4L^2} t}}{(L^2 / n\pi\alpha) \sin(\frac{n\pi}{2})}$$

$$\times \left\{ \sum_{i=1}^p \frac{B_i}{\frac{n^2 \pi^2 \alpha}{4L^2} + \beta_i} + \sum_{j=1}^s \frac{\alpha F A_j}{k \left( \frac{n^2 \pi^2 \alpha}{4L^2} \right) \left( \frac{n^2 \pi^2 \alpha}{4L^2} + \lambda_j \right)} \right\} \quad (10)$$

$$+ \sum_{j=1}^s \frac{\alpha F A_j e^{\lambda_j t}}{k \lambda_j} \left\{ 1 - \frac{\cosh \sqrt{\frac{\lambda_j}{\alpha}} x_1}{\cosh \sqrt{\frac{\lambda_j}{\alpha}} L_1} \right\}$$

in the fuel and moderator, respectively.

The equivalent solutions in cylindrical geometry are derived in Appendix A and are given here as

$$\begin{aligned} \theta_f(x, t) = & \sum_{i=1}^p \frac{B_i I_0 \left( \sqrt{\frac{\beta_i}{\alpha}} r \right) e^{\beta_i t}}{I_0 \sqrt{\frac{\beta_i}{\alpha}} R} + \sum_{n=1}^{\infty} \frac{J_0 \left( \frac{\omega_n r}{R} \right) e^{-\frac{\omega_n^2 \alpha}{R^2} t}}{\frac{R^2}{2\omega_n \alpha} J_1(\omega_n)} \\ & \times \left\{ \sum_{i=1}^p \frac{B_i}{\frac{\omega_n^2 \alpha}{R^2} + \beta_i} + \sum_{j=1}^s \frac{q_{oo} \alpha A_j I_0(\kappa R)}{k \left( \frac{\omega_n^2 \alpha}{R^2} + \lambda_j \right) \left( \frac{\omega_n^2 \alpha}{R^2} + \alpha \kappa^2 \right)} \right\} \\ & - \sum_{j=1}^s \frac{A_j q_{oo} \alpha e^{\lambda_j t}}{k (\alpha \kappa^2 - \lambda_j)} \left\{ I_0(\kappa r) - \frac{I_0(\kappa R) I_0 \left( \sqrt{\frac{\lambda_j}{\alpha}} r \right)}{I_0 \left( \sqrt{\frac{\lambda_j}{\alpha}} R \right)} \right\} \end{aligned} \quad (11)$$

and

$$\begin{aligned} \theta_m(x, t) = & \sum_{i=1}^p B_i \left\{ \frac{K_1 \left( \sqrt{\frac{\beta_i}{\alpha}} R \right) I_0 \left( \sqrt{\frac{\beta_i}{\alpha}} r \right) + I_1 \left( \sqrt{\frac{\beta_i}{\alpha}} R \right) K_0 \left( \sqrt{\frac{\beta_i}{\alpha}} r \right)}{K_1 \left( \sqrt{\frac{\beta_i}{\alpha}} R \right) I_0 \left( \sqrt{\frac{\beta_i}{\alpha}} R \right) + I_1 \left( \sqrt{\frac{\beta_i}{\alpha}} R \right) K_0 \left( \sqrt{\frac{\beta_i}{\alpha}} R \right)} \right\} e^{\beta_i t} \\ & + \sum_{n=1}^{\infty} \frac{2 \sqrt{\rho_n \alpha} \left[ K_1 \left( \sqrt{\frac{\rho_n}{\alpha}} R \right) I_0 \left( \sqrt{\frac{\rho_n}{\alpha}} r \right) + I_1 \left( \sqrt{\frac{\rho_n}{\alpha}} R \right) K_0 \left( \sqrt{\frac{\rho_n}{\alpha}} r \right) \right] e^{\rho_n t}}{R \left[ K_1 \left( \sqrt{\frac{\rho_n}{\alpha}} R \right) I_1 \left( \sqrt{\frac{\rho_n}{\alpha}} R \right) - K_1 \left( \sqrt{\frac{\rho_n}{\alpha}} R \right) I_1 \left( \sqrt{\frac{\rho_n}{\alpha}} R \right) - I_0 \left( \sqrt{\frac{\rho_n}{\alpha}} R \right) K_0 \left( \sqrt{\frac{\rho_n}{\alpha}} R \right) + I_0 \left( \sqrt{\frac{\rho_n}{\alpha}} R \right) K_0 \left( \sqrt{\frac{\rho_n}{\alpha}} R \right) \right]} \end{aligned}$$

$$\begin{aligned}
& \times \sum_{i=1}^p \left\{ \frac{B_i}{\rho_n - \beta_i} - \sum_{j=1}^s \frac{\alpha F A_j}{k \rho_n (\rho_n - \lambda_j)} \right\} \quad (12) \\
& + \sum_{j=1}^s \frac{\alpha F A_j e^{\lambda_j t}}{k} \left\{ \frac{K_i \sqrt{\frac{\lambda_j}{\alpha}} R_i I_0 \sqrt{\frac{\lambda_j}{\alpha}} r + I_i \sqrt{\frac{\lambda_j}{\alpha}} R_i K_0 \sqrt{\frac{\lambda_j}{\alpha}} r}{K_i \sqrt{\frac{\lambda_j}{\alpha}} R_i I_0 \sqrt{\frac{\lambda_j}{\alpha}} R + I_i \sqrt{\frac{\lambda_j}{\alpha}} R K_0 \sqrt{\frac{\lambda_j}{\alpha}} R} \right\}
\end{aligned}$$

where  $\omega_n$ 's are the roots of the equation,  $J_0(x) = 0$

and  $\rho_n$ 's are the roots of the equation,

$$[K_i (\sqrt{\frac{S}{\alpha}} R_i) I_0 (\sqrt{\frac{S}{\alpha}} R) + I_i (\sqrt{\frac{S}{\alpha}} R_i) K_0 (\sqrt{\frac{S}{\alpha}} R)] = 0$$

The solutions to the transient heat transfer equations in slab geometry in which the time dependence of the heat generation rate and the first derivative of the surface temperature with respect to  $x$  are  $\sum_{j=1}^{s'} A_j e^{\lambda_j t}$  and  $\sum_{i=1}^{p'} B_i e^{\beta_i t}$  respectively are derived in Appendix A and are given here as

$$\theta_f(x, t) = \sum_{j=1}^{p'} \frac{B_i \cosh(\sqrt{\frac{\beta_i}{\alpha}} x) e^{\beta_i t}}{\sqrt{\frac{\beta_i}{\alpha}} \sinh(\sqrt{\frac{\beta_i}{\alpha}} L)} - \frac{B_i \alpha}{B_i L} - \sum_{n=1}^{\infty} \frac{\cos \frac{n\pi x}{2L} e^{\frac{n^2 \pi^2 \alpha}{4L^2} t}}{(L/\alpha) \cos n\pi}$$

$$\begin{aligned}
& \times \left\{ \sum_{i=1}^{p'} \frac{B_i}{\frac{n^2 \pi^2 \alpha}{4L^2} + \beta_i} + \sum_{j=1}^{s'} \frac{q_{oo} \alpha A_j \kappa \sinh \kappa L}{k (\frac{n^2 \pi^2 \alpha}{4L^2} + \lambda_j) (\frac{n^2 \pi^2 \alpha}{4L^2} + \alpha \kappa^2)} \right\} \quad (13)
\end{aligned}$$

$$\begin{aligned}
& - \sum_{j=1}^{s'} \frac{q_{oo} \alpha A_j e^{\lambda_j t}}{k (\alpha \kappa^2 - \lambda_j)} \left\{ \cosh \kappa x - \frac{\kappa \sinh(\kappa L) \cosh(\sqrt{\frac{\lambda_j}{\alpha}} x)}{\sqrt{\frac{\lambda_j}{\alpha}} \sinh(\sqrt{\frac{\lambda_j}{\alpha}} L)} \right\} \\
& - \frac{q_{oo} \alpha A_j \sinh \kappa L}{k \lambda_j L \kappa}
\end{aligned}$$

and

$$\theta_m(s, t) = \sum_{i=1}^{p'} \frac{B_i \cosh(\sqrt{\frac{\beta_i}{\alpha}} x) e^{\beta_i t}}{\sqrt{\frac{\beta_i}{\alpha}} \sinh \sqrt{\frac{\beta_i}{\alpha}} L} - \frac{B_i \alpha}{\beta_i L}$$

$$- \sum_{n=1}^{\infty} \frac{\cos \frac{n\pi x}{2L} e^{-\frac{n^2 \pi^2 \alpha}{4L^2} t}}{(L/\alpha) \cos n\pi} \left\{ \sum_{i=1}^{p'} \frac{B_i \alpha}{\frac{n^2 \pi^2 \alpha}{4L^2} + \beta_i} \right\} \quad (14)$$

$$+ \sum_{j=1}^{s'} \frac{\alpha F A_j}{k (\lambda_j)} (e^{\lambda_j t} - 1)$$

in the fuel and moderator, respectively.

The solution to the transient heat transfer equation in slab geometry in which the time dependence of the heat generation rate and the surface temperature are represented by  $\sum_{j=1}^s A_j e^{\lambda_j t}$  and  $\sum_{i=1}^p B_i \cos \beta_i t$  respectively are derived in Appendix A and are given here as

$$\theta_f(x, t) = \sum_{i=1}^p B_i Z_i^{\frac{1}{2}} \cos(\beta_i t + \varphi_i) - \sum_{n=1,3,5,\dots}^{\infty} \frac{\cos \frac{n\pi x}{2L} e^{-\frac{n^2 \pi^2 \alpha}{4L^2} t}}{(L^2 / n\pi\alpha) \sin \frac{n\pi}{2}}$$

$$\times \left\{ \sum_{i=1}^p \frac{B_i \left( \frac{n^2 \pi^2 \alpha}{4L^2} \right)}{\left( \frac{n^2 \pi^2 \alpha}{16L^4} + \beta_i^2 \right)} + \sum_{j=1}^s \frac{q_{\infty} \alpha A_j \cosh \kappa L}{k \left( \frac{n^2 \pi^2 \alpha}{4L^2} + \alpha \kappa^2 \right) \left( \frac{n^2 \pi^2 \alpha}{4L^2} + \lambda_j \right)} \right\} \quad (15)$$

$$- \sum_{j=1}^s \frac{q_{\infty} \alpha A_j e^{\lambda_j t}}{k (\alpha \kappa^2 - \lambda_j)} \left\{ \cosh \kappa x - \frac{\cosh(\kappa L) \cosh(\sqrt{\frac{\lambda_j}{\alpha}} x)}{\cosh(\sqrt{\frac{\lambda_j}{\alpha}} L)} \right\}$$

and

$$\theta_m(x, t) = \sum_{i=1}^p B_i Z_i^{\frac{1}{2}} \cos(\beta_i t + \varphi_i) + \sum_{n=1,3,5,\dots}^{\infty} \frac{\cos \frac{n\pi x}{2L} e^{-\frac{n^2 \pi^2 \alpha}{4 L^2} t}}{(L^2 / n\pi \alpha) \sin \frac{n\pi}{2}}$$

$$x \left\{ \sum_{i=1}^p \frac{B_i \frac{n^2 \pi^2 \alpha}{4 L^2}}{\frac{n^2 \pi^2 \alpha}{16 L^4} + \beta_i^2} - \sum_{j=1}^s \frac{\alpha F A_j}{k \left( \frac{n^2 \pi^2 \alpha}{4 L^2} + \alpha \kappa^2 \right) \left( \frac{n^2 \pi^2 \alpha}{4 L^2} + \lambda_j \right)} \right\} \quad (16)$$

$$+ \sum_{j=1}^s \frac{\alpha F A_j e^{\lambda_j t}}{k \lambda_j} \left\{ 1 - \frac{\cosh(\sqrt{\frac{\lambda_j}{\alpha}} x)}{\cosh(\sqrt{\frac{\lambda_j}{\alpha}} L)} \right\}$$

where

$$Z_1 = \frac{\cos^2(\sqrt{\frac{\beta_1}{2\alpha}} x) \cosh^2(\sqrt{\frac{\beta_1}{2\alpha}} x) + \sin^2(\sqrt{\frac{\beta_1}{2\alpha}} x) \sinh^2(\sqrt{\frac{\beta_1}{2\alpha}} x)}{\cos^2(\sqrt{\frac{\beta_1}{2\alpha}} L) \cosh^2(\sqrt{\frac{\beta_1}{2\alpha}} L) + \sin^2(\sqrt{\frac{\beta_1}{2\alpha}} L) \sinh^2(\sqrt{\frac{\beta_1}{2\alpha}} L)}$$

and

$$\varphi_1 = \tan^{-1} \frac{\sin(\sqrt{\frac{\beta_1}{2\alpha}} x) \sinh(\sqrt{\frac{\beta_1}{2\alpha}} x)}{\cos(\sqrt{\frac{\beta_1}{2\alpha}} L) \cosh(\sqrt{\frac{\beta_1}{2\alpha}} L)} - \tan^{-1} \frac{\sin(\sqrt{\frac{\beta_1}{2\alpha}} L) \sinh(\sqrt{\frac{\beta_1}{2\alpha}} L)}{\cos(\sqrt{\frac{\beta_1}{2\alpha}} L) \cosh(\sqrt{\frac{\beta_1}{2\alpha}} L)}$$

2.2.1 Temperature Distributions. Equations (15) and (16) of the previous section can be evaluated to obtain the temperature as a function of position and time in any unit cell of a reactor if the heat generation rate,  $q(x,t)$ , and the fuel surface temperature,  $\theta_f(L,t)$ , are known and can be expressed in the appropriate analytical form. The experimental values of these variables during applicable transient tests on the SPERT-I reactor system were obtained in graphical form from "Sub-cooled Transient Tests in the SPERT-I-A Reactor - Experimental Data" by J. C. Haire (25). Numerical power and temperature data were obtained from the graphs. These numerical data were normalized to a zero initial temperature then fit empirically by an even trigonometric series,  $\sum_{i=1}^P A_i \cos \beta_i t$ , for the temperature traces. The power traces were reduced to give the heat generation rate in the center of a central fuel element and moderator region and then fit empirically by an exponential series,  $\sum_{j=1}^S A_j e^{\lambda_j t}$ . The reduction of the power data to give the appropriate heat generation rate in the fuel region was accomplished in the following manner. The SPERT-I core contained 28 assemblies, 51 plates per assembly and an active volume of  $7.523 \text{ cm}^3$  per plate. Therefore,

$$\begin{aligned} \bar{H}_{\text{plate}}(t) &= \left( \frac{P(t) \times 10^6}{28 \text{ assemblies}} \right) \left( \frac{1 \text{ assembly}}{51 \text{ plates}} \right) \left( \frac{1 \text{ plate}}{7.523 \text{ cm}^3} \right) \\ &= 97.78 P(t) \text{ watts/cm}^3 \end{aligned} \quad (16)$$

was the "average heat generation rate in an average fuel plate, where  $P(t)$  is the total power in megawatts. Converting this to the required dimensions of  $\text{cal/sec-cm}^3$  yielded  $\bar{H}_{\text{plate}}(t) = 23.37 P(t) \text{ cal/sec cm}^3$ . The heat generation rate in the center of the fuel plate is found in terms of the average heat generation rate since the heat generation rate is proportional to the neutron flux distribution.

$$\bar{H}_{\text{plate}}(t) = \frac{\int_0^L C \Phi(x) A dx}{\int_0^L A dx} = \frac{\int_0^L H_0 \cosh \kappa x dx}{L} = \frac{H_0 \sinh \kappa L}{\kappa L} \quad (17)$$

where  $L$  is half-thickness of plate, 0.0254 cm,

and  $\bar{H}_0$  is heat generation rate at center of the average fuel plate.

$\kappa$  was determined from the neutron transport theory relationship for heavy absorbers (44),

$$\frac{\kappa}{\Sigma_{\text{tot}}} = \tanh \frac{\kappa}{\Sigma_s} \quad (18)$$

to be  $0.7973 \text{ cm}^{-1}$ .

$$\kappa L / \sinh \kappa L = \frac{0.02025}{0.02025} = 1.0 \quad (19)$$

Therefore,

$$\bar{H}_{\text{of}}(t) = \bar{H}_{\text{plate}}(t) = 23.37 P(t) \text{ cal/sec cm}^3. \quad (20)$$

The correction from the average fuel element to the one of interest, a central fuel element, required a maximum to average correction. Therefore,

$$H'_{\text{of}}(t) = \bar{H}_{\text{of}}(t) (\Phi_{\text{max}} / \bar{\Phi}) = 23.37 P(t) (1.9) = 44.38 P(t) \text{ cal/cm}^3 \text{ sec}. \quad (21)$$

The final correction was to assume that approximately 5% of the power was generated in the moderator. Therefore,

$$H_{\text{of}}(t) = 0.95 H'_{\text{of}}(t) = 42.16 P(t) \text{ cal/cm}^3 \text{ sec}. \quad (22)$$

The relation used to calculate the heat generation rate in the moderator was

$$q_m(t) = 0.05 \bar{q}_f(t) \frac{V_f}{V_m} = 0.05 \bar{q}_f(t) \frac{L_f}{L_m} = 0.05 H_{\text{of}}(t) \left( \frac{0.0254}{0.071755} \right) = 0.017695 H_{\text{of}}(t) \quad (23)$$



where  $\bar{q}_f$  is average heating rate in the fuel,

$V_f$  is volume of the fuel,

$V_m$  is volume of the moderator,

$L_f$  is half-thickness of the fuel,

$L_m$  is half-thickness of the moderator,

and  $q_m$  is the heat generation rate in the moderator.

The above equation assumes that there is a flat spatial distribution of the heating rate, that approximately 5% of the total heat generation takes place in the moderator and that the average heat generation rate in the fuel is well approximated by the heat generation rate in the center of the fuel.

As previously mentioned that data from the temperature traces were fit with a finite number of terms of a Fourier series of the form

$$\sum_{n=0}^p b_n \cos \frac{2\pi n t}{a} \quad (24)$$

where

$$b_0 = \frac{2}{a} \int_0^a y(t) dt,$$

$$b_n = \frac{1}{a} \int_0^a y(t) \cos \frac{2\pi n t}{a} dt,$$

$y(t)$  = experimental temperature trace data,

and  $a$  = interval of periodicity.

The data reduced from the power traces, actually  $H_{of}(t)$ , were fitted with a finite number of terms of an exponential function of the form,

$$\sum_{j=1}^s A_j e^{\lambda_j t}, \quad (25)$$

where  $A_j$  and  $\lambda_j$  were parameters which were determined by trial and error to give the best fit. The best fit parameters were determined by means

of an IBM-650 computer program described in Appendix B. This program resulted from a very minor modification of one written by L. R. Foulke (17). The data for  $H_{of}(t)$  and the approximating equations are shown in Figures 8 through 11.

The thermal, nuclear and geometric constants used in determining the temperature distributions are given in Table 1.

Table 1. Constants Used to Evaluate the Temperature Distributions

Constant	Fuel	Moderator
$\alpha$ , Thermal Diffusivity, $\text{cm}^2/\text{sec}$	0.82	0.001512
$\kappa$ , Inverse Diffusion Length, $\text{cm}^{-1}$	0.7973	0.0
$L$ , Half-thickness of Region, $\text{cm}$	0.0254	0.071755
$k$ , Thermal Conductivity, $\text{cal/cm sec } ^\circ\text{C}$	0.5002	0.001488

2.2.2 Surface Heat Flow. The heat flow rate out of the fuel and into the moderator as a function of time was evaluated by forming the partial derivative with respect to position evaluating it at the outside of the respective region and multiplying by the respective thermal conductivity. The heat flow out of the fuel and into the moderator are, respectively,

$$(q/A)_f(t) = -k_f \left. \frac{\partial \theta_f(x,t)}{\partial x} \right|_{x=L} \quad (26)$$

and

$$(q/A)_m(t) = -k_m \left. \frac{\partial \theta_m(x,t)}{\partial x} \right|_{x=L} \quad (27)$$

Evaluating the above equations yields in the fuel

$$\begin{aligned}
 (q/A)_f(t) = & -k_f \left\{ \sum_{i=1}^p \left( \sqrt{\frac{\beta_i}{2\alpha}} \right) B_i (D_i \cos \beta_i t + E_i \sin \beta_i t) \right. \\
 & + \sum_{n=1,3,5,\dots(L^2/n\pi\alpha)}^{\infty} \frac{\left(\frac{n\pi}{2L}\right) e^{-\frac{n^2\pi^2\alpha}{4L^2}t}}{L^2/n\pi\alpha} \left[ \sum_{i=1}^p \frac{B_i \left(\frac{n^2\pi^2\alpha}{4L^2}\right)}{\frac{n^2\pi^2\alpha}{16L^4} + \beta_i^2} + \sum_{j=1}^s \frac{q_{\infty} \alpha A_j \cosh \kappa L}{k_f \left(\frac{n^2\pi^2\alpha}{4L^2} + \lambda_j\right) \left(\frac{n^2\pi^2\alpha}{4L^2} + \alpha \kappa^2\right)} \right] \\
 & + \sum_{j=1}^s \frac{q_{\infty} \alpha A_j e^{\lambda_j t}}{k_f (\alpha \kappa^2 - \lambda_j)} \left[ \frac{\sqrt{\frac{\lambda_j}{\alpha}} \cosh(\kappa L) \sinh\left(\sqrt{\frac{\lambda_j}{\alpha}} L\right)}{\cosh\left(\sqrt{\frac{\lambda_j}{\alpha}} L\right)} - \kappa \sinh \kappa L \right] \left. \right\}
 \end{aligned}$$

and in the moderator

$$\begin{aligned}
 (q/A)_m(t) = & -k_m \left\{ \sum_{i=1}^p \left( \sqrt{\frac{\beta_i}{2\alpha}} \right) B_i (D_i \cos \beta_i t + E_i \sin \beta_i t) \right. \\
 & + \sum_{n=1,3,5,\dots L^2/n\pi\alpha}^{\infty} \frac{\left(\frac{n\pi}{2L}\right) e^{-\frac{n^2\pi^2\alpha}{4L^2}t}}{L^2/n\pi\alpha} \left[ \sum_{j=1}^s \frac{\alpha F A_j}{k_m \left(\frac{n^2\pi^2\alpha}{4L^2} + \lambda_j\right) \left(\frac{n^2\pi^2\alpha}{4L^2}\right)} + \sum_{i=1}^p \frac{B_i \left(\frac{n^2\pi^2\alpha}{4L^2}\right)}{\frac{n^2\pi^2\alpha}{16L^4} + \beta_i^2} \right] \\
 & - \sum_{j=1}^s \frac{\alpha F A_j}{k_m \lambda_j} \left( \frac{\sqrt{\frac{\lambda_j}{\alpha}} \sinh\left(\sqrt{\frac{\lambda_j}{\alpha}} L\right)}{\cosh\left(\sqrt{\frac{\lambda_j}{\alpha}} L\right)} \right) \left. \right\},
 \end{aligned}$$

$$\text{where } D_i = \frac{\cosh\left(\sqrt{\frac{\beta_i}{2\alpha}} L\right) \sinh\left(\sqrt{\frac{\beta_i}{2\alpha}} L\right) - \cos\left(\sqrt{\frac{\beta_i}{2\alpha}} L\right) \sin\left(\sqrt{\frac{\beta_i}{2\alpha}} L\right)}{\cos^2\left(\sqrt{\frac{\beta_i}{2\alpha}} L\right) \cosh^2\left(\sqrt{\frac{\beta_i}{2\alpha}} L\right) + \sin^2\left(\sqrt{\frac{\beta_i}{2\alpha}} L\right) \sinh^2\left(\sqrt{\frac{\beta_i}{2\alpha}} L\right)}$$

$$\text{and } E_1 = \frac{\cosh(\sqrt{\frac{\beta}{2\alpha}} L) \sinh(\sqrt{\frac{\beta}{2\alpha}} L) + \cos(\sqrt{\frac{\beta}{2\alpha}} L) \sin(\sqrt{\frac{\beta}{2\alpha}} L)}{\cos^2(\sqrt{\frac{\beta}{2\alpha}} L) \cosh^2(\sqrt{\frac{\beta}{2\alpha}} L) + \sin^2(\sqrt{\frac{\beta}{2\alpha}} L) \sinh^2(\sqrt{\frac{\beta}{2\alpha}} L)}.$$

### 2.3 Reactivity Effects Due to Temperature Coefficient and Fuel Expansion

It is pointed out by Deverall and Griffing (9) that the temperature rise in the moderator in the central unit cell cannot be used directly to determine reactivity changes. "Since the temperature coefficient of reactivity,  $\alpha$ , was determined under conditions of a uniform temperature throughout the core - a condition that does not exist in a transient - it is necessary to define a properly weighted average temperature. This average temperature would then produce the same change in reactivity as if an actual uniform temperature change of this amount had been made. This average is defined by

$$\overline{\Delta T} = \frac{\int I(\vec{x}) \Delta T(\vec{x}) d\vec{x}}{\int I(\vec{x}) d\vec{x}} \quad (30)$$

where

$\Delta T(\vec{x})$  is the change of temperature at position  $\vec{x}$ ,

$I(\vec{x})$  is the statistical importance at position  $\vec{x}$ ,

and the integration is carried out over the whole volume of the reactor."

The authors also show that for SPERT I-A (17/28) core, the system under consideration,

$$\frac{\overline{\Delta T}}{\Delta T_{\max}} = 0.65 \quad (31)$$

Therefore,

$$\Delta k = 0.65 \alpha(T) \Delta T_{\max}. \quad (32)$$

A value for  $\alpha(t)$  of  $0.9 \times 10^{-4} (\Delta k / ^\circ C)$  was used yielding

$$\Delta k = (-5.85 \times 10^{-5} / ^\circ C) \Delta T_{\max}. \quad (33)$$

A similar problem was faced by Forbes (13). In determining the reactivity effect due to fuel plate expansion he stated,

"In order to obtain the reactivity change, the temperature distribution and void importance function in the core must be combined to obtain the dynamic reactivity coefficient as opposed to the static coefficient which applies only to uniform void distributions. Applying the observed distribution functions for temperature and void worth, it is found that the effective average temperature rise under dynamic conditions can be obtained from the temperature rise at the center of the core by the relation

$$\Delta \theta = 0.7 \Delta \theta_{\max}. \quad (34)$$

The reactivity change due to plate expansion,  $\Delta k_1$ , will be

$$\Delta k_1 = \left( \overline{\frac{\partial k}{\partial v}} \right) 3 a v (0.7 \Delta \theta_{\max}), \quad (35)$$

where  $\left( \overline{\frac{\partial k}{\partial v}} \right)$  is the average void coefficient for the core,

$a$  is the linear expansion coefficient of aluminum,

$v$  is the volume of the aluminum which is heated (i.e., the volume of fuel plates proper),

$\overline{\Delta \theta^v}$  is the average temperature rise of the aluminum

and  $\Delta \theta_{\max}$  is the temperature rise at center of the core.

For the SPERT I-A (17/28) core the appropriate constants are the following:

$$a = 2.5 \times 10^{-5} / ^\circ C$$

$$v = 2.8 \times 10^4 \text{ cm}^3$$

$$\left(\frac{\partial k}{\partial v}\right) = -3.5 \times 10^{-6} \Delta k / \text{cm}^3$$

Therefore, the expression for the reactivity change becomes

$$\Delta k_1 = (-5 \times 10^{-6} \frac{\Delta k}{^\circ\text{C}}) (\Delta \theta_{\text{max}}). \quad (36)$$

In order to avoid erroneously taking into account the void formation due to fuel element expansion in both the temperature coefficient and in the fuel element expansion calculation, the fuel element expansion was calculated only for the temperature rise in the fuel over the temperature rise in the moderator. Therefore, the reactivity effects due to the temperature coefficient,  $\Delta k_T$ , and due to the fuel plate expansion,  $\Delta k_E$ , are

$$\Delta k_T(t) = -5.85 \times 10^{-5} (\Delta k / ^\circ\text{C}) \bar{\theta}_{\text{mod}}(t) \quad (37)$$

$$\text{and} \quad \Delta k_E(t) = -5 \times 10^{-6} (\Delta k / ^\circ\text{C}) (\bar{\theta}_{\text{fuel}}(t) - \bar{\theta}_{\text{mod}}(t)) \quad (38)$$

where  $\bar{\theta}_{\text{mod}}(t)$  is the average temperature rise in the moderator at time  $t$

$\bar{\theta}_{\text{fuel}}(t)$  is the average temperature rise in the fuel at time  $t$  as obtained from Tables 2 through 5.

#### 2.4 Reactivity Effects Due to Steam Formation

The calculation of the steam production was based on the same assumptions as those used in the "Conduction Boiling Model for Reactor Self-Shutdown" suggested by S. G. Forbes (15). In Forbes' work the steam volume,  $V_s$ , was assumed to be proportional to a fraction,  $f_{as}$ , of the energy,  $E_s$ , transferred to the moderator after the time boiling first occurred



in the core. The steam volume is given by

$$V_s = \frac{f_{as} E_s}{h_s}, \quad (39)$$

where  $h_s$  is the energy required to form a unit volume of steam from boiling water at standard pressure (1.35 watt-sec/cm<sup>3</sup> steam). The term  $f_{as}$  was regarded as a combination of factors involving the fraction of the energy actually forming steam during nucleate boiling (about 1%) and the fraction of the core heat transfer area,  $A$ , which is involved in boiling heat transfer (about 10%) (15). The reactivity effect of the steam is

$$\Delta k_s = V_s C_v = \frac{f_{as} E_s}{h_s} C_v, \quad (40)$$

where  $C_v$  is the void coefficient in the center of the core, ( $C_v = -7.2 \times 10^{-6} \Delta k/cm^3$  for Spert I-A). In this investigation the factor  $f_{as}$  was divided into its two components, the fraction of the core involved in boiling,  $f_a$ , and the fraction of the energy actually forming steam during nucleate boiling,  $f_s$ . This was done since it was possible to approximate  $f_a$  directly from the fuel surface temperature and the assumption that the gross temperature distribution over the core was proportional to the bare core power distribution. It is expected that the final factor,  $f_s$ , will be independent of the pulse parameters for a particular system and that it will prove essentially independent of the reactor parameters in any heterogeneous water moderated system. In effect, the final parameter,  $f_s$ , was left to be calibrated by any particular pulse. The test of this model was of course a constant  $f_s$ . For the two boiling runs considered, the values of  $f_s$  calculated were  $3.7 \times 10^{-3}$  and  $3.3 \times 10^{-3}$  which differ



by less than 2%. The 2% difference is less than would be expected for the accuracy of the input data. The reactivity effect of the steam is then

$$\begin{aligned}\Delta k_s(t) &= \left( \frac{-7.28 \times 10^{-6}}{1.35 \times 10^{-6}} \Delta k/\text{MW-sec} \right) (f_a f_s E_s(t)) \\ &= -1.87 \times 10^{-2} f_a E_s(t)\end{aligned}\quad (41)$$

$f_a$  is fraction of core heat transfer area involved in boiling,

$f_s$  is fraction of energy actually forming steam,

and  $E_s(t)$  is total energy into core after initial boiling in MW-sec.

The fraction  $f_a$  was calculated assuming the gross core temperature distribution had reached a dynamic equilibrium with the power and the power distribution could be approximated by that of an equivalent bare core with an effective height,  $2Z_e$ , and radius,  $R_e$ . The gross temperature distribution in the core is then

$$\theta(r, Z) = \theta_o J_o\left(\frac{2.4048 r}{R_e}\right) \cos \frac{\pi Z}{2Z_e} \quad (42)$$

where  $\theta_o$  is the surface temperature at the time of interest on the axial center line of a central fuel element. The maximum value of  $Z$ ,  $Z_{\max}$ , for which boiling will occur on any plate can then be obtained knowing the boiling temperature,  $\theta_b$ , and the axial centerline surface temperature,

$$\theta_o J_o\left(\frac{2.4048 r}{R_e}\right).$$

That is

$$\cos \frac{\pi Z_{\max}}{2 Z_e} = \frac{\theta_b}{\theta_o J_o\left(\frac{2.4048 r}{R_e}\right)} \quad (43)$$

so that

$$\frac{Z_{\max}}{Z_e} = \frac{2}{\pi} \cos^{-1} \left( \frac{\theta_b}{\theta_o J_o \left( \frac{2.4048 r}{R_e} \right)} \right)$$

The maximum value of  $r$  for which boiling will occur,  $r_{\max}$ , on the core axial centerline can be obtained from

$$\theta_b = \theta_o J_o \left( \frac{2.4048 r_{\max}}{R_e} \right)$$

so that

(44)

$$\frac{r_{\max}}{R_e} = \frac{1}{2.4048} J_o^{-1} \left( \frac{\theta_b}{\theta_o} \right)$$

where  $y = J_o^{-1}(x)$  is the inverse of  $x = J_o(y)$ .

The volume fraction of the core having a fuel surface temperature above the boiling temperature is

$$\begin{aligned} f_v &= \frac{1}{\pi R_e^2 (2Z_e)} \int_0^{r_{\max}} 2 Z_{\max} 2\pi r dr \\ &= \frac{2}{R_e^2} \int_0^{r_{\max}} \frac{Z_{\max}}{Z_e} r dr \end{aligned}$$

Making the change in variable  $\eta = r/R_e$ , the integral becomes

$$f_v = 2 \int_0^{\eta_{\max}} \frac{Z_{\max}(\eta)}{Z_e} \eta d\eta \quad (46)$$

Substituting the value of  $Z_{\max}/Z_e$  from equation (43) yields

$$f_v = 4/\pi \int_0^{\eta_{\max}} \cos^{-1} \frac{\theta_b}{\theta_o J_o \left( \frac{2.4048 \eta}{1} \right)} \eta d\eta \quad (47)$$

This integration was then carried out numerically using the value of  $\eta_{\max} = r_{\max}/R_e$  determined from equation (44). Since there is a

constant heat transfer area per unit volume in the core then  $\underline{f_v} = \underline{f_a}$ . For the two boiling runs  $\tau = 15.8$  msec and 23 msec,  $\underline{f_a}$  was equal to 0.116 and 0.084, respectively.

The total energy transferred to the moderator after the time of initial boiling was obtained by considering the moderator volume associated with unit surface area in the central fuel element. The heat content of the moderator at the time boiling temperatures were reached at the surface and at the time of peak power were calculated based on the conduction model. While this model gave a somewhat erroneous temperature distribution above boiling temperatures it accurately represented the heat flow into the moderator. The difference between the moderator heat content at the time of interest and at the time boiling temperatures were first reached was the energy available for boiling per unit fuel surface area. Plots of the central fuel surface temperature and the average moderator temperature in a central element used to calculate the moderator heat contents are shown in Figures 2 and 3. The total energy available for steam formation is obtained by multiplying by the total heat transfer surface area of the core. This somewhat overestimates the total energy but is probably the best estimate of the energy of interest since the boiling region is confined to a rather small central portion of the core. Therefore

$$E_s(t) = (\bar{\theta}_m(t) - \bar{\theta}_m(t_b)) C_p M$$

where  $C_p$  is the heat capacity of the moderator

$M$  is the mass of the moderator in the system

$\bar{\theta}_m(t)$  is the average moderator

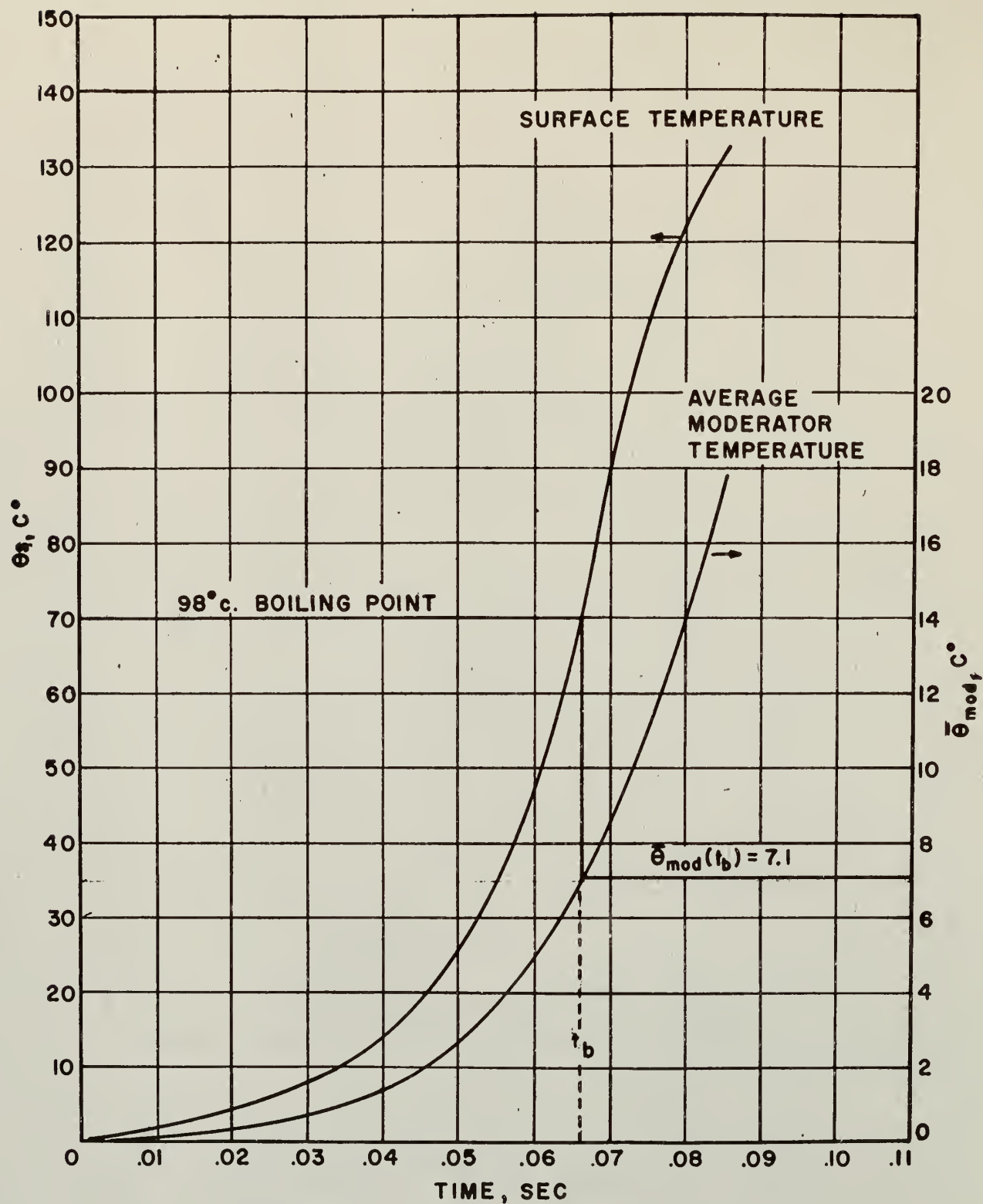


Figure 2. Graph used to determine the moderator energy for boiling calculations during a transient with an initial period of 15.8 msec.

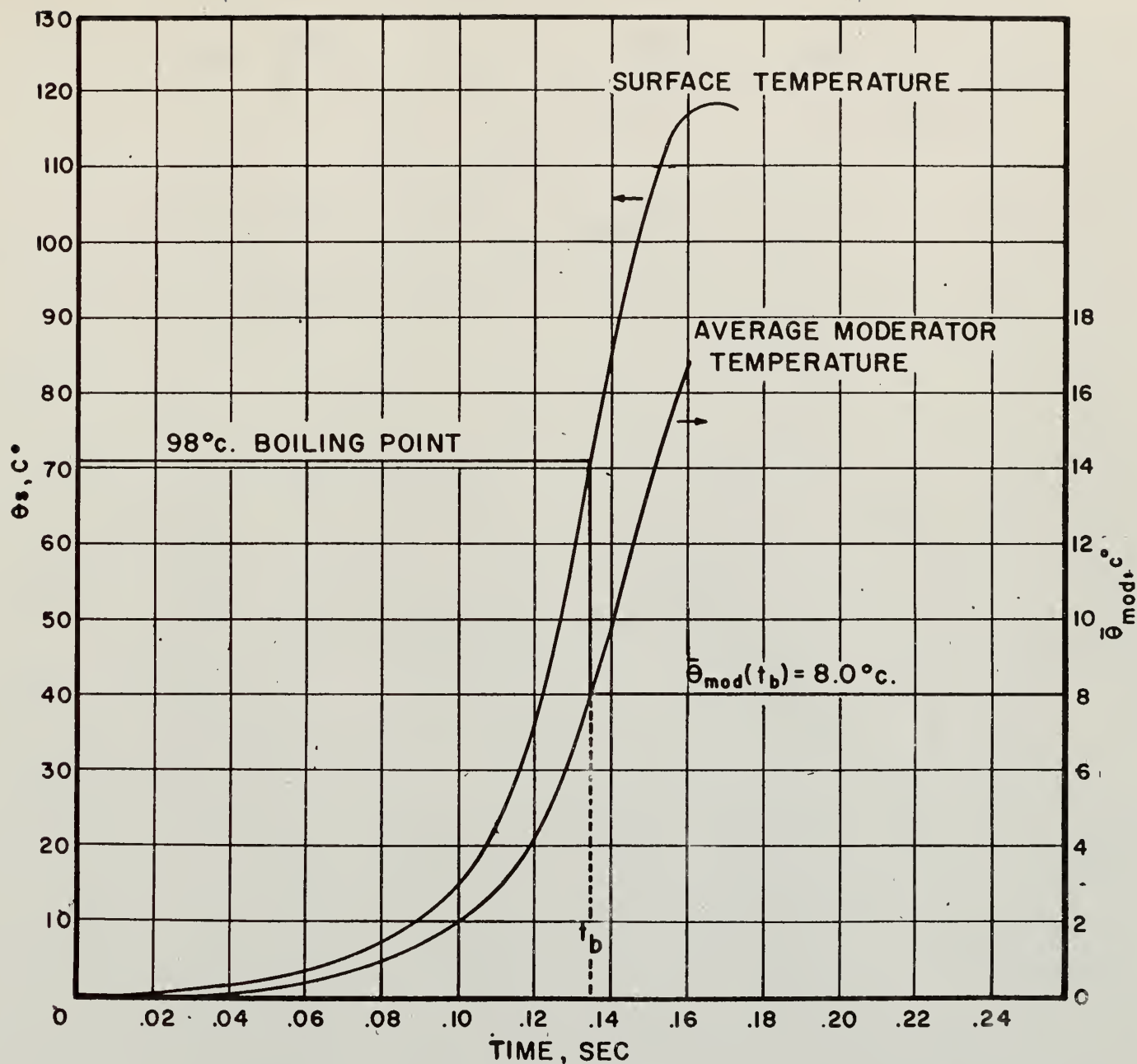


Figure 3. Graph used to determine the moderator energy content for boiling calculations during a transient with an initial period of 23 msec.

### 3.0 RESULTS AND DISCUSSION

#### 3.1 Temperature Distribution and Surface Heat Flow

The temperature distributions as obtained from equations 15 and 16 are shown in Figures 4 through 7. These plots were obtained using experimental data from four transient tests on the SPERT I-A (17/28) reactor having initial periods,  $\tau$ , of 15.8, 23, 120, and 150 msec, respectively. The transient burst for  $\tau$  equal 15.8 and 23 msec show regions in the moderator which have temperatures above the boiling point at a pressure of one atmosphere. It is not believed that this superheating takes place. These temperature distributions are shown since such a small portion of the moderator is above the saturation point that it is not likely that it will materially affect the temperature in the remainder of the moderator or the average moderator temperature. One possibility which must be considered in calculating the reactivity effects if that pressure transients are developed which raise the boiling point above the temperatures observed in the core. This appears not to be the case for two reasons. First, experimental measurements of the pressures do not indicate sufficient rises in pressure and second, the total reactivity compensations at peak power indicate that boiling must have taken place.

The experimental surface temperature traces and the approximate analytical fits for the four transient tests are shown in Figures 8 through 11. The parameters for the analytical fits,  $\theta(L,t) = \sum_{i=1}^P B_i \cos \beta_i t$ , are shown in Table 2. The experimental power traces, actually  $H_{of}(t)$ , and the approximate analytical fits for the same four transient tests



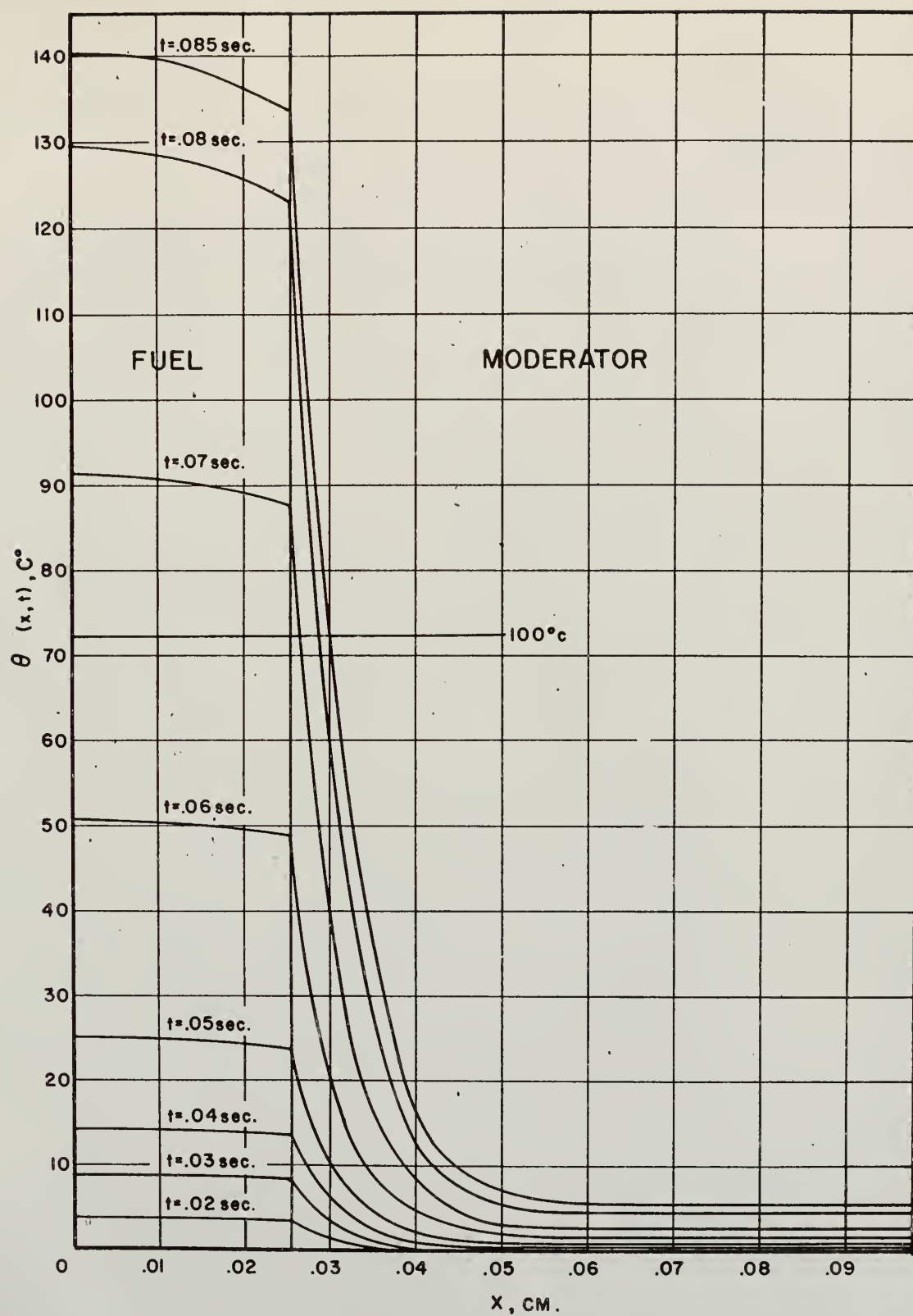


Figure 4. Temperature distributions,  $\theta(x,t)$ , vs position in fuel and moderator based on pure conduction during a transient with an initial period of 15.8 msec.

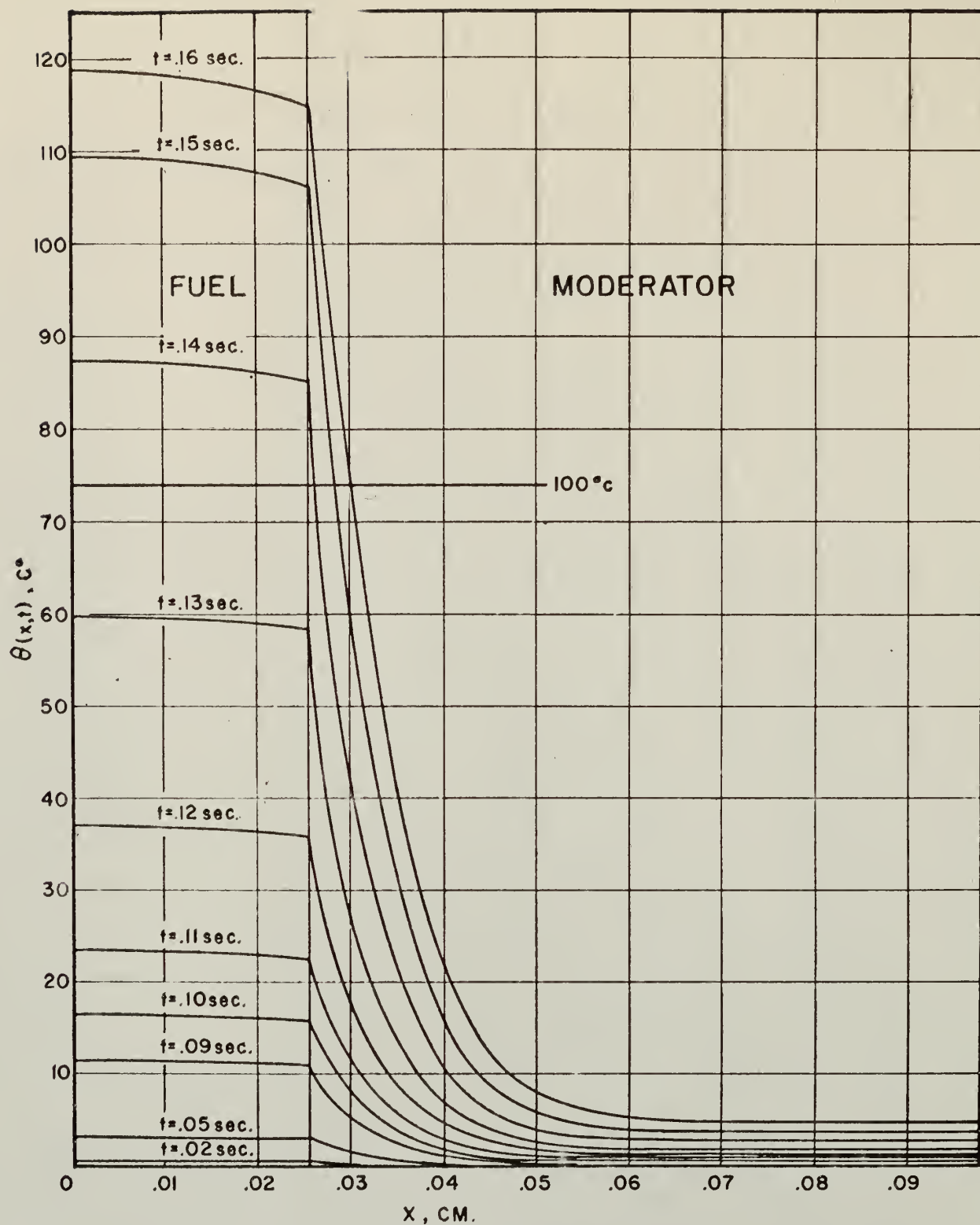


Figure 5. Temperature distributions,  $\theta(x,t)$ , vs position in fuel and moderator based on pure conduction during a transient with an initial period of 23 msec.

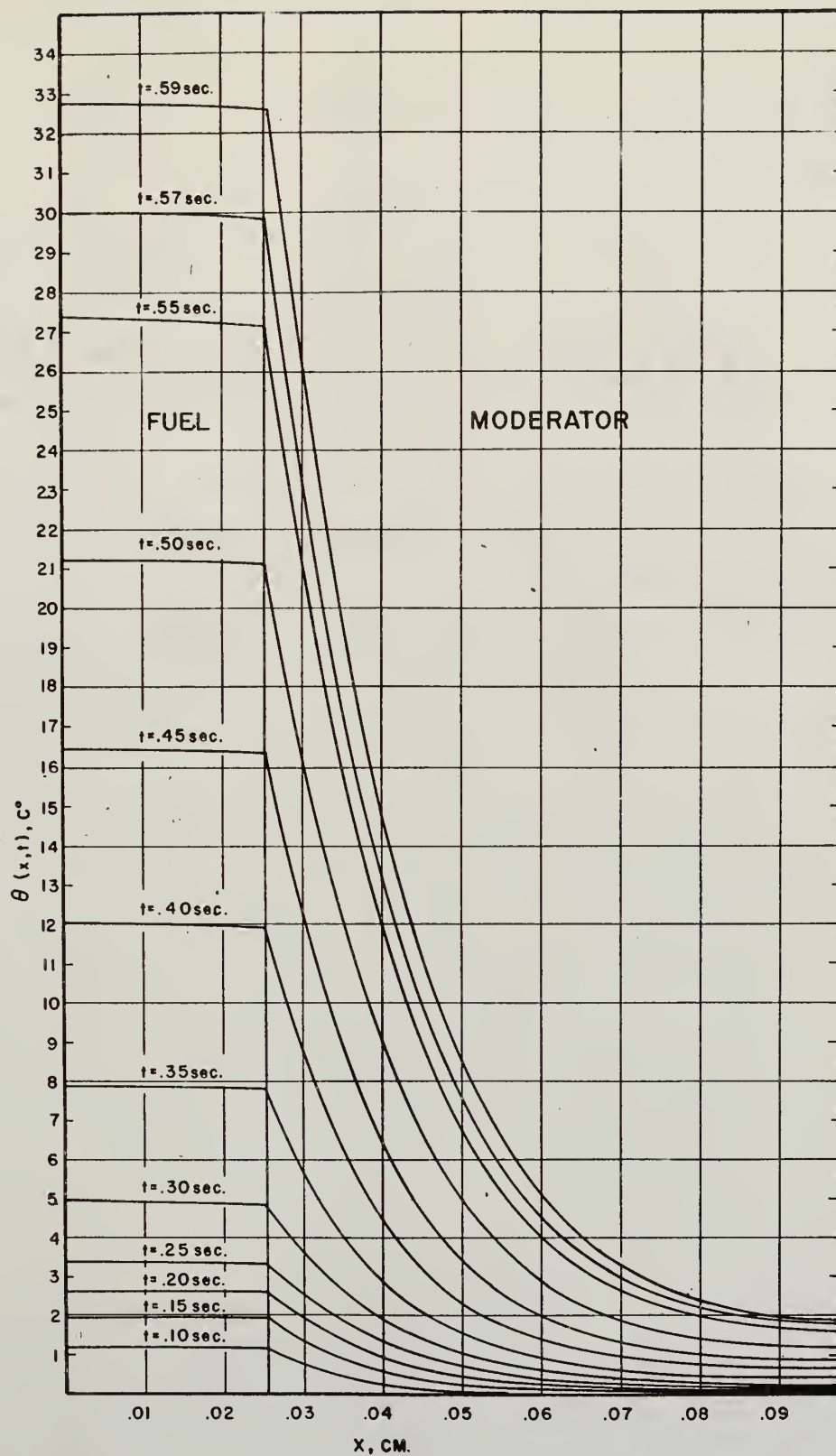


Figure 6. Temperature distributions,  $\theta(x,t)$ , vs position in fuel and moderator based on pure conduction during a transient with an initial period of 120 msec.

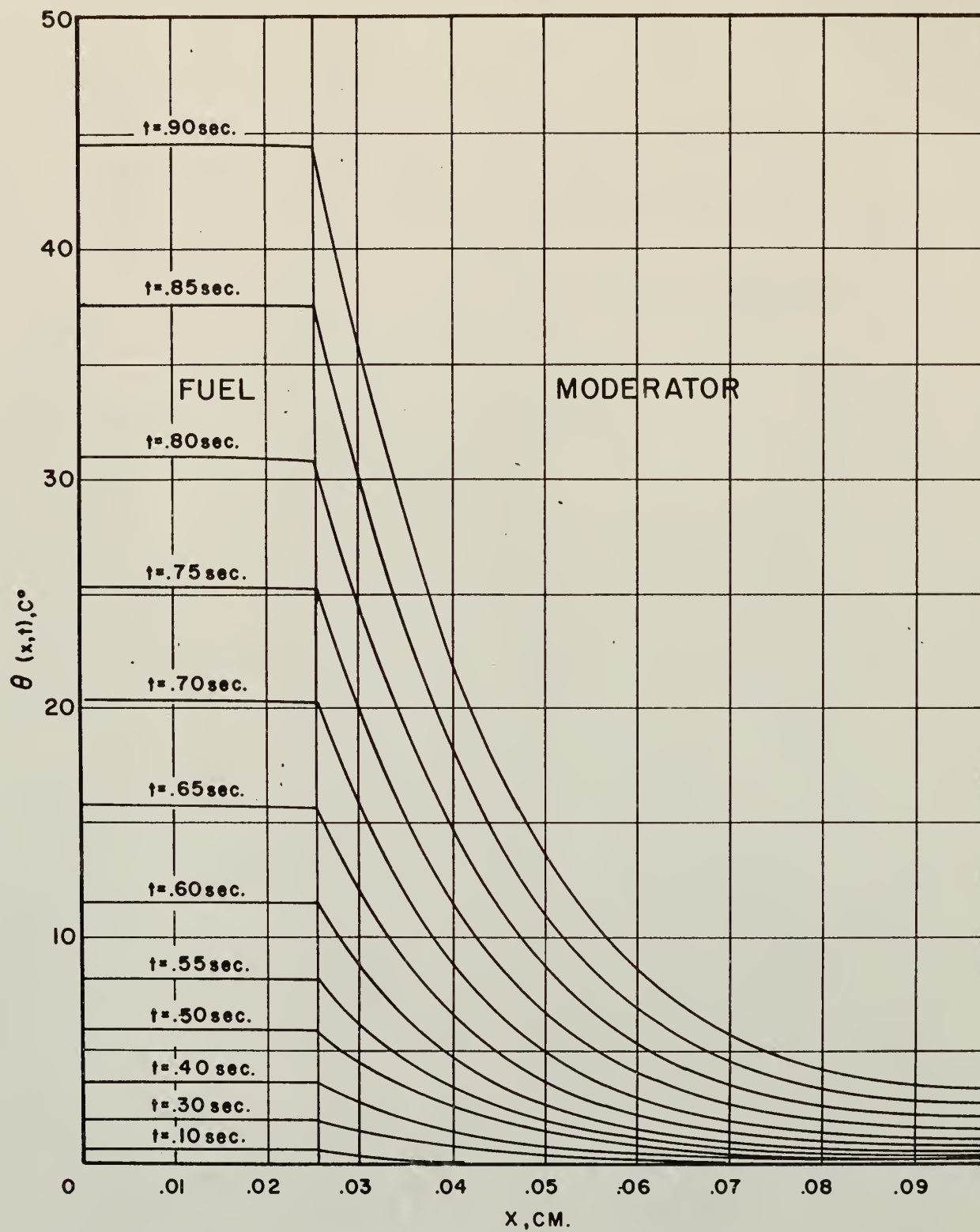


Figure 7. Temperature distributions,  $\theta(x,t)$ , vs position in fuel and moderator based on pure conduction during a transient with an initial period of 150 msec.

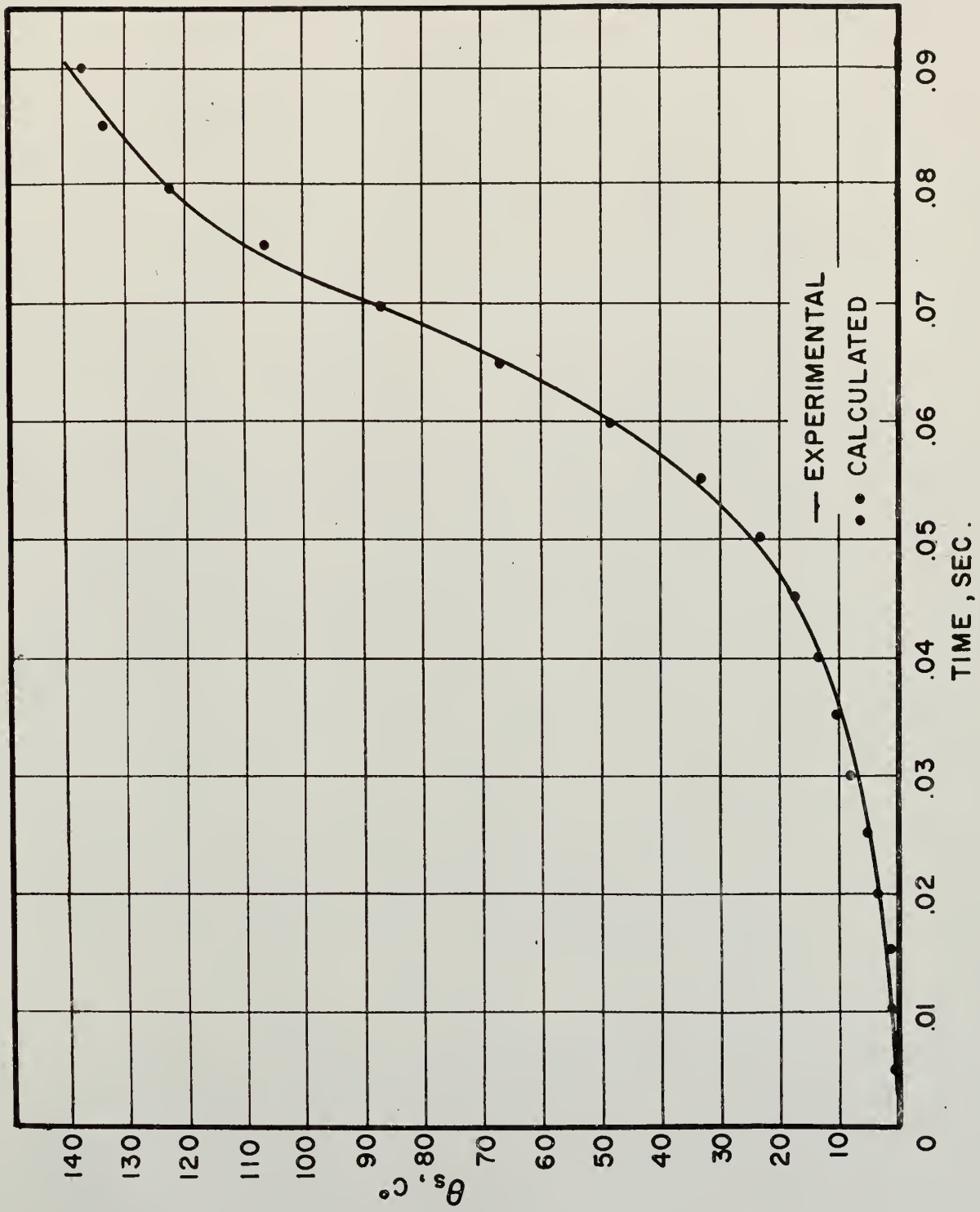


Figure 8. Interface temperatures,  $\theta_s$ , vs arbitrary time during a transient with an initial period of 15.8 msec.

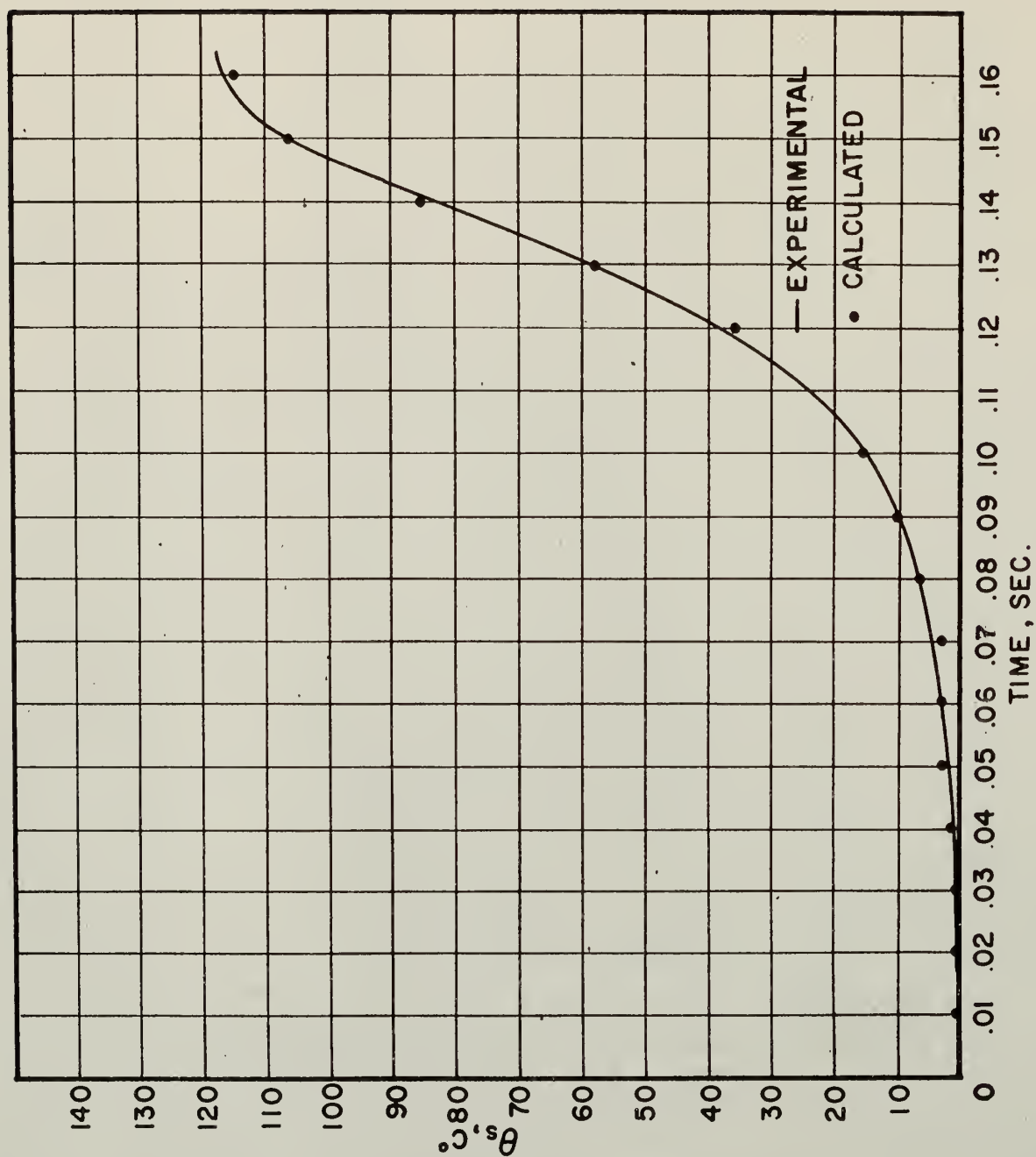


Figure 9. Interface temperatures,  $\theta_s$ , vs arbitrary time during a transient with an initial period of 23 msec.



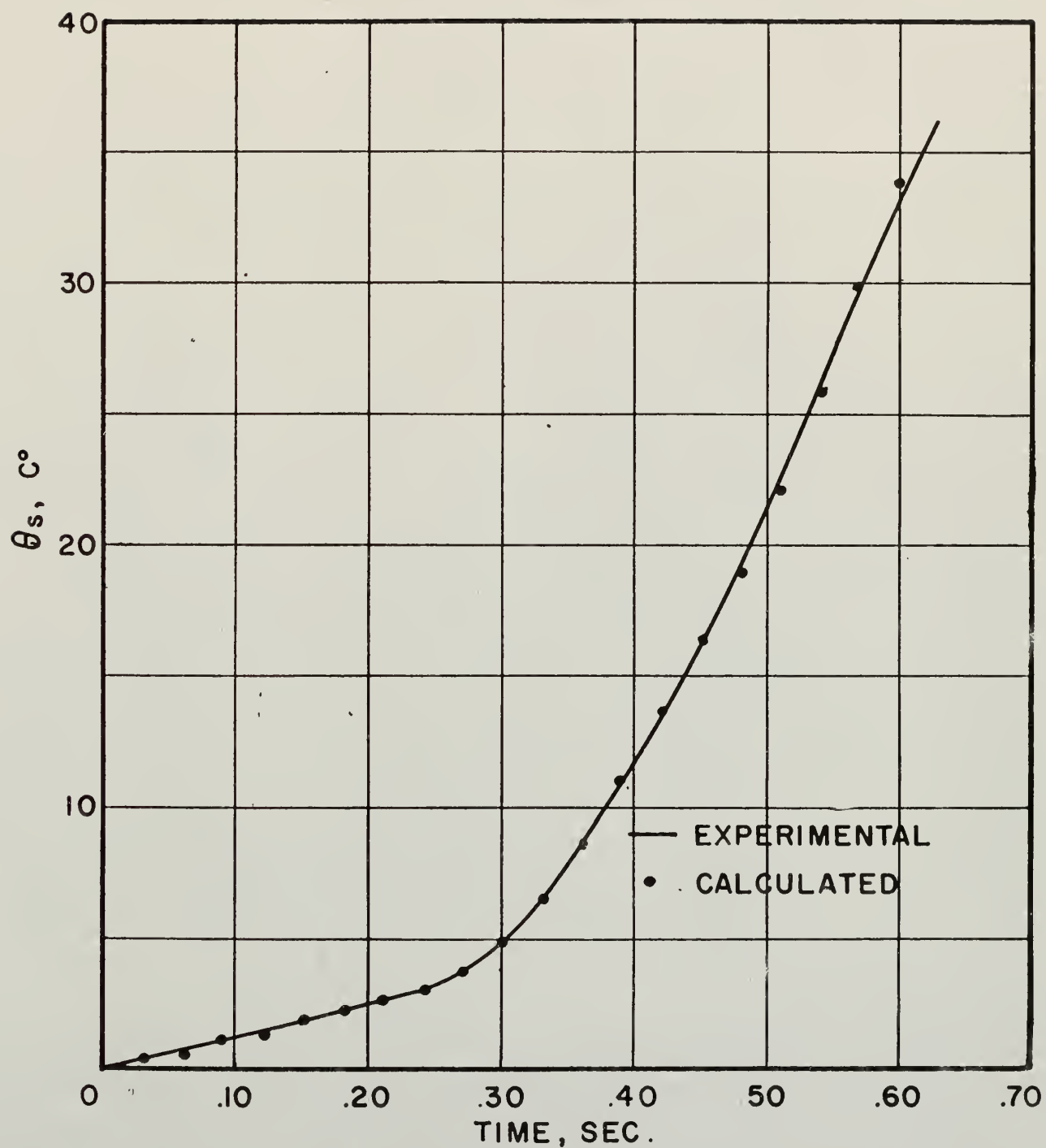


Figure 10. Interface temperatures,  $\theta_s$ , vs arbitrary time during a transient with an initial period of 120 msec.

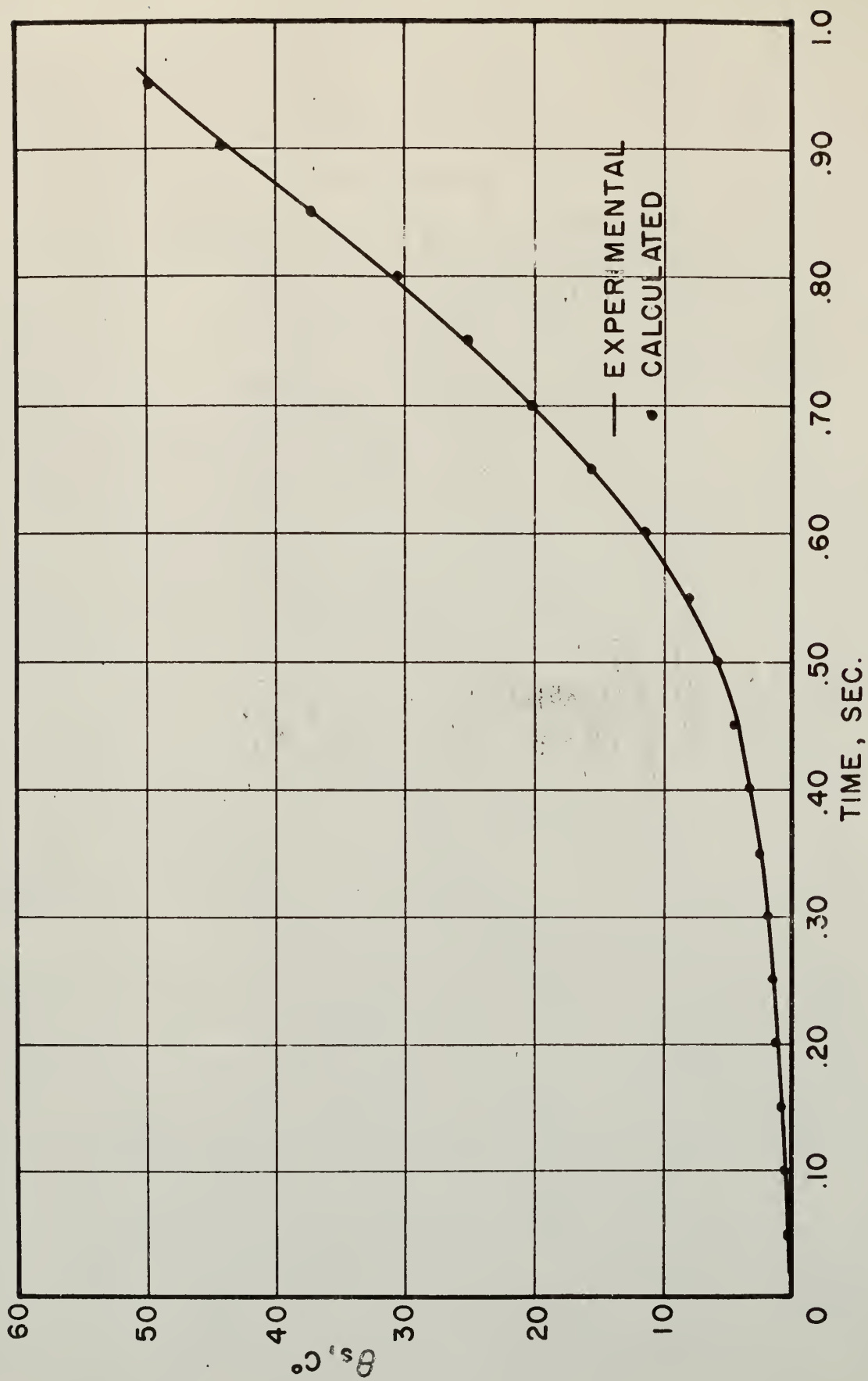


Figure 11. Interface temperatures,  $\theta_s$ , vs arbitrary time during a transient with an initial period of 150 msec.

Table 2. Numerical Values of Parameters for Empirical Fits of  $\theta(L,t)$  Used in Equations (15) and (16)

$\tau, \text{msec}$	$B_1$ $\beta_1$	$B_2$ $\beta_2$	$B_3$ $\beta_3$	$B_4$ $\beta_4$	$B_5$ $\beta_5$	$B_6$ $\beta_6$	$B_7$ $\beta_7$	$B_8$ $\beta_8$
150	+14.593 0.00	-20.958 3.1416	+9.474 6.2832	-3.763 9.4279	+1.313 12.566	-0.871 15.708	+0.582 18.850	-0.447 21.991
120	+12.033 0.00	-15.831 4.760	+5.875 9.520	-2.067 14.280	+6.817 19.040	-0.829 23.800	+0.399 28.560	-0.100 33.320
23	+35.752 0.00	-54.937 17.405	+26.246 34.810	-7.248 52.215	-2.118 69.620	+4.476 87.024	-3.802 104.429	+2.413 121.834
15.8 $\mu$	42.074 0.00	-59.957 34.906	+25.821 69.812	-9.279 104.718	+1.094 139.624	0.838 174.530	-- --	-- --

are shown in Figures 12 through 15. The parameters for the analytical fits,  $H_{of}(t) = \sum_{j=1}^8 A_j e^{\lambda_j t}$  are shown in Table 3.

One physical check on the solutions not required by the mathematical formulation of the problem is that the heat flow out of the fuel must equal the heat flow into the moderator. The heat flow data are shown in Figures 16 through 19. It is obvious from inspection of these data that the equivalent heat flow condition is not well satisfied. There are several possible explanations for this discrepancy. First, the heat flow data is somewhat more sensitive to the analytical fits of the surface temperature and the heat generation rates than the average temperatures. Second, the cladding between the meat and the moderator was neglected in calculating the temperature distributions. Again, the average temperatures are far less sensitive to this approximation than the heat flow calculations. Finally, it can be seen by investigating the heat flow equations that the discrepancies could be decreased by introducing a positive phase angle to the surface temperature fits. This could be attributed to a delay time in the surface temperature measurements.

The average temperatures in the fuel and moderator as a function of time were calculated by means of a numerical integration of the calculated temperature distributions. These data are given in Tables 4 through 7.

### 3.2 Reactivity Effects

The reactivity compensations

$$\Delta k_c(t) = \Delta k(o) - \Delta k(t)$$

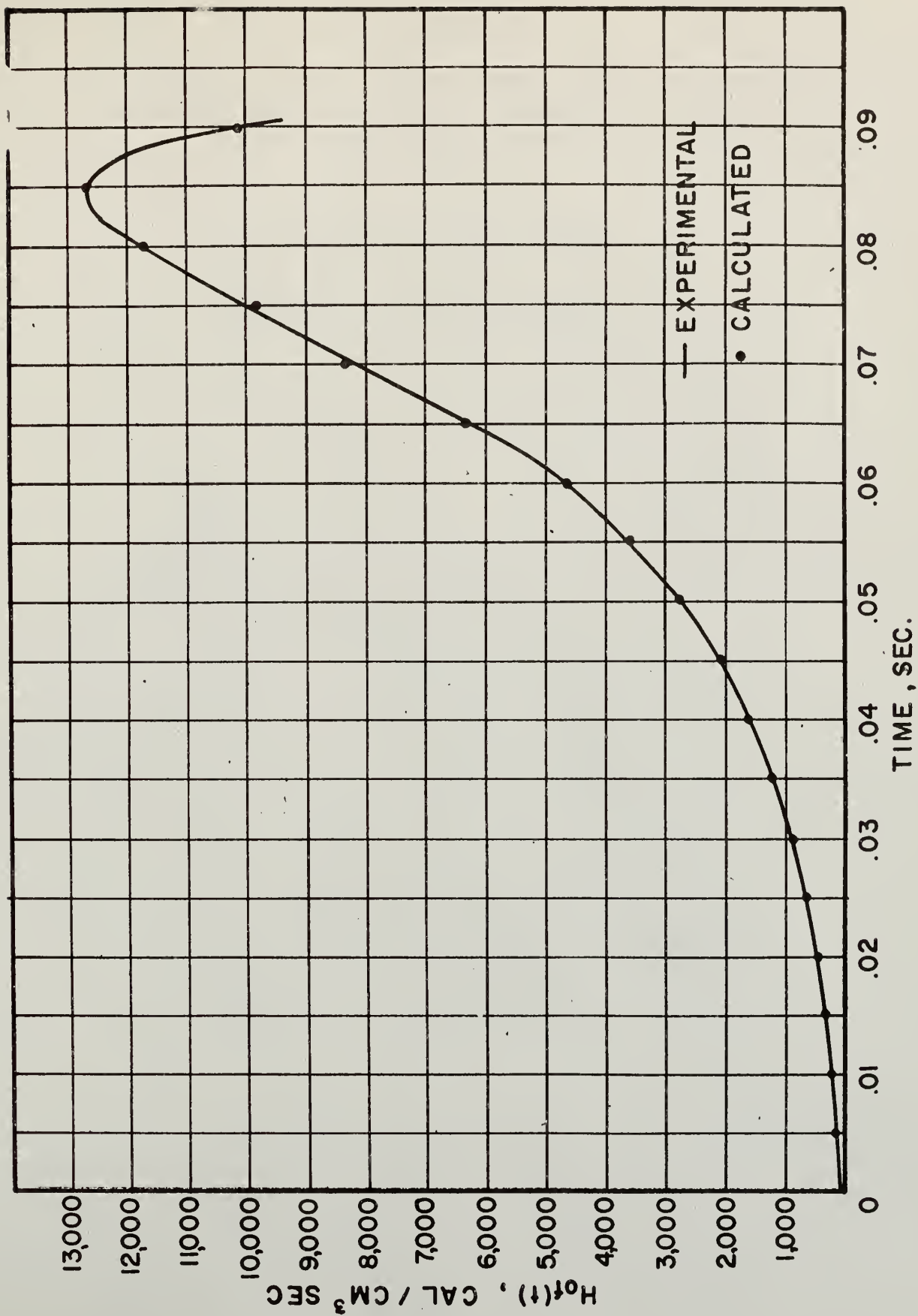


Figure 12. Interthal plate heat generation rate,  $H_{of}(t)$ , vs arbitrary time during a transient with an initial period of 15.8 msec.

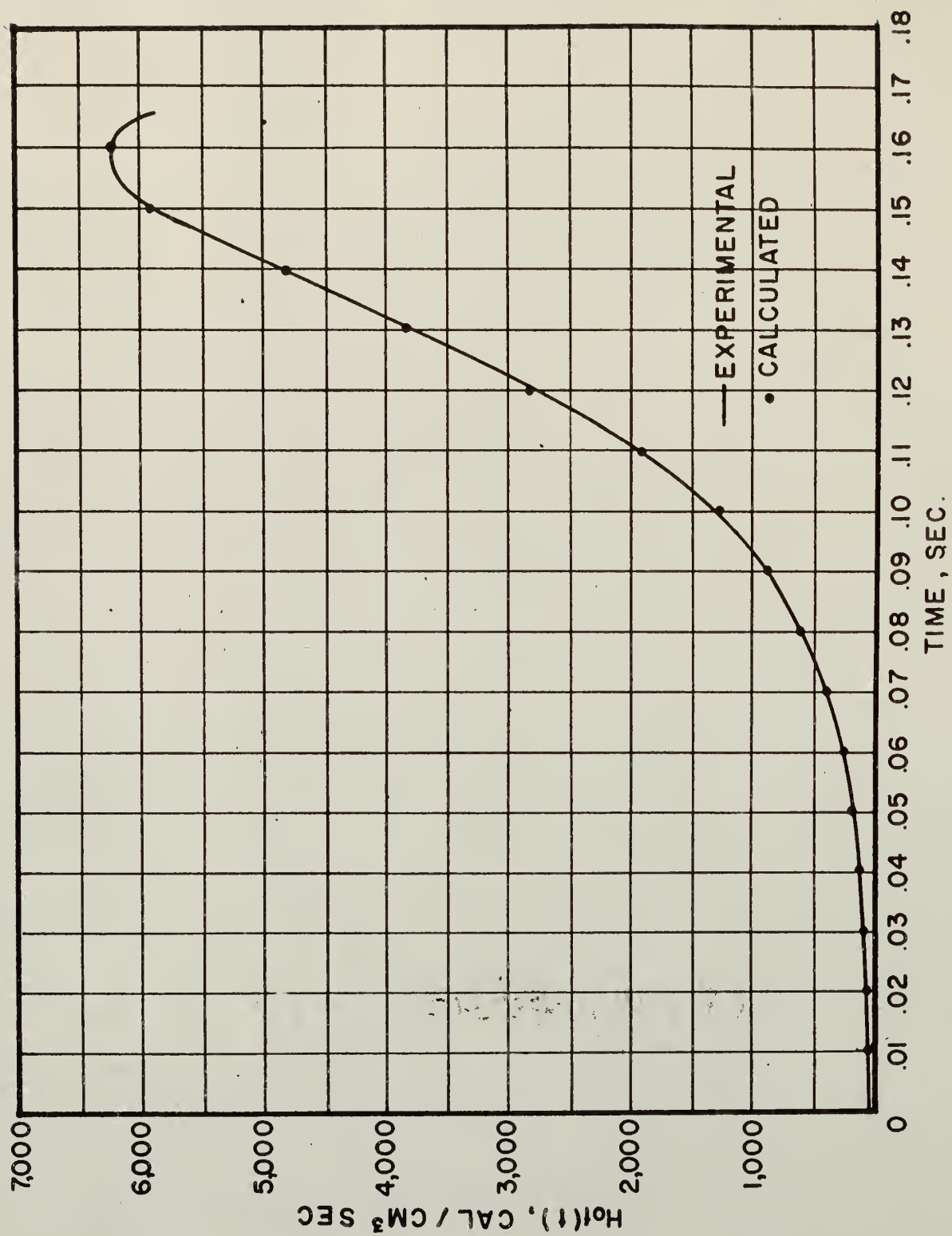


Figure 13. Internal plate heat generation rate,  $H_{0f}(t)$ , vs arbitrary time during a transient with an initial period of 23 msec.



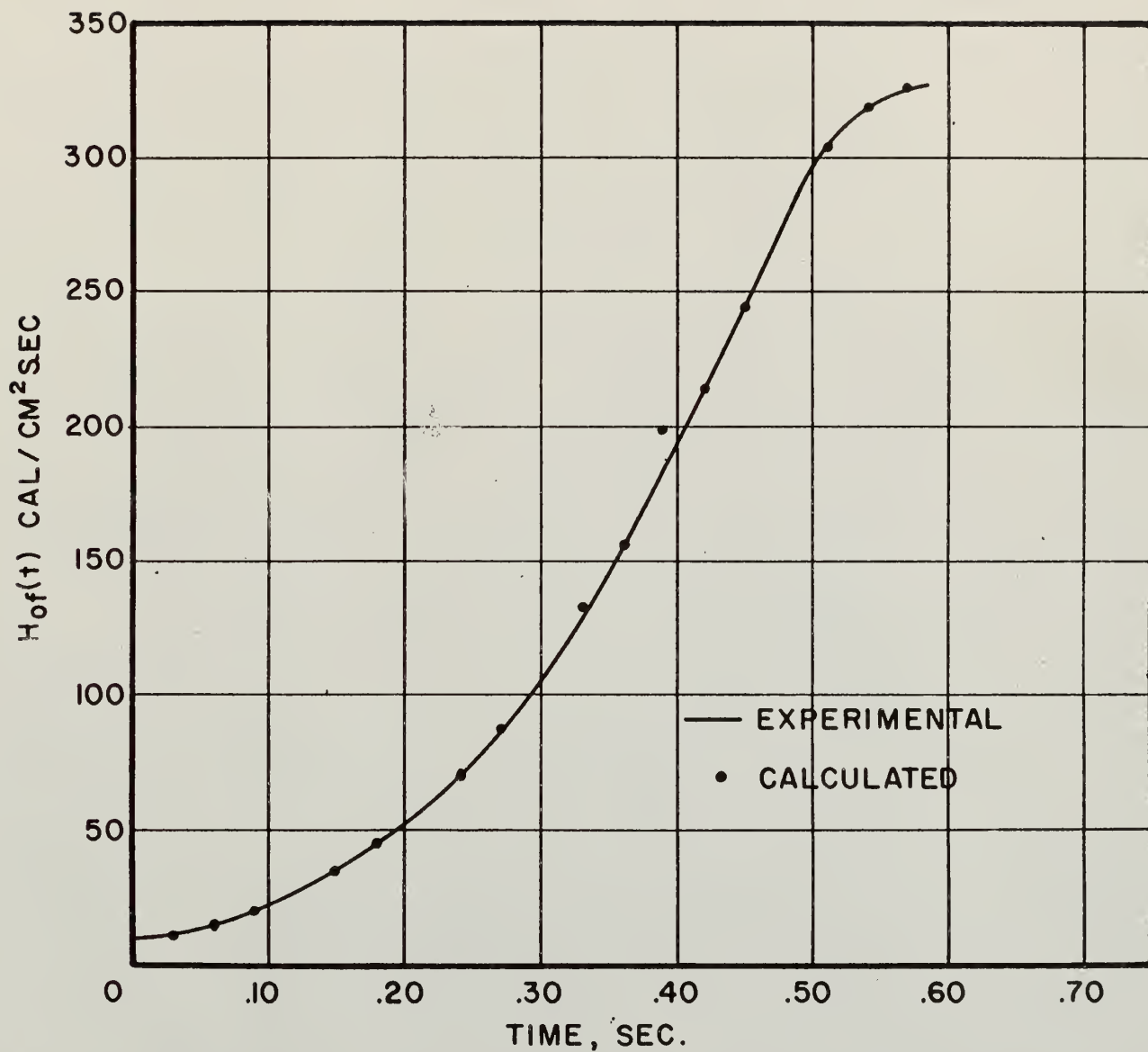


Figure 14. Internal plate heat generation rate,  $H_{of}(t)$ , vs arbitrary time during a transient with an initial period of 120 msec.

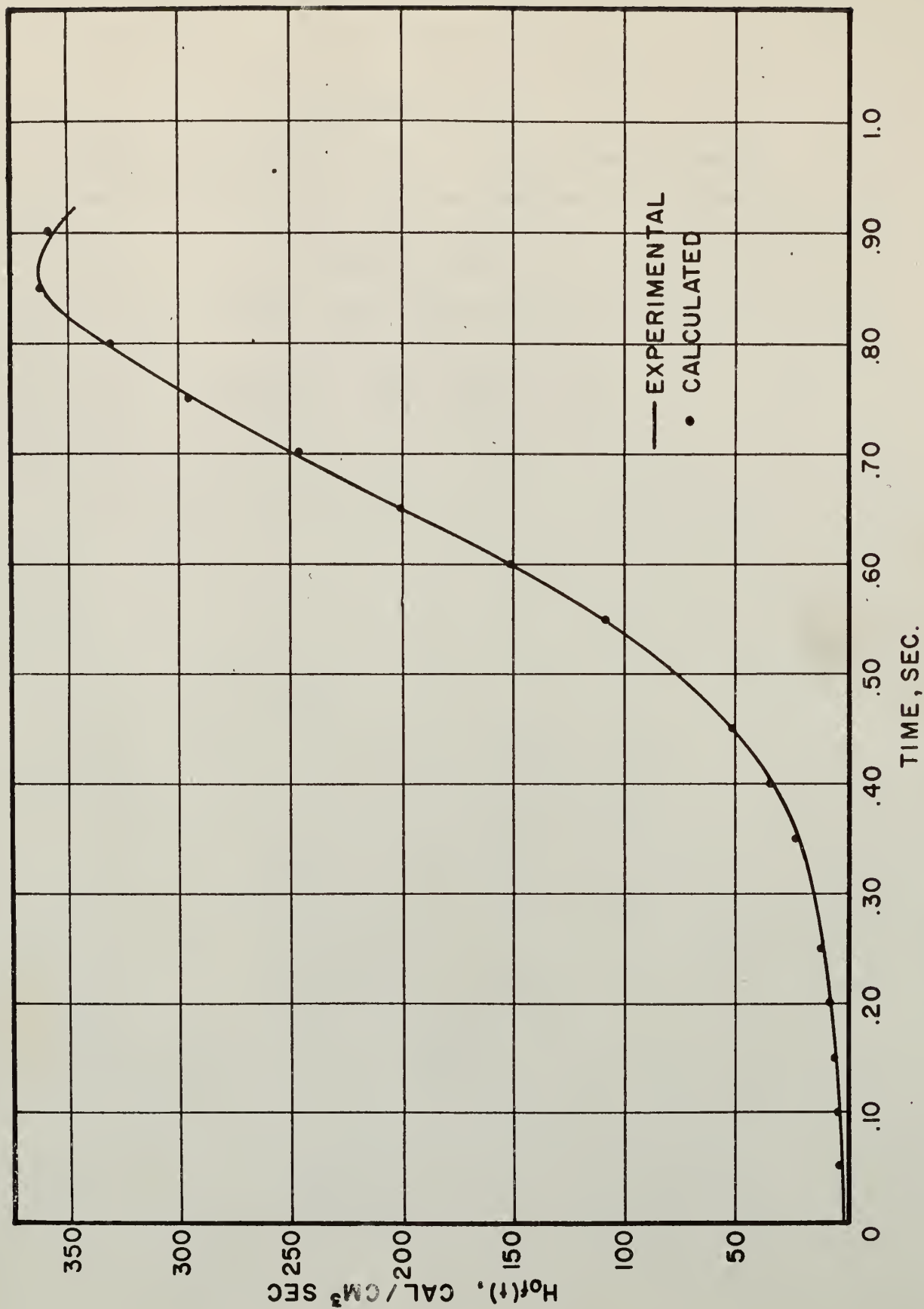


Figure 15. Internal plate heat generation rate,  $H_{of}(t)$ , vs arbitrary time during a transient with an initial period of 150 msec.

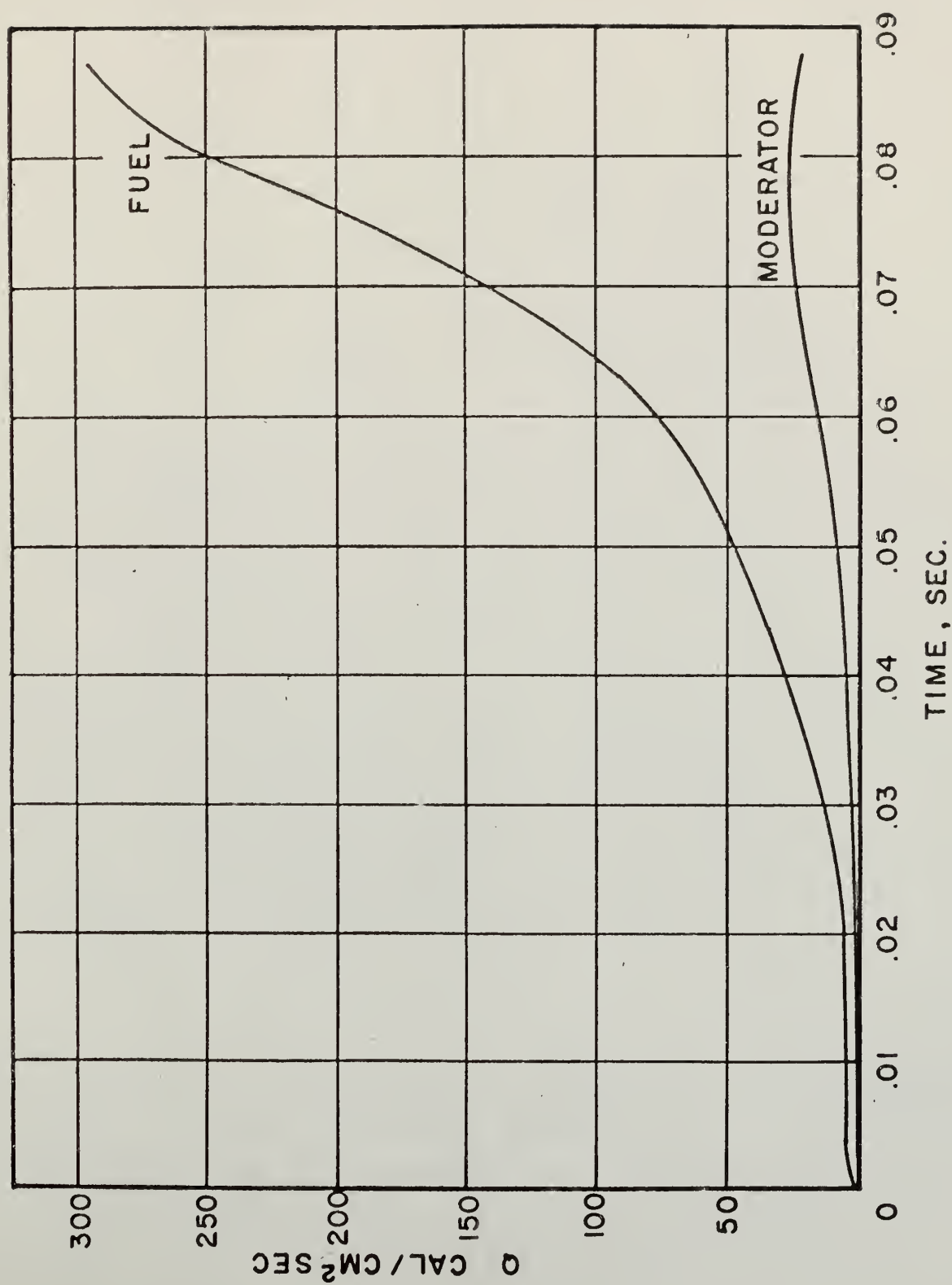


Figure 16. Comparison of  $Q$ , heat flow rates per unit area out of the fuel and into the moderator vs arbitrary time during a transient with an initial period of 15.8 msec.

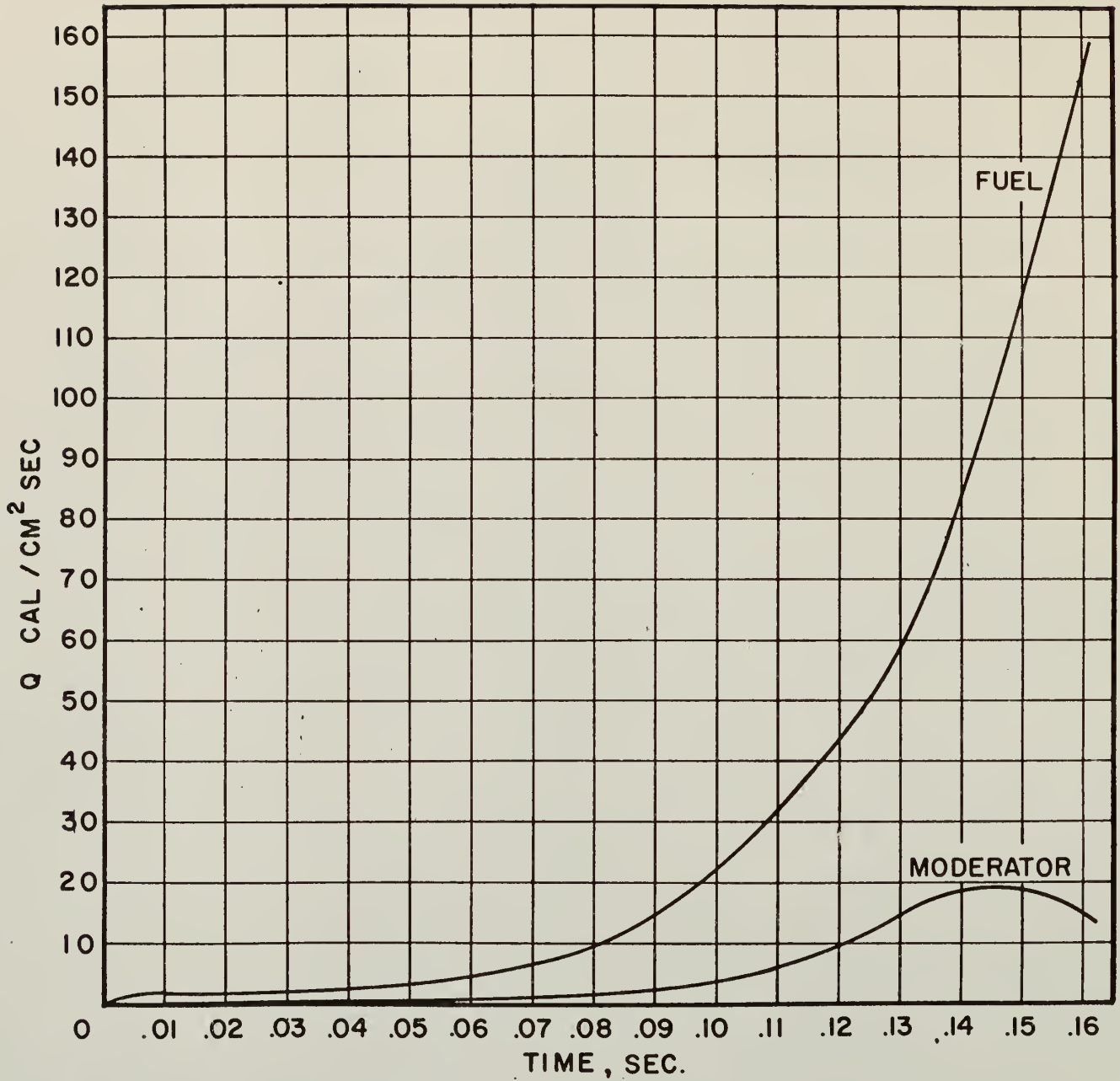


Figure 17. Comparison of,  $Q$ , heat flow rates per unit area out of the fuel and into the moderator vs arbitrary time during a transient with an initial period of 23 msec.

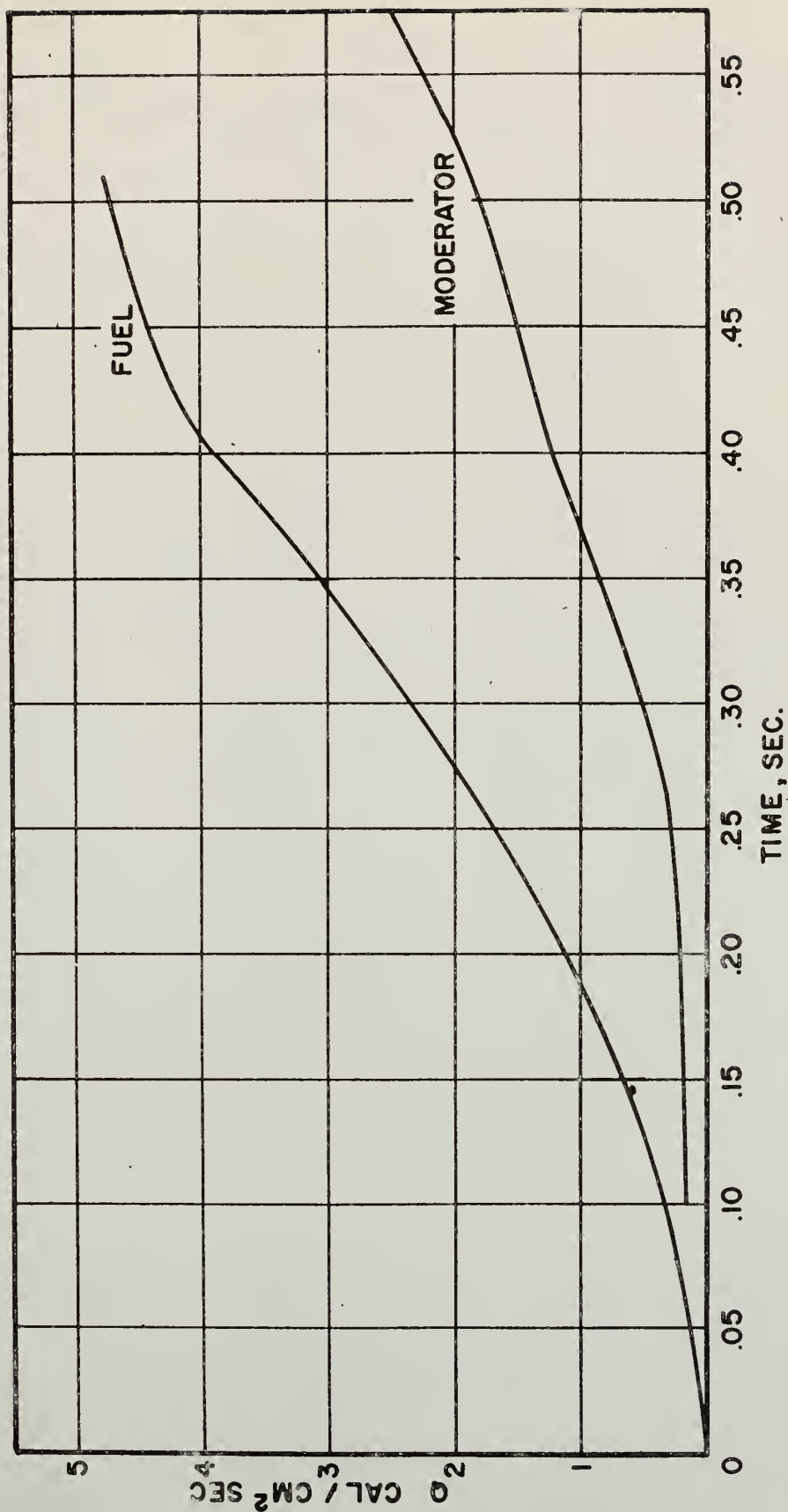


Figure 18. Comparison of  $Q$ , heat flow rates per unit area out of the fuel and into the moderator vs arbitrary time during a transient with an initial period of 120 msec.

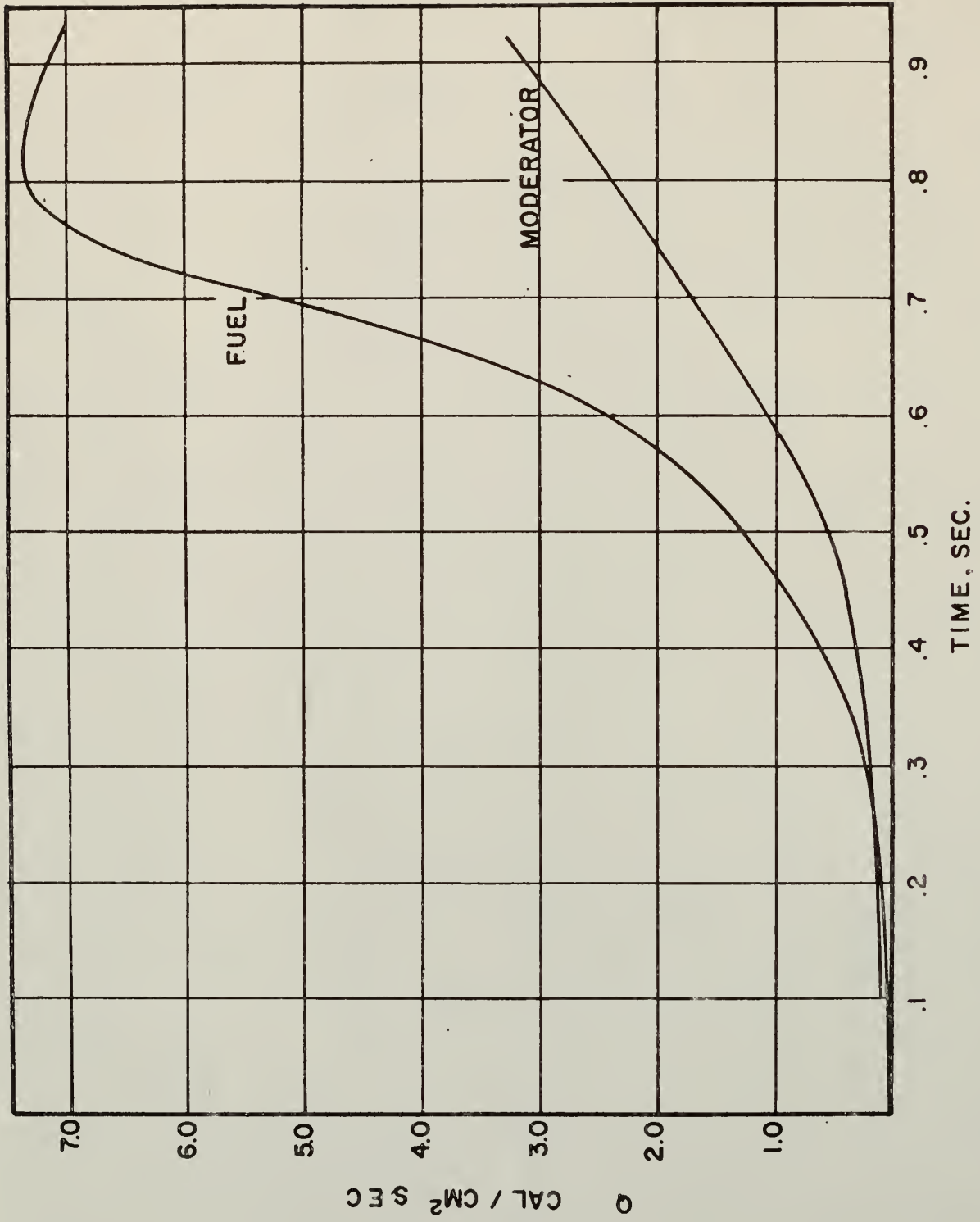


Figure 19. Comparison of  $Q$ , heat flow rates per unit area out of the fuel and into the moderator vs arbitrary time during a transient with an initial period of 150 msec.



Table 3. Numerical Values of Parameters for Empirical Fits of  $H_{of}(t)$  Used in Equations (15) and (16)

$\tau, \text{msec}$	$A_1$ $\lambda_1$	$A_2$ $\lambda_2$	$A_3$ $\lambda_3$	$A_4$ $\lambda_4$	$A_5$ $\lambda_5$
150	+1.912 7.426	-2.097 $\times 10^{-5}$ 21.090	+6.062 $\times 10^{-8}$ 27.260	---	---
120	9.218 9.204	-6.486 $\times 10^{-2}$ 20.233	+3.564 $\times 10^{-4}$ 30.093	-1.856 $\times 10^{-7}$ 42.208	+3.019 $\times 10^{-19}$ 85.147
23	2.414 $\times 10^1$ 39.761	-4.364 $\times 10^{-5}$ 124.03	9.563 $\times 10^{-10}$ 187.61	---	---
15.8	1.364 $\times 10^2$ 64.573	-2.993 104.11	---	---	---

Table 4. Average Temperature Rise in the Fuel and Moderator for  $\tau = 15.8$  msec.

$t, \text{sec.}$	$\bar{\theta}_{\text{fuel}}(t), ^\circ\text{C}$	$\bar{\theta}_{\text{mod}}(t), ^\circ\text{C}$	$(\bar{\theta}_{\text{fuel}} - \bar{\theta}_{\text{mod}}), ^\circ\text{C}$
.085	138.53	16.732	121.80
.080	127.34	13.99	113.35
0.075	110.34	10.81	99.53
.070	89.99	8.664	81.33
.060	50.12	4.87	45.25
.050	24.58	2.446	22.13
.040	13.91	1.333	12.58
.030	8.51	0.692	7.82
.020	3.52	.271	3.25
.010	1.039	.0767	.962

Table 5. Average Temperature Rise in the Fuel and Moderator for  $\tau = 23$  msec.

$t, \text{sec.}$	$\bar{\theta}_{\text{fuel}}(t), ^\circ\text{C}$	$\bar{\theta}_{\text{mod}}(t), ^\circ\text{C}$	$(\bar{\theta}_{\text{fuel}} - \bar{\theta}_{\text{mod}}), ^\circ\text{C}$
.16	117.76	16.832	100.93
.15	108.71	13.371	95.34
.14	86.92	9.764	77.16
.13	59.48	6.459	53.02
.12	36.58	4.218	32.35
.11	23.17	2.759	20.41
.10	16.28	1.869	15.21
.09	11.25	1.231	10.02
.05	3.13	.260	2.87

Table 6. Average Temperature Rise in the Fuel  
and Moderator for  $\tau = 120$  msec.

$t, \text{sec.}$	$\bar{\theta}_{\text{fuel}}(t), ^\circ\text{C}$	$\bar{\theta}_{\text{mod}}(t), ^\circ\text{C}$	$(\bar{\theta}_{\text{fuel}} - \bar{\theta}_{\text{mod}}), ^\circ\text{C}$
.59	32.66	8.572	24.09
.57	29.95	7.738	22.21
.55	27.33	6.935	20.39
.50	21.15	5.212	15.94
.45	16.40	3.834	12.57
.40	11.98	2.660	9.32
.35	7.84	1.744	6.10
.30	4.89	1.143	3.75
.20	2.59	.534	2.06
.10	1.17	.164	1.01

Table 7. Average Temperature Rise in the Fuel  
and Moderator for  $\tau = 150$  msec.

$t, \text{sec.}$	$\bar{\theta}_{\text{fuel}}(t), ^\circ\text{C}$	$\bar{\theta}_{\text{mod}}(t), ^\circ\text{C}$	$(\bar{\theta}_{\text{fuel}} - \bar{\theta}_{\text{mod}}), ^\circ\text{C}$
.90	44.46	12.994	31.47
.85	37.49	10.630	26.86
.80	30.87	8.510	22.36
.75	25.23	6.678	18.55
.70	20.31	5.111	15.20
.65	15.70	4.644	11.06
.60	11.48	2.750	8.73
.55	8.11	1.989	6.12
.50	4.86	1.472	4.39
.40	3.58	.834	2.75
.30	1.91	.431	1.48
.10	.602	.0652	.537

where  $\Delta k(o)$  is the initial reactivity insertion to start the transient and  $\Delta k(t)$  is the excess reactivity of the system at any time,  $t$ , are shown as a function of time in Tables 8 through 11. Tables 8 through 11 also show the components of the compensated reactivity due to the temperature coefficient  $\Delta k_T(t)$ , fuel plate expansion  $\Delta k_E(t)$  and steam formation,  $\Delta k_s(t)$ . The excess reactivity  $\Delta k(t)$  for two of the transients,  $\tau$  equals 120 and 150 msec respectively, is compared with equivalent data obtained from a kinetic analysis of the power burst shapes by Miller (34) in Figures 20 and 21. The reactivity compensation at peak power, is shown along with comparable data from the kinetic analysis in Figure 22. Figure 22 also includes the components of the reactivity compensations for a model suggested by S. G. Forbes (15) as well as for the model suggested in this report.

### 3.3 Conclusions

The forms of all of the solutions shown in equations (9) through (16) are such that three terms are developed. The first term represents the steady state solution resulting from the surface temperature boundary condition. The second term includes the transient portion of both the surface temperature boundary condition and the forcing function, the heat generation rate. The final term represents the steady state or equilibrium solution resulting from the forcing function. It has been common in several previous works (27,36) to assume that the temperature is separable in space and time. It can be seen from the derived solutions that this will be a good approximation of the temperature distribution only when the second term, the transient solution, has died out. The

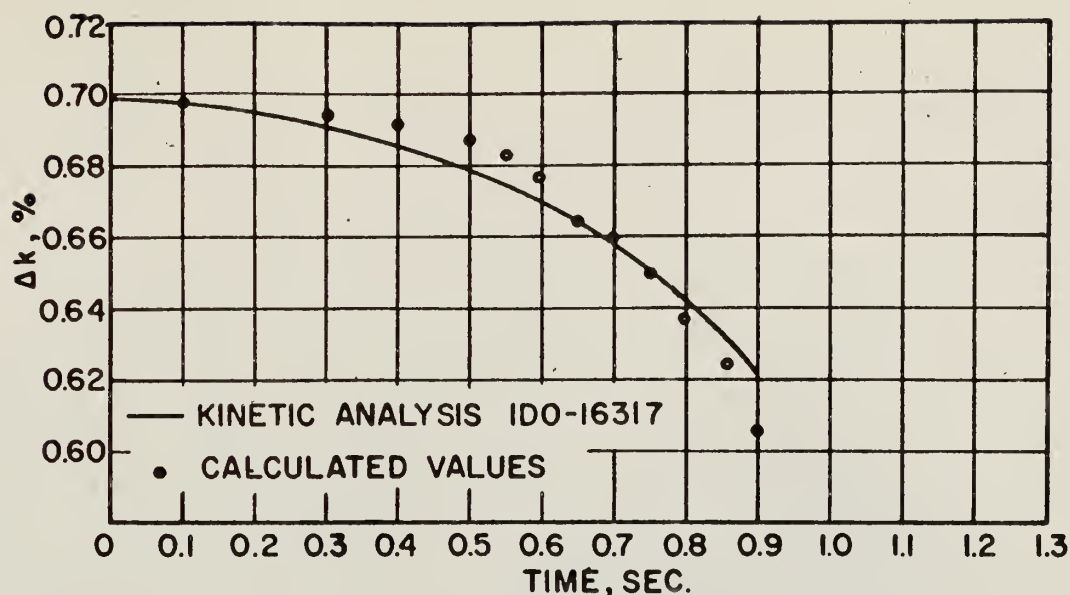


Figure 20. Comparison of calculated percent excess reactivities,  $\Delta k$ , and those obtained by kinetic analysis vs arbitrary time during a transient with an initial period of 120 msec.

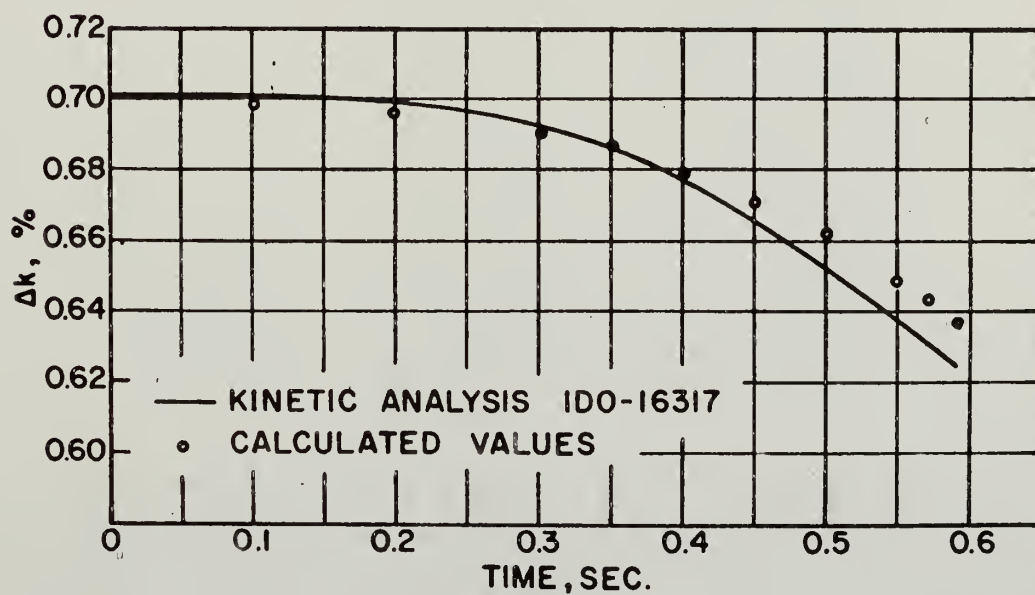


Figure 21. Comparison of calculated percent excess reactivities,  $\Delta k$ , and those obtained by kinetic analysis vs arbitrary time during a transient with an initial period of 150 msec.

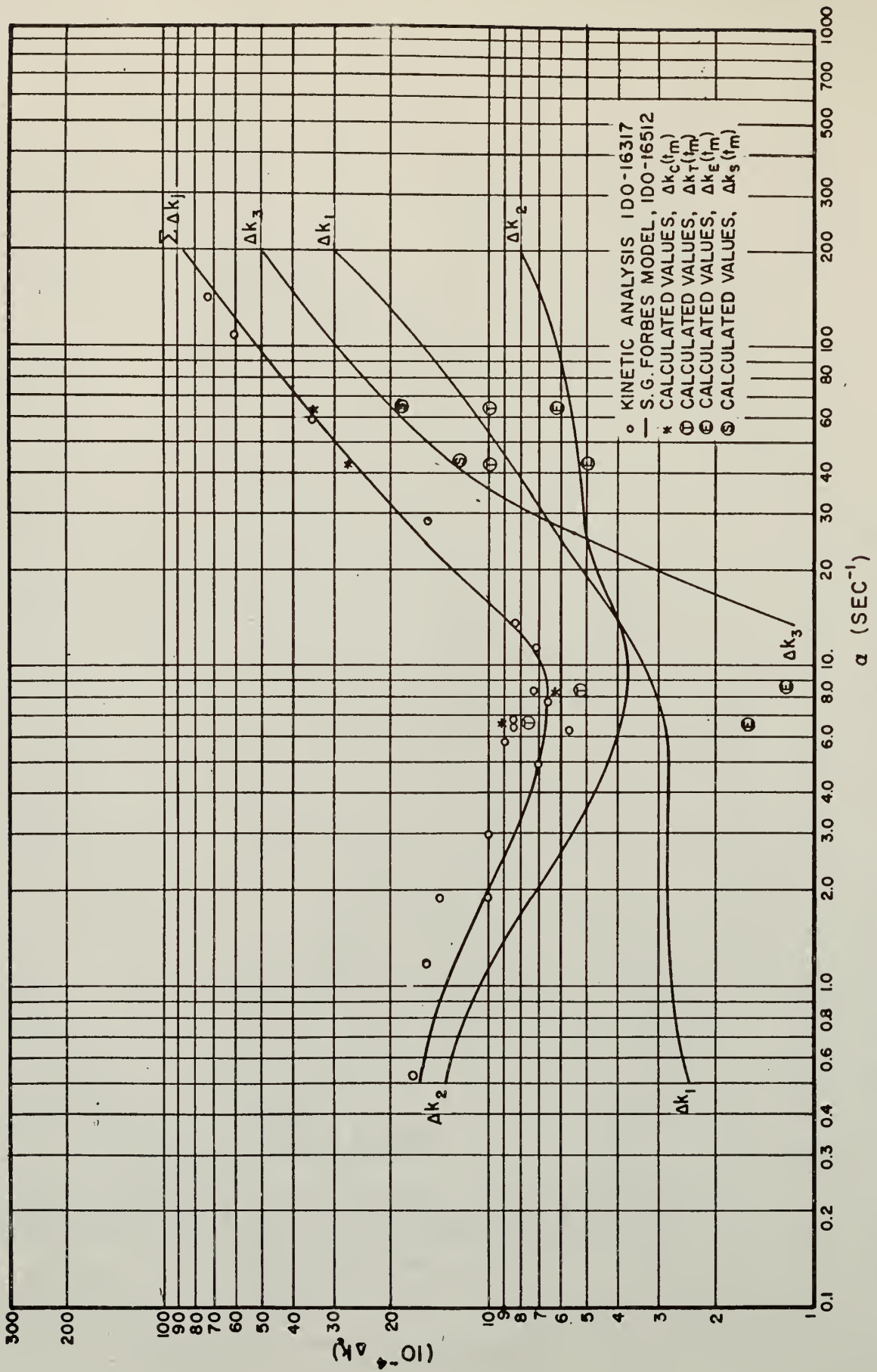


Figure 22. Peak power compensated reactivities,  $\Delta k_c$ , vs reciprocal period,  $\alpha$ .



Table 8. Compensated Reactivities for  
 $\tau = 15.8$  msec Run

t, sec	$\Delta k_T(t)$	$\Delta k_E(t)$	$\Delta k_S(t)$	$\Delta k_C(t)$
0.084	$0.979 \times 10^{-3}$	$0.609 \times 10^{-3}$	$1.86 \times 10^{-3}$	$3.45 \times 10^{-3}$
0.080	$0.818 \times 10^{-3}$	$0.546 \times 10^{-3}$	$1.21 \times 10^{-3}$	$2.60 \times 10^{-3}$
0.075	$0.632 \times 10^{-3}$	$0.498 \times 10^{-3}$	$0.46 \times 10^{-3}$	$1.59 \times 10^{-3}$
0.070	$0.684 \times 10^{-3}$	$0.407 \times 10^{-3}$	$0.13 \times 10^{-3}$	$1.22 \times 10^{-3}$
0.060	$0.285 \times 10^{-3}$	$0.226 \times 10^{-3}$	0.0	$0.51 \times 10^{-3}$
0.050	$0.143 \times 10^{-3}$	$0.111 \times 10^{-3}$	0.0	$0.25 \times 10^{-3}$
0.040	$0.078 \times 10^{-3}$	$0.063 \times 10^{-3}$	0.0	$0.14 \times 10^{-3}$
0.030	$0.050 \times 10^{-3}$	$0.039 \times 10^{-3}$	0.0	$0.08 \times 10^{-3}$
0.020	$0.016 \times 10^{-3}$	$0.016 \times 10^{-3}$	0.0	$0.03 \times 10^{-3}$
0.010	$0.004 \times 10^{-3}$	$0.005 \times 10^{-3}$	0.0	$0.01 \times 10^{-3}$

Table 9. Compensated Reactivities for  
 $\tau = 23$  msec Run

t, sec	$\Delta k_T(t)$	$\Delta k_E(t)$	$\Delta k_S(t)$	$\Delta k_C(t)$
0.16	$0.985 \times 10^{-3}$	$0.505 \times 10^{-3}$	$1.21 \times 10^{-3}$	$2.70 \times 10^{-3}$
0.15	$0.782 \times 10^{-3}$	$0.468 \times 10^{-3}$	$0.54 \times 10^{-3}$	$1.79 \times 10^{-3}$
0.14	$0.571 \times 10^{-3}$	$0.386 \times 10^{-3}$	$0.003 \times 10^{-3}$	$0.96 \times 10^{-3}$
0.13	$0.378 \times 10^{-3}$	$0.265 \times 10^{-3}$	0.0	$0.64 \times 10^{-3}$
0.12	$0.247 \times 10^{-3}$	$0.162 \times 10^{-3}$	0.0	$0.41 \times 10^{-3}$
0.11	$0.161 \times 10^{-3}$	$0.102 \times 10^{-3}$	0.0	$0.26 \times 10^{-3}$
0.10	$0.109 \times 10^{-3}$	$0.076 \times 10^{-3}$	0.0	$0.18 \times 10^{-3}$
0.09 "	$0.072 \times 10^{-3}$	$0.050 \times 10^{-3}$	0.0	$0.12 \times 10^{-3}$
0.05	$0.015 \times 10^{-3}$	$0.014 \times 10^{-3}$	0.0	$0.03 \times 10^{-3}$

Table 10. Compensated Reactivities for  
 $\tau = 120$  msec Run

t, sec	$\Delta k_T(t)$	$\Delta k_E(t)$	$\Delta k_S(t)$	$\Delta k_C(t)$
0.59	$0.501 \times 10^{-3}$	$0.120 \times 10^{-3}$	0.0	$0.621 \times 10^{-3}$
0.57	$0.453 \times 10^{-3}$	$0.111 \times 10^{-3}$	0.0	$0.564 \times 10^{-3}$
0.55	$0.406 \times 10^{-3}$	$0.100 \times 10^{-3}$	0.0	$0.506 \times 10^{-3}$
0.50	$0.305 \times 10^{-3}$	$0.080 \times 10^{-3}$	0.0	$0.385 \times 10^{-3}$
0.45	$0.224 \times 10^{-3}$	$0.063 \times 10^{-3}$	0.0	$0.287 \times 10^{-3}$
0.40	$0.156 \times 10^{-3}$	$0.047 \times 10^{-3}$	0.0	$0.203 \times 10^{-3}$
0.35	$0.102 \times 10^{-3}$	$0.030 \times 10^{-3}$	0.0	$0.132 \times 10^{-3}$
0.30	$0.067 \times 10^{-3}$	$0.019 \times 10^{-3}$	0.0	$0.086 \times 10^{-3}$
0.20	$0.031 \times 10^{-3}$	$0.010 \times 10^{-3}$	0.0	$0.041 \times 10^{-3}$
0.10	$0.010 \times 10^{-3}$	$0.005 \times 10^{-3}$	0.0	$0.015 \times 10^{-3}$

Table 11. Compensated Reactivities for  
 $\tau = 150$  msec Run

t, sec	$\Delta k_T(t)$	$\Delta k_E(t)$	$\Delta k_S(t)$	$\Delta k_C(t)$
0.90	$0.760 \times 10^{-3}$	$0.157 \times 10^{-3}$	0.0	$0.915 \times 10^{-3}$
0.85	$0.622 \times 10^{-3}$	$0.134 \times 10^{-3}$	0.0	$0.756 \times 10^{-3}$
0.80	$0.498 \times 10^{-3}$	$0.112 \times 10^{-3}$	0.0	$0.610 \times 10^{-3}$
0.75	$0.391 \times 10^{-3}$	$0.093 \times 10^{-3}$	0.0	$0.484 \times 10^{-3}$
0.70	$0.299 \times 10^{-3}$	$0.076 \times 10^{-3}$	0.0	$0.375 \times 10^{-3}$
0.65	$0.272 \times 10^{-3}$	$0.055 \times 10^{-3}$	0.0	$0.327 \times 10^{-3}$
0.60	$0.161 \times 10^{-3}$	$0.044 \times 10^{-3}$	0.0	$0.205 \times 10^{-3}$
0.55	$0.116 \times 10^{-3}$	$0.031 \times 10^{-3}$	0.0	$0.147 \times 10^{-3}$
0.50	$0.086 \times 10^{-3}$	$0.022 \times 10^{-3}$	0.0	$0.108 \times 10^{-3}$
0.40	$0.049 \times 10^{-3}$	$0.014 \times 10^{-3}$	0.0	$0.063 \times 10^{-3}$
0.30	$0.025 \times 10^{-3}$	$0.007 \times 10^{-3}$	0.0	$0.032 \times 10^{-3}$
0.10	$0.004 \times 10^{-3}$	$0.003 \times 10^{-3}$	0.0	$0.007 \times 10^{-3}$

numerical results obtained from evaluating the set of equations (9) and (10) and the set of equations (15) and (16) show that the transient term is negligible for all times of interest in the fuel region but it makes a significant contribution for all times of interest in the moderator.

In one sense it would be more informative to investigate the reactor burst behavior using the minimum of input data (i.e. the physical dimensions and the initial reactivity insertion) and test for corroboration of all of the experimentally measured variables. However, it seemed better in analyzing for the shutdown mechanisms to use as much of the data as possible leaving only the compensated reactivities as a check on the validity of the model. The compensated reactivity was established as a criterion because of its extreme sensitivity to the state of the system and because of its direct influence on the safety of nuclear reactors.

The results of this work are two-fold. First, a more accurate view of distribution of the energy during a transient burst is presented and second, a model based on the energy distribution was shown to predict the reactivity effects as well as any of the existing models. The advantage of this model is that assuming the fractional energy associated with void formation can be determined as the mechanism of transient boiling becomes better understood, the final empiricism can be removed from the model.

### 3.4 Further Investigation

There are several avenues of attack for further work in determining the inherent shutdown mechanisms. First, additional data on Spert I-A should be tested on the model proposed in this report to make certain that it is as capable of determining reactivity effects as these preliminary runs indicate. Second, application of this model to any new system

will mean that the surface temperatures and power traces would not be available. This problem can be circumvented by studying the two region conduction problem subject only to the heat generation rate forcing function. The heat generation rate can be calculated from the initial reactivity insertion, allowing a feedback from the induced negative reactivity to the heat generation rate through the reactor kinetics equations. This suggests an analog solution or possibly a digital analog combination. Third, application of the heat transfer equations developed in this report should be used to determine the mode of heat transfer during transient operation by investigating a single plate in as much detail as possible. The application of this study can probably be done more simply using electrical heating. Fourth, a detailed study of nucleate boiling at low heat fluxes is necessary before complete understanding of the mechanisms of shutdown can be obtained. This study should provide a direct measurement of the fraction of the energy used to produce steam,  $f_g$ . Fifth, work on this model should be extended to investigate further available evidence on other Spert reactors to see if it will account for changes in other parameters such as neutron lifetime, pressure and coolant flow. Finally, experimental and analytical work should be done on the zirconium hydride moderated Triga systems since qualitatively they show the greatest inherent safety that has been demonstrated to date.

## ACKNOWLEDGEMENT

The author wishes to express his gratitude to Dr. W. R. Kimel and Dr. J. O. Mingle under whose direction this work has been done. In addition, I wish to extend sincerest thanks to Dr. C. A. Halijak and Professor R. C. Baillie for their efforts in the most difficult phases of this work. Sincere appreciation is given to the Kansas State University Engineering Experiment Station, the Department of Nuclear Engineering and the National Science Foundation for their financial support of this research.

## LITERATURE CITED

1. Arpaci, V. S. and Clark, J. A.  
Dynamic Response of Heat Exchangers Having Internal Heat Sources. J. Heat Transfer, 81, 253-66 (1959).
2. Bright, G. O. et. al.  
An Elementary Model for Reactor Burst Behavior. IDO-16393 (August 1957).
3. Bonilla, C. F.  
Nuclear Engineering. McGraw-Hill (1957).
4. Chernick, J.  
BNL-173 (T-30) (1951).
5. Clark, E. T.  
Analysis of Initial Shutdown in SPERT-I. NYO-4726 (1956).
6. Clark, E. T.  
Initial Shutoff in a SPERT Type Reactor Transient. Paper presented at the June 1957 meeting of the American Nuclear Society.
7. Deitrich, J. R. and Layman, D. C.  
Transients and Steady State Characteristics of a Boiling Reactor The BORAX Experiments. AECD-3840 (1953).
8. Deitrich, J. R.  
Experimental Investigations of the Self-limitation of Power During Reactivity Transients in a Subcooled, Water-moderated Reactor. AECD-3688 (1954).
9. Deverall, L. I. and Griffing, G. W.  
Kinetic Studies on the SPERT-I Reactor, II, On the Initial Shutdown of the SPERT-I Reactor for Periods Greater Than Fifty Milliseconds. IDO-16404 (December 1957).
10. Deverall, L. I. and Griffing, G. W.  
Kinetic Studies on the SPERT-I Reactor, I, Initial Behavior by the Energy Model. IDO-16397 (April 1958).
11. Epel, L. G.  
Transient Temperatures in Infinite Plates, Infinite Cylinders and Spheres Following a Simultaneous Step Change in Internal Heat Generation Rate, Coolant Temperature and Heat Transfer Coefficient. ORNL-2597 (1958).
12. Ermakov, V. S. and Ivanov, V.  
Investigations of Non-Uniform Heat Transfer in Nuclear Reactor Heat Releasing Elements. Inzhener, Fiz. Zhur., Akad, Nauk Belorus. S.S.R., 1, No. 12, 960112 (1958).



13. Forbes, S. G.  
Quarterly Progress Report. IDO-16452, p. 38 (September 1958).
14. Forbes, S. G.  
Conduction Boiling Model - Quarterly Progress Report. IDO-16489, pp. 71-88 (January 1959).
15. Forbes, S. G.  
Calculation of Thermal Shutdown Effects in SPERT I-A. Quarterly Progress Report. IDO-16512 (May 1959).
16. Forbes, S. G., et. al.  
Analysis of Self-Shutdown Behavior in the SPERT-I Reactor. IDO-16528 (July 1959).
17. Foulke, L. R.  
K.S.U. Pile Standardization and Study of Slowing Down and Diffusion Models. Kansas Engineering Experiment Station Special Report Number 8, (1961).
18. French, P.  
Analytical Treatment of Transient Heat Conduction During Reactor Power Excursions - Quarterly Progress Report. IDO-16512 (May 1959).
19. French, P.  
Insulated Core Experiment - Quarterly Progress Report. IDO-16539 (November 1959).
20. French, P. and Forbes, S. G.  
Preliminary Moderator Expulsion Experiments. IDO-16539 (November 1959).
21. Fuchs, Klaus  
Efficiency for Very Slow Assembly. LA-596 (August 1946).
22. Glasstone, S. and Edlund, M. C.  
Elements of Nuclear Reactor Theory. Van Nostrand (1952).
23. Graham, R. H. and Boyer, D. G.  
AEC Steps Up Reactor Safety Experiments. Nucleonics. Vol. 14, No. 3, (1956).
24. Greenspan, H.  
Argonne Quarterly Report for September - November 1952. ANL-4951 (1952).
25. Haire, J. C.  
Subcooled Transient Tests in the SPERT-I Reactor - Experimental Data. IDO-16343 (July 1958).

26. Horning, W. A.  
Theory of Power Transient in the SPERT-I Reactor. IDO-16434  
(January 1958).
27. Iriarte, M., Jr.  
An Accurate Transfer Function for the Dynamic Analysis of  
Temperature and Heat Release in Cylindrical Fuel Elements. Nuclear  
Science and Engineering. 7 26-32 (1960).
28. Kaminsky, S.  
Study of Nucleation and Bubble Dynamics to Evaluate Void  
Shutdown Mechanism in a Heterogeneous Water Moderated Reactor.  
KLX-1809 (May 1959).
29. Kattwinkel, Willy  
The Question of the Temperature Distribution in a Bare Cylindrical  
Fuel Element of Great Length in the Non-steady State Heating  
Up. Atomkern-Energie, 3, 342-5 (1958).
30. Kirchenmayer, A.  
The Transient Behavior of the Heat Transfer from Fuel Elements to  
a Coolant of Constant (Boiling) Temperature in a One Dimensional  
Heat Flux. Atomkern-Energie, 3, 337-41 (1958).
31. Margulies, R. S.  
GNL-200 (T-47) (1954).
32. McMurray, W. L.  
Temperature Distribution in a Fuel Plate with Exponentially  
Rising Power. IDO-16214 (March 1955).
33. Mickley, H. S., Sherwood, T. K. and Reed, C. E.  
Applied Mathematics in Chemical Engineering. McGraw-Hill (1957).
34. Miller, R. W.  
Calculations of Reactivity Behavior During SPERT-I Transients.  
IDO-16317, (June 1957).
35. Miller, R. W.  
The "Clipped Exponential" Power Burst Model - Quarterly Progress  
Report. IDO-16489, pp. 88-96 (January 1959).
36. Miller, R. W.  
Photographic Investigations of Reactor Shutdown Mechanisms.  
IDO-16584 (April 1960).
37. Murray, Raymond L.  
Nuclear Reactor Physics. Prentice-Hall (1957).
38. Nicholson, R. B.  
The Doppler Effect in Fast Neutron Reactors. APDA-139 (1960).

39. Nyer, W. E. et. al.  
Experimental Investigations of Reactor Transients. IDO-16285  
(1956).
40. Stein, R. P.  
Transient Heat Transfer in Reactor Coolant Channels. AECU-3600  
(1957).
41. Technical Foundations of TRIGA. General Atomic, Division of General  
Dynamic GA-471 (1958).
42. Walker, R.  
An Investigation of the Poison Model for Reactor Self-Shutdown -  
Quarterly Progress Report. IDO-16489, p. 960110 (January 1959).
43. Wilson, T. R.  
An Engineering Description of the SPERT-I Reactor Facility.  
IDO-16318.
44. Wylie, C. R., Jr.  
Advanced Engineering Mathematics. McGraw-Hill (1960).

## APPENDICES

## APPENDIX A

Derivations of Solutions for the  
Temperature Distribution in the  
Fuel and Moderator of a Unit Cell

The differential equations governing the time dependent temperature distribution in the fuel and moderator are

$$\nabla^2 \theta_f(x, t) + \sum_{j=1}^s \frac{q_{\infty} \cosh(\kappa x) a_j e^{\lambda_j t}}{k} = \frac{1}{\alpha} \frac{\partial \theta_f(x, t)}{\partial t} \quad (A-1)$$

and

$$\nabla^2 \theta_m(x, t) + \sum_{j=1}^s \frac{F A_j e^{\lambda_j t}}{k} = \frac{1}{\alpha} \frac{\partial \theta_m(x, t)}{\partial t} \quad (A-2)$$

The differential equations, (A-1) and (A-2), are most easily solved by use of Laplace transforms. Considering the fuel region first and transforming the time variable in equation (1) yields

$$\nabla^2 \Phi_f(x, S) + \sum_{j=1}^s \frac{q_{\infty} \cosh(\kappa x) A_j}{k (S - \lambda_j)} = \frac{1}{\alpha} [S \Phi_f(x, S) - \theta(x, 0)]. \quad (A-3)$$

$\Phi(x, S)$  is the transform of  $\theta(x, t)$ , and  $\theta(x, 0)$  is the initial temperature distribution. Assuming the initial temperature distribution to be flat, the equation can be normalized by letting  $\theta(x, 0)$  equal zero. Thus  $\theta(x, t)$  is the temperature excess in the fuel over the initial temperature. The initially flat temperature distribution in the fuel is unreal but it is a good approximation if the transients are started from low power levels.

Letting  $\theta(x, 0) = 0$  and rearranging the terms in equation (A-3) yields

$$\nabla^2 \Phi_f(x, S) - \frac{S}{\alpha} \Phi_f(x, S) = - \sum_{j=1}^s \frac{q_{\infty} \cosh(\kappa x) A_j}{k (S - \lambda_j)} \quad (A-4)$$

The usual one-dimensional slab assumption is made and  $\nabla^2$  becomes  $\frac{\partial^2}{\partial x^2}$ . This assumption neglects the axial flow of heat in the fuel compared to the radial. While this might be the limiting assumption in the analysis, it is probably not seriously in error.

The homogeneous solution to the one dimensional form of equation (A-4) is well known and is derived in many standard texts. This solution is

$$\Phi_{fh}(x, S) = A \cosh \sqrt{\frac{S}{\alpha}} x + B \sinh \sqrt{\frac{S}{\alpha}} x \quad (A-5)$$

The particular solution is found by the method of undetermined coefficients and is

$$\Phi_{fp}(x, S) = \sum_{j=1}^s \frac{q_{oo} \alpha A_j \cosh \kappa x}{k(S - \lambda_j)(S - \alpha \kappa_j^2)} \quad (A-6)$$

Therefore,

$$\Phi_{fp}(x, S) = A \cosh \sqrt{\frac{S}{\alpha}} x + B \sinh \sqrt{\frac{S}{\alpha}} x + \sum_{j=1}^s \frac{q_{oo} \alpha A_j \cosh(\kappa x)}{k(S - \lambda_j)(S - \alpha \kappa_j^2)} \quad (A-7)$$

The boundary conditions used to determine the constants A and B are as follows. First, the temperature gradient in the center of the region ( $x = 0$ ) is zero for all time. Second, the surface temperature is matched with the experimental data. The surface temperature is expressed as a sum of exponentials,  $\sum_{i=1}^p B_i e^{\beta_i t}$  or a Fourier series,  $\sum_{i=1}^p B_i \cos \beta_i t$ . First consider the solution in which the exponential boundary condition is used.

The transformed boundary conditions are



$$\mathcal{L} \left\{ \frac{\partial \theta_f(x,t)}{\partial x} \right\}_{x=0} = \mathcal{L} \{0\} \quad \text{or} \quad \frac{d\Phi_f(x,S)}{dx} = 0 \quad \text{at } x=0 \quad (\text{A-8})$$

and

$$\mathcal{L} \left\{ \theta_f(L,t) \right\} = \mathcal{L} \left\{ \sum_{i=1}^p B_i e^{\beta_i t} \right\} \quad \text{or} \quad \Phi_f(L,S) = \sum_{i=1}^p \frac{B_i}{(S-\beta_i)} \quad (\text{A-9})$$

Applying equation (A-8) to equation (A-7) shows that  $B$  must equal zero.  $A$  is determined by evaluating equation (A-9). The solution in the transform domain is shown in equation (A-10).

$$\Phi_f(x,S) = \sum_{i=1}^p \frac{B_i \cosh \sqrt{\frac{S}{\alpha}} x}{(S-\beta_i) \cosh \sqrt{\frac{S}{\alpha}} L} - \sum_{j=1}^s \frac{q_{\infty} \alpha A_j}{k(S-\lambda_j)(S-\alpha \kappa^2)} \left\{ \cosh(\kappa x) - \frac{\cosh(\kappa L) \cosh \sqrt{\frac{S}{\alpha}} x}{\cosh \sqrt{\frac{S}{\alpha}} L} \right\} \quad (\text{A-10})$$

Transforming equation (A-10) back into the time domain is greatly simplified since no poles of order greater than one occur in the inversion integral. It is interesting to note that it is the occurrence of higher order poles which complicates the solution to the multiple region problem. Equation (A-11), shown below, (33) can be used to invert transformed functions of the form  $\bar{f}(s) = j(s) / \lambda(s)$  if the degree of  $\lambda(s)$  is at least one greater than  $j(s)$  and only poles of order one occur,

$$\mathcal{L}^{-1} \{ \bar{f}(s) \} = \sum_{n=1}^m \frac{j(\rho_n)}{\lambda'(\rho_n)} e^{\rho_n t} \quad (\text{A-11})$$

$\rho_n$  denotes the  $n$  simple poles of  $\bar{f}(S)$  and  $\ell^{(0)}_n$  denotes the value of  $\frac{d\ell(S)}{dS}$  evaluated at  $S = \rho_n$ .

The inversion of equation (A-10) is shown in detail below. First consider the third term of equation (A-10).

$$\mathcal{L}^{-1} \left\{ \sum_{j=1}^S \frac{q_{\infty} \alpha \cosh \kappa L A_j \cosh \sqrt{\frac{S}{\alpha}} x}{k(S - \lambda_j)(S - \alpha \kappa^2) \cosh \sqrt{\frac{S}{\alpha}} L} \right\} = \sum_{j=1}^S \frac{q_{\infty} \alpha \cosh (\kappa L) A_j}{k} \mathcal{L}^{-1} \{ I \} \quad (A-12)$$

The obvious poles of  $I$  are at  $S = \lambda_j$  and  $S = \alpha \kappa^2$ . Additional roots of the denominator exist for  $\cosh \sqrt{\frac{S}{\alpha}} L = 0$ . The roots of  $\cosh \sqrt{\frac{S}{\alpha}} L$  are obtained by making the transformation  $S = -\mathcal{A}$ . This is done since  $\cosh \sqrt{\frac{S}{\alpha}} L$  cannot equal zero for real values of the argument and  $\alpha$  and  $L$  are always positive, real constants.

$$\cosh \sqrt{\frac{S}{\alpha}} L = \cosh i \sqrt{\frac{\mathcal{A}}{\alpha}} L = \cos \sqrt{\frac{\mathcal{A}}{\alpha}} L = 0 \quad (A-13)$$

therefore

$$\begin{aligned} \sqrt{\frac{\mathcal{A}}{\alpha}} R_0 &= \frac{n\pi}{2}, \quad n \text{ odd} \\ \mathcal{A}_n &= \frac{n^2 \pi^2 \alpha}{4L^2} \\ S_n &= -\frac{n^2 \pi^2 \alpha}{4L^2} \end{aligned} \quad (A-14)$$

Evaluating  $\mathcal{L}^{-1} \{ I \}$  by means of equation (A-11) at the poles  $\underline{\rho = \alpha \kappa^2}$ ,  $\underline{\rho = \lambda_j}$  and  $\underline{\rho = -\frac{n^2 \pi^2 \alpha}{4L^2}}$  yields equation (A-15).

$$\mathcal{L}^{-1} \{I\} = \frac{\cosh(\sqrt{\frac{\lambda_j}{\alpha}} x) e^{\lambda_j t}}{\cosh(\sqrt{\frac{\lambda_j}{\alpha}} L) (\lambda_j - \alpha \kappa^2)} + \frac{\cosh(\kappa x) e^{\alpha \kappa^2 t}}{\cosh(\kappa L) \alpha \kappa^2 - \lambda_j} \quad (A-15)$$

$$+ \sum_{n=1,3,5,\dots}^{\infty} \frac{\cos \frac{n\pi x}{2L} e^{-\frac{n^2 \pi^2 \alpha}{4L^2} t}}{(\frac{n^2 \pi^2 \alpha}{4L^2} + \lambda_j) (\frac{n^2 \pi^2 \alpha}{4L^2} + \alpha \kappa^2) (\frac{2L^2}{n\pi \alpha}) \sin(\frac{n\pi}{2})}$$

Considering the second term in equation (A-10), the inversion as obtained through use of equation (A-11) is given in equation (A-16).

$$\mathcal{L}^{-1} \sum_{j=1}^s \frac{q_{\infty} \alpha A_j}{k} \frac{1}{(S - \lambda_j)(S - \alpha \kappa^2)} = \sum_{j=1}^s \frac{q_{\infty} \alpha A_j}{k} \left( \frac{e^{\lambda_j t}}{(\lambda_j - \alpha \kappa^2)} + \frac{e^{\alpha \kappa^2 t}}{(\alpha \kappa^2 - \lambda_j)} \right) \quad (A-16)$$

In a similar manner the first term of equation (A-10), the inversion, again using equation (A-11), is given in equation (A-17).

$$\mathcal{L}^{-1} \left\{ \sum_{i=1}^p \frac{C_i \cosh \sqrt{\frac{s}{\alpha}} x}{(S - \beta_i) \cosh \sqrt{\frac{s}{\alpha}} L} \right\} = \sum_{i=1}^p \frac{B_i \cosh(\sqrt{\frac{\beta_i}{\alpha}} x) e^{\beta_i t}}{\cosh(\sqrt{\frac{\beta_i}{\alpha}} L)} \quad (A-17)$$

$$- \frac{n^2 \pi^2 \alpha}{4L^2} t$$

$$+ \sum_{i=1}^p \sum_{n=1,3,5,\dots}^{\infty} \frac{B_i \cos \frac{n\pi x}{2L} e^{-\frac{n^2 \pi^2 \alpha}{4L^2} t}}{(-\frac{n^2 \pi^2 \alpha}{4L^2} - \beta_i) \frac{L^2}{n\pi \alpha} (\sin \frac{n\pi}{2})}$$

The temperature distribution in the fuel plate,  $\theta_f(x, t)$  is obtained by substituting equation (A-15) in equation (A-12) and adding equations (A-12), (A-16) and (A-17). The result is

$$\begin{aligned}
\theta_f(x, t) = & \sum_{i=1}^p \frac{B_i \cosh \sqrt{\frac{\beta_i}{\alpha}} x}{\cosh \sqrt{\frac{\beta_i}{\alpha}} L} e^{-\beta_i t} - \sum_{n=1,3,5,\dots}^{\infty} \frac{\cos \frac{n\pi x}{2L} e^{-\frac{n^2 \pi^2 \alpha}{4L^2} t}}{\left(\frac{L^2}{\alpha n \pi}\right) \sin\left(\frac{n\pi}{2}\right)} \\
& \times \left\{ \sum_{i=1}^p \frac{B_i}{\frac{n^2 \pi^2 \alpha}{4L^2} + \beta_i} + \sum_{j=1}^s \frac{q_{\infty} \alpha A_j \cosh \kappa L}{k \left(\frac{n^2 \pi^2 \alpha}{4L^2} + \lambda_j\right) \left(\frac{n^2 \pi^2 \alpha}{4L^2} + \alpha \kappa^2\right)} \right\} \quad (A-18) \\
& - \sum_{j=1}^s \frac{A_j q_{\infty} \alpha e^{-\lambda_j t}}{k(\alpha \kappa^2 - \lambda_j)} \left\{ \cosh(\kappa x) - \frac{\cosh(\kappa L) \cosh\left(\sqrt{\frac{\lambda_j}{\alpha}} x\right)}{\cosh\left(\sqrt{\frac{\lambda_j}{\alpha}} L\right)} \right\}
\end{aligned}$$

As seen by comparing (A-1) and (A-2) the differential equations to be solved in the fuel and moderator are almost the same, the only difference being in the heat generation term. Thus, the total differential equation for the moderator in the Laplace transform domain after having applied the zero initial temperature condition is given in equation (A-19)

$$\nabla^2 \Phi_m(x, s) - \frac{s}{\alpha} \Phi_m(x, s) = - \sum_{j=1}^s \frac{F A_j}{k (s - \lambda_j)} \quad (A-19)$$

The homogeneous solutions are the same as before and particular solutions are easily obtained, as before, from the method of undetermined coefficients. Therefore, the solutions to equation (A-19) in the transform domain are

$$\Phi_m(x, s) = C \cosh \sqrt{\frac{s}{\alpha}} x + D \sinh \sqrt{\frac{s}{\alpha}} x + \sum_{j=1}^s \frac{F \alpha A_j}{k s (s - \lambda_j)} \quad (A-20)$$

The transform boundary conditions for the moderator are same as those for the fuel if the origin in the moderator is taken at the outside of the unit cell, i.e.,

$$\bar{\Phi}_m(L, S) = \sum_{i=1}^P \frac{B_i}{S - \beta_i} \quad \text{and} \quad \left. \frac{d\bar{\Phi}(x_i, S)}{dx_i} \right|_{x_i=0} = 0. \quad (\text{A-21})$$

Thus  $\underline{D}$  equals zero and  $\underline{A}$  takes the same form as for the solution in the fuel. The complete solution in the transform domain is given in equation (A-22).

$$\bar{\Phi}_m(x, S) = \sum_{i=1}^P \frac{B_i \cosh \sqrt{\frac{S}{\alpha}} x_i}{(S - \beta_i) \cosh \sqrt{\frac{S}{\alpha}} L_i} + \sum_{j=1}^S \frac{\alpha F A_j}{k S (S - \lambda_j)} \left[ 1 - \frac{\cosh \sqrt{\frac{S}{\alpha}} x_i}{\cosh \sqrt{\frac{S}{\alpha}} L_i} \right]. \quad (\text{A-22})$$

The inversion of this solution is easily accomplished by the same method used for the fuel region. The solution for the temperature is

$$\begin{aligned} \theta_m(x, t) = & \sum_{i=1}^P \frac{B_i \cosh(\sqrt{\frac{\beta_i}{\alpha}} x_i) e^{\beta_i t}}{\cosh(\sqrt{\frac{\beta_i}{\alpha}} L_i)} - \sum_{n=1, 3, 5, \dots}^{\infty} \frac{\cos \frac{n\pi x_i}{2L_i} e^{-\frac{n^2 \pi^2 \alpha}{4L_i^2} t}}{\left(\frac{L_i^2}{n\pi\alpha}\right) \sin\left(\frac{n\pi}{2}\right)} \\ & \times \left\{ \sum_{i=1}^P \frac{B_i}{\frac{n^2 \pi^2 \alpha}{4L_i^2} + \beta_i} + \sum_{j=1}^S \frac{\alpha F A_j}{\frac{n^2 \pi^2 \alpha}{4L_i^2} + \lambda_j} \right\} \\ & + \sum_{j=1}^S \frac{\alpha F A_j e^{\lambda_j t}}{k \lambda_j} \left\{ 1 - \frac{\cosh \sqrt{\frac{\lambda_j}{\alpha}} x_i}{\cosh \sqrt{\frac{\lambda_j}{\alpha}} L_i} \right\}. \end{aligned} \quad (\text{A-23})$$

This solution could have been obtained from the solution in the fuel by setting  $\kappa = 0$  and  $\underline{q}_{oo} = \underline{F}$ .

The equivalent solution in cylindrical geometry (r dependence only) for the exponential boundary condition is obtained in the same general manner, however, several important differences do occur. The equations governing the temperature in the fuel and moderator are

$$\nabla^2 \theta_f(r, t) + \sum_{j=1}^s \frac{q_{oo} I_o(\kappa r) A_j e^{\lambda_j t}}{k} = \frac{1}{\alpha} \frac{\partial \theta_f(r, t)}{\partial t} \quad (A-24)$$

and

$$\nabla^2 \theta_m(r, t) + \sum_{j=1}^s \frac{F A_j e^{\lambda_j t}}{k} = \frac{1}{\alpha} \frac{\partial \theta_m(r, t)}{\partial t} \quad (A-25)$$

Considering the fuel region first, transforming with respect to time and applying the zero initial condition yields

$$\nabla^2 \Phi(r, S) - \frac{S}{\alpha} \Phi(r, S) = - \sum_{j=1}^s \frac{q_{oo} A_j I_o(\kappa r)}{k (S - \lambda_j)} \quad (A-26)$$

The spatial operator for this case is

$$\nabla^2 = \frac{\partial^2}{\partial r^2} + \frac{1}{r} \frac{\partial}{\partial r} \quad (A-27)$$

The particular solution, again by the method of undetermined coefficients, is

$$\Phi_p(r, S) = \frac{q_{oo} \alpha A_j I_o(\kappa r)}{k(S - \lambda_j) (S - \alpha \kappa^2)} \quad (A-28)$$

The homogeneous solution, noting the fact that  $\Phi(0, S)$  if finite is

$$\Phi_h(r, s) = A I_o \sqrt{\frac{S}{\alpha}} r \quad (A-29)$$



The final constant  $\underline{A}$  is evaluated by use of the surface temperature boundary condition and the solution in the transform domain is

$$q_f(r, s) = \sum_{i=1}^p \frac{B_i}{s - \beta_i} \frac{I_0 \sqrt{\frac{s}{\alpha}} r}{I_0 \sqrt{\frac{s}{\alpha}} R_0} + \sum_{j=1}^s \frac{q_{\infty} \alpha A_j}{k(s - \lambda_j)(s - \alpha \kappa^2)} \left( I_0(\kappa r) - \frac{I_0(\kappa R_0) \sqrt{\frac{s}{\alpha}} r}{I_0 \sqrt{\frac{s}{\alpha}} R_0} \right) \quad (A-30)$$

Inverting this expression is entirely analogous to the inversion of the equivalent expression, equation (A-9) of this appendix. The analogy carries even to the point that in determining the zeros of  $I_0 \sqrt{\frac{s}{\alpha}} R_0$  as in determining the zeros of  $\cosh \sqrt{\frac{s}{\alpha}} L$  imaginary values of  $s$  yield an infinite set of zeros. In this case the zeros are

$$I_0 \sqrt{\frac{s}{\alpha}} R_0 = I_0 \sqrt{\frac{-\mathcal{A}}{\alpha}} R_0 = I_0 i \sqrt{\frac{\mathcal{A}}{\alpha}} R_0 = J_0 \sqrt{\frac{\mathcal{A}}{\alpha}} R_0 = 0 \quad (A-31)$$

therefore,

$$\sqrt{\frac{\mathcal{A}}{\alpha}} R_0 = \omega_n, \text{ where } \omega_n = 2.4048, 5.5201, \text{ etc. (the zeros of } J(\omega_n) = 0)$$

$$\frac{\mathcal{A}}{\alpha} R_0^2 = \omega_n^2,$$

$$\mathcal{A}_n = \frac{\omega_n^2 \alpha}{R_0^2} \quad (A-32)$$

$$\text{and} \quad S_n = \frac{\omega_n^2 \alpha}{R_0^2}$$

The details of the remainder of the inversion are not included.

The result is

$$\theta_f(x, t) = \sum_{i=1}^p \frac{B_i I_0(\sqrt{\frac{\beta_i}{\alpha}} r) e^{\beta_i t}}{I_0(\sqrt{\frac{\beta_i}{\alpha}} R)} + \sum_{n=1,2,3,\dots}^{\infty} \frac{J_0(\frac{\omega_n r}{R}) e^{-\frac{\omega_n^2 \alpha}{R^2} t}}{\frac{R^2}{2\omega_n^2 \alpha} J_0(\frac{\omega_n}{R})}$$

$$X \left\{ \sum_{i=1}^p \frac{B_i}{\frac{\omega_n^2 \alpha}{R^2} + \beta_i} + \sum_{j=1}^s \frac{q_{\infty} \alpha A_j I_0(\kappa R_0)}{k \left( \frac{\omega_n^2 \alpha}{R^2} + \lambda_j \right) \left( \frac{\omega_n^2 \alpha}{R^2} + \alpha \kappa^2 \right)} \right\} \quad (A-33)$$

$$- \sum_{j=1}^s \frac{A_j q_{\infty} \alpha e^{\lambda_j t}}{k(\alpha \kappa^2 - \lambda_j t)} \left\{ [I_0(\kappa r)] - \frac{[I_0(\kappa R) I_0(\sqrt{\frac{\lambda_j}{\alpha}} r)]}{I_0(\sqrt{\frac{\lambda_j}{\alpha}} R)} \right\},$$

where the  $\omega_n$ 's are the roots of the equation,  $J_0(X) = 0$ .

The solution for the cylindrical geometry in the moderator is complicated only by the fact that the symmetry condition cannot be located at the coordinate  $r = 0$ . Thus both terms  $I_0(\sqrt{\frac{S}{\alpha}} r)$  and  $K_0(\sqrt{\frac{S}{\alpha}} r)$  of the homogeneous solution must be retained. The details of this solution are not included. The result is

$$\theta_m(x, t) = \sum_{i=1}^p B_i \left\{ \frac{K_1(\sqrt{\frac{\beta_i}{\alpha}} R_1) I_0(\sqrt{\frac{\beta_i}{\alpha}} r) + I_1(\sqrt{\frac{\beta_i}{\alpha}} R_1) K_0(\sqrt{\frac{\beta_i}{\alpha}} r)}{(K_1(\sqrt{\frac{\beta_i}{\alpha}} R_1) I_0(\sqrt{\frac{\beta_i}{\alpha}} R) + I_1(\sqrt{\frac{\beta_i}{\alpha}} R) K_0(\sqrt{\frac{\beta_i}{\alpha}} R))} \right\} e^{\beta_i t}$$

$$+ \sum_{n=1}^{\infty} \frac{2 \sqrt{\rho_n \alpha} \left[ K_1 \left( \sqrt{\frac{\rho_n}{\alpha}} R \right) I_0 \left( \sqrt{\frac{\rho_n}{\alpha}} r \right) + I_1 \left( \sqrt{\frac{\rho_n}{\alpha}} R \right) K_0 \left( \sqrt{\frac{\rho_n}{\alpha}} r \right) \right] e^{\rho_n t}}{R \left[ K_1 \left( \sqrt{\frac{\rho_n}{\alpha}} R \right) I_1 \left( \sqrt{\frac{\rho_n}{\alpha}} R \right) - K_0 \left( \sqrt{\frac{\rho_n}{\alpha}} R \right) I_0 \left( \sqrt{\frac{\rho_n}{\alpha}} R \right) \right] + I_0 \left( \sqrt{\frac{\rho_n}{\alpha}} R \right) K_0 \left( \sqrt{\frac{\rho_n}{\alpha}} R \right) - I_1 \left( \sqrt{\frac{\rho_n}{\alpha}} R \right) K_1 \left( \sqrt{\frac{\rho_n}{\alpha}} R \right)}$$

$$+ \left\{ \sum_{i=1}^p \frac{B_i}{\rho_n - \beta_i} - \sum_{j=1}^s \frac{\alpha F A_j}{k \rho_n (\rho_n - \lambda_j)} \right\} + \sum_{j=1}^s \frac{\alpha F A_j e^{\lambda_j t}}{k} \quad (A-34)$$

$$\times \left\{ \frac{K_1 \left( \sqrt{\frac{\lambda_j}{\alpha}} R \right) I_0 \left( \sqrt{\frac{\lambda_j}{\alpha}} r \right) + I_1 \left( \sqrt{\frac{\lambda_j}{\alpha}} R \right) K_0 \left( \sqrt{\frac{\lambda_j}{\alpha}} r \right)}{K_1 \left( \sqrt{\frac{\lambda_j}{\alpha}} R \right) I_0 \left( \sqrt{\frac{\lambda_j}{\alpha}} R \right) - I_1 \left( \sqrt{\frac{\lambda_j}{\alpha}} R \right) K_0 \left( \sqrt{\frac{\lambda_j}{\alpha}} R \right)} \right\},$$

where the  $\rho_n$ 's are the roots of the equation,

$$K_1 \left( \sqrt{\frac{S}{\alpha}} R \right) I_0 \left( \sqrt{\frac{S}{\alpha}} R \right) + I_1 \left( \sqrt{\frac{S}{\alpha}} R \right) K_0 \left( \sqrt{\frac{S}{\alpha}} R \right) = 0$$

The next solution considered again uses an exponential fit for the heat generation rate, however, the boundary condition was that the first derivative with respect to  $x$  evaluated at the outside of the plate or effectively the heat flow out of the plate could be expressed as a sum of exponentials. The general solution with the exception of the evaluation of the final constant  $A$  is exactly the same as the first derivation in this appendix. Including the one undetermined coefficient the solution is

$$\Phi_f(x, S) = A \cosh \sqrt{\frac{S}{\alpha}} x + \sum_{j=1}^s \frac{q_{00} \alpha A_j \cosh \kappa x}{k(S - \lambda_j) (S - \alpha \kappa^2)} \quad (A-35)$$

Evaluation of A through use of the boundary condition leads to

$$\Phi_f(x, S) = \sum_{i=1}^{p'} \frac{B_i \cosh(\sqrt{\frac{S}{\alpha}} x)}{(S - \beta_i) \sqrt{\frac{S}{\alpha}} \sinh(\sqrt{\frac{S}{\alpha}} L)} + \sum_{j=1}^{s'} \frac{q_{\infty} \alpha A_j}{k(S - \lambda_j)(S - \alpha \kappa^2)} \quad (A-36)$$

$$\left( \cosh \kappa x - \frac{\cosh(\kappa L) \cosh(\sqrt{\frac{S}{\alpha}} x)}{\cosh(\sqrt{\frac{S}{\alpha}} L)} \right)$$

The details of this inversion are not included. The result is

$$\theta_f(x, t) = \sum_{i=1}^{p'} \left( \frac{B_i \cosh(\sqrt{\frac{\beta_i}{\alpha}} x) e^{\beta_i t}}{\sqrt{\frac{\beta_i}{\alpha}} \sinh(\sqrt{\frac{\beta_i}{\alpha}} L)} - \frac{B_i \alpha}{\beta_i L} \right) - \sum_{n=1}^{\infty} \frac{\cos\left(\frac{n\pi x}{2L}\right) e^{-\frac{n^2 \pi^2 x}{4L^2}}}{\frac{L}{\alpha} \cos n\pi}$$

$$\times \left\{ \sum_{i=1}^{p'} \frac{B_i}{\frac{n^2 \pi^2 \alpha}{4L^2} + \beta_i} + \sum_{j=1}^{s'} \frac{q_{\infty} \alpha A_j \kappa \sinh \kappa L}{k\left(\frac{n^2 \pi^2 \alpha}{4L^2} + \lambda_j\right)\left(\frac{n^2 \pi^2 \alpha}{4L^2} + \alpha \kappa^2\right)} \right\} \quad (A-37)$$

$$- \sum_{j=1}^{s'} \frac{q_{\infty} \alpha A_j e^{\lambda_j t}}{k(\alpha \kappa^2 - \lambda_j)} \left[ \cosh \kappa x - \frac{\kappa \sinh(\lambda L) \cosh(\sqrt{\frac{\lambda_j}{\alpha}} x)}{\sqrt{\frac{\lambda_j}{\alpha}} \sinh(\sqrt{\frac{\lambda_j}{\alpha}} L)} \right] - \frac{q_{\infty} \alpha A_j \sinh \kappa L}{k \lambda_j \kappa L}.$$

The time dependent temperature distribution in the moderator for the comparable boundary conditions is obtained by setting  $\kappa$  equal to zero and  $q_{\infty}$  equal to  $\underline{F}$  in equation (A-37). The result is

$$\theta_m(x, t) = \sum_{i=1}^{p'} \left( \frac{B_i \cosh(\sqrt{\frac{\beta_i}{\alpha}} x) e^{\beta_i t}}{\sqrt{\frac{\beta_i}{\alpha}} \sinh(\sqrt{\frac{\beta_i}{\alpha}} L)} - \frac{B_i \alpha}{\beta_i L} \right)$$

$$\begin{aligned}
& - \sum_{n=1}^{\infty} \frac{\cos \frac{n\pi x}{2L} e^{-\frac{n^2 \pi^2 \alpha}{4L^2} t}}{\left(\frac{L}{\alpha}\right) \cos n\pi} \left\{ \sum_{i=1}^{p'} \frac{B_i}{\frac{n^2 \pi^2 \alpha}{4L^2} + \beta_i} \right\} \\
& + \sum_{j=1}^{s'} \frac{\alpha F A_j}{k(\lambda_j)} (e^{\lambda_j t} - 1). \quad (A-38)
\end{aligned}$$

The final solution considered again used a sum of exponentials to represent the time dependence of the heat generation rate, however, the surface temperature boundary condition was approximated by an even Fourier series,  $\sum_{i=1}^p B_i \cos \beta_i t$ . With the exception of the steady state term resulting from the surface temperature boundary condition the derivation follows exactly the first derivation of this appendix. The steady state term is handled most easily in a slightly different manner as shown below. The general solution in the transform domain is

$$\begin{aligned}
\Phi_f(x, S) = & \sum_{i=1}^p \frac{B_i S \cosh(\sqrt{\frac{S}{\alpha}} x)}{(S^2 + \beta_i^2) \cosh(\sqrt{\frac{S}{\alpha}} L)} + \sum_{j=1}^s \frac{q_{\infty} \alpha A_j}{k(S - \lambda_j) (S - \alpha \kappa^2)} \\
& \left[ \cosh \kappa x - \frac{\cosh(\kappa L) \cosh(\sqrt{\frac{S}{\alpha}} x)}{\cosh(\sqrt{\frac{S}{\alpha}} L)} \right] \quad (A-39)
\end{aligned}$$

The first term presents the only change and there only for the poles at  $S = \pm j\beta_i$ . The terms generated from the inversion integral by these two poles are

$$\rho_1 \Big|_{S=j\beta_1} = \frac{B_1 j \beta_1 \cosh(\sqrt{\frac{j\beta_1}{\alpha}} x)}{2 j \beta_1 \cosh(\sqrt{\frac{j\beta_1}{\alpha}} L)} e^{j\beta_1 t} \quad (A-40)$$

and

$$\rho_2 = \frac{B_1 (-j\beta_1) \cosh(\sqrt{\frac{-j\beta_1}{\alpha}} x)}{2 (-j\beta_1) \cosh(\sqrt{\frac{-j\beta_1}{\alpha}} L)} e^{-j\beta_1 t} \quad (A-41)$$

$s = -j\beta_1$

These terms are most easily handled by recognizing the fact that the sum  $\rho_1 + \rho_2$  is the sum of a function and its conjugate. That is

$$\rho_1 + \rho_2 = f(z) + \overline{f(z)} = f(z) + \overline{f(\bar{z})} \quad \text{since } z \text{ is a pure imaginary number.}$$

Therefore

$$\begin{aligned} \rho_1 + \rho_2 &= 2 \operatorname{Re} \left\{ f(z) \right\} = 2 \operatorname{Re} \left\{ \rho_1 \right\} \\ &= 2 \operatorname{Re} \left\{ \frac{B_1 \cosh(\sqrt{\frac{j\beta_1}{\alpha}} x)}{2 \cosh(\sqrt{\frac{j\beta_1}{\alpha}} L)} e^{j\beta_1 t} \right\} \quad (A-42) \\ &= B_1 \operatorname{Re} \left\{ \frac{\cosh(\sqrt{\frac{j\beta_1}{\alpha}} x)}{\cosh(\sqrt{\frac{j\beta_1}{\alpha}} L)} e^{j\beta_1 t} \right\} \\ &= B_1 \operatorname{Re} \left[ \frac{\cosh(\sqrt{\frac{j\beta_1}{\alpha}} x)}{\cosh(\sqrt{\frac{j\beta_1}{\alpha}} L)} e^{j(\beta_1 t + \arg \left\{ \frac{\cosh \sqrt{\frac{j\beta_1}{\alpha}} x}{\cosh \sqrt{\frac{j\beta_1}{\alpha}} L} \right\})} \right] \\ &= B_1 Z_1^{\frac{1}{2}}(x) \cos [\beta_1 t + \varphi_1(x)], \end{aligned}$$

where

$$Z_1(x) = \left| \frac{\cosh \sqrt{\frac{j\beta_1}{\alpha}} x}{\cosh \sqrt{\frac{j\beta_1}{\alpha}} L} \right|^2 = \left| \frac{\cosh(\sqrt{\frac{\beta_1}{2\alpha}} x) \cos(\sqrt{\frac{\beta_1}{2\alpha}} x) + j \sin(\sqrt{\frac{\beta_1}{2\alpha}} x) \sinh(\sqrt{\frac{\beta_1}{2\alpha}} x)}{\cosh(\sqrt{\frac{\beta_1}{2\alpha}} L) \cos(\sqrt{\frac{\beta_1}{2\alpha}} L) + j \sin(\sqrt{\frac{\beta_1}{2\alpha}} L) \sinh(\sqrt{\frac{\beta_1}{2\alpha}} L)} \right|^2$$



$$= \left\{ \frac{\cos^2(\sqrt{\frac{\beta_1}{2\alpha}} x) \cosh^2(\sqrt{\frac{\beta_1}{2\alpha}} x) + \sin^2(\sqrt{\frac{\beta_1}{2\alpha}} x) \sinh^2(\sqrt{\frac{\beta_1}{2\alpha}} x)}{\cos^2(\sqrt{\frac{\beta_1}{2\alpha}} L) \cosh^2(\sqrt{\frac{\beta_1}{2\alpha}} L) + \sin^2(\sqrt{\frac{\beta_1}{2\alpha}} L) \sinh^2(\sqrt{\frac{\beta_1}{2\alpha}} L)} \right\} \quad (A-43)$$

and

$$\begin{aligned} \varphi_1(x) &= \arg \left\{ \frac{\cosh \sqrt{\frac{j\beta_1}{\alpha}} x}{\cosh \sqrt{\frac{j\beta_1}{\alpha}} L} \right\} = \arg \left\{ \cosh \sqrt{\frac{j\beta_1}{\alpha}} x \right\} - \left\{ \arg \cosh \sqrt{\frac{j\beta_1}{\alpha}} L \right\} \\ &= \tan^{-1} \left( \frac{\sin \sqrt{\frac{\beta_1}{2\alpha}} x \sinh(\sqrt{\frac{\beta_1}{2\alpha}} x)}{\cos \sqrt{\frac{\beta_1}{2\alpha}} x \cosh(\sqrt{\frac{\beta_1}{2\alpha}} x)} \right) - \tan^{-1} \left( \frac{\sin(\sqrt{\frac{\beta_1}{2\alpha}} L) \sinh(\sqrt{\frac{\beta_1}{2\alpha}} L)}{\cos(\sqrt{\frac{\beta_1}{2\alpha}} L) \cosh(\sqrt{\frac{\beta_1}{2\alpha}} L)} \right) \quad (A-44) \end{aligned}$$

The resultant time dependent temperature distributions are

$$\begin{aligned} \theta_f(x, t) &= \sum_{i=1}^p B_i Z_i^{1/2} \cos(\beta_i t + \varphi_i) - \sum_{n=1,3,5,\dots}^{\infty} \frac{\cos \frac{n\pi x}{2L} e^{-\frac{n^2 \pi^2 \alpha}{4L^2} t}}{(L^2/n\pi\alpha) \sin \frac{n\pi}{2}} \\ &\times \left\{ \sum_{i=1}^p \frac{B_i \frac{(n^2 \pi^2 \alpha)}{4L^2}}{(\frac{n^2 \pi^2 \alpha}{4L^2} + \beta_i^2)} + \sum_{j=1}^s \frac{q_{\infty} \alpha A_j \cosh \kappa L}{k(\frac{n^2 \pi^2 \alpha}{4L^2} + \alpha \kappa^2)(\frac{n^2 \pi^2 \alpha}{4L^2} + \lambda_j^2)} \right\} \quad (A-45) \\ &- \sum_{j=1}^s \frac{q_{\infty} \alpha A_j e^{\lambda_j t}}{k(\alpha \kappa^2 - \lambda_j^2)} \left\{ \cosh \kappa x - \frac{\cosh(\kappa L) \cosh(\sqrt{\frac{\lambda_j}{\alpha}} x)}{\cosh(\sqrt{\frac{\lambda_j}{\alpha}} L)} \right\} \end{aligned}$$

and

$$\begin{aligned}
 \theta_m(x, t) = & \sum_{i=1}^p B_i Z_i^{\frac{1}{2}} \cos(\beta_i t + \varphi_i) + \sum_{n=1,3,5,\dots}^{\infty} \frac{\cos \frac{n\pi x}{2L} e^{-\frac{n^2 \pi^2 \alpha}{4L^2} t}}{(L^2 / n\pi\alpha) \sin \frac{n\pi}{2}} \\
 & \times \left\{ \sum_{i=1}^p \frac{B_i \left( \frac{n^2 \pi^2 \alpha}{4L^2} \right)}{\frac{n^2 \pi^2 \alpha}{16L^4} + \beta_i^2} - \sum_{j=1}^p \frac{\alpha F A_j}{k \left( \frac{n^2 \pi^2 \alpha}{4L^2} + \alpha \kappa^2 \right) \left( \frac{n^2 \pi^2 \alpha}{4L^2} + \lambda_j \right)} \right\} \quad (A-46) \\
 & + \sum_{j=1}^s \frac{\alpha F A_j e^{\lambda_j t}}{k(\lambda_j)} \left\{ 1 - \frac{\cosh \sqrt{\frac{\lambda_j}{\alpha}} x}{\cosh \sqrt{\frac{\lambda_j}{\alpha}} L} \right\}
 \end{aligned}$$

in the fuel and moderator, respectively.

## APPENDIX B

Description and Explanation of the IBM-650  
Computer Program Used for Fitting Empirically  
Experimental Data with the Sum of Several  
Terms of Exponential Form

The computer code was written to fit an analytical function of the form of the sum of exponentials to the experimentally determined power traces during a transient burst. The program was written in SOAP II and floating point form. The object program is listed and the logic diagram is shown in this appendix.

The criteria that the machine inspected was that the sum of the squares of the residuals between the experimental data and the calculated values should be made as small as possible. Each of the fitting parameters was varied in turn by a specified increment, holding all other parameters constant, until such a time that a specified increment could make no further reduction in the sum of the squares of the residuals. This parameter was then stored as the best available estimate of the particular empirical parameter. When none of the parameters could be varied by the specified increment to give a smaller sum of the squares of the residuals, the increments were refined and the trial and error process was repeated with the refined increments. This procedure continued until the increments were less than a specified precision.

The data were fit empirically with a function of the form

$$P_i = \sum_{j=1}^s A_j e^{\lambda_j t_i} \quad s \leq 10 \quad (B-1)$$

As stated above, the best fit criterion was that

$$\text{ERROR} = \sum_{i=1}^c \frac{1}{w_i^2} \sum_{j=1}^s (A_j e^{\lambda_j t_i} - \bar{P}_i)^2 \quad (B-2)$$

be a minimum.

The program required, in addition to the experimental data and their respective times, initial estimates for a specific number of parameters. The program had a capacity for up to 20 data points and 10 terms in the summation of equation (B-1). These input data were read into the machine along with the program deck on one-word load cards. Each one-word load card contained a particular constant or an initial value and its specified storage location. Table B-1 lists the various input data needed for this program.

Table B-1. Input data required for use of the IBM-650 program which fit empirically experimental data with several terms of Exponential form.

Symbol	Explanation	Storage Location
ZERD	0.00	0073
FPONE	1.00	0129
FOUR	4.00	0185
TEN	10.00	0158
HNDRD	100.00	0090
ONE	Index Number 1 (0000000001)	0392
EIGHT	Index Number 8 (0000000008)	0024
INDXB	Number of Exponential Terms (00000000xx)	0412
INDXA	Number of Data Points (00000000xx)	0062
ONEHD	Precision	0168
DELB <sub>j</sub>	Initial increments of the Amplitude, B <sub>j</sub>	(1800 + i)
DELR <sub>j</sub>	Initial increments of R <sub>j</sub>	(1810 + j)
BINIT <sub>j</sub>	Initial estimate of B <sub>j</sub>	(1300 + j)
RINIT <sub>j</sub>	Initial estimate of R <sub>j</sub>	(1310 + j)
Z <sub>i</sub>	Time of ith data point	(1200 + i)
FLUX <sub>i</sub>	Experimental data at ith point	(1200 + i)
W <sub>i</sub>	Weighting function at ith point	(1750 + i)

The machine yielded an answer card having a capacity of 8 words, a word being ten digit numbers and a sign. For the first answer the machine punched out the initial estimates of the fitting parameters on as many cards as was necessary to accommodate them.  $\underline{A}$  and  $\underline{\lambda}$  for the first term were stored in word locations 1 and 2, respectively. After a card was filled to its 8 word capacity, it was punched and a new card began to fill. This procedure continued until all of the fitting parameters had been punched out. Then a separate card was punched giving in the word 8 location, the value of the sum of the weighted of the residuals between the experimental data and the calculated values. The machine then punched out values of the time, residual and correct values at the last data point in word locations 1, 2 and 3, respectively and the next to last data point in word locations 5, 6 and 7, respectively. The same information for two previous data points was punched out on a second card in the same format and this procedure was continued until the position residual and correct value was punched out for each data point. Subsequent improvements in the parameters and the weighted sum of squares of the residuals were printed out after each cycle of trying to vary each parameter. The positions, residuals and correct values at each data point were obtained at this time if the console instruction was negative. When the fitting parameters could not be further improved with the most refined increment specified, the punching of the best fit parameters, the sum of the weighted square of the residuals, the position, residual and correct values took place according to the procedure described above.





## OBJECT PROGRAM-APPENDIX B

	BLR	1200	1830	1	0000	00	0000	0000
	BLR	1951	1960	2	0000	00	0000	0000
	BLR	1977	1985	3	0000	00	0000	0000
	SYM	START	1999	4	0000	00	0000	0000
	SYM	Z	1800	5	0000	00	0000	0000
	SYM	FLUX	1880	6	0000	00	0000	0000
	SYM	G	1240	7	0000	00	0000	0000
	SYM	B	1260	8	0000	00	0000	0000
	SYM	BREST	1270	9	0000	00	0000	0000
	SYM	R	1280	10	0000	00	0000	0000
	SYM	RBEST	1290	11	0000	00	0000	0000
	SYM	RINIT	1300	12	0000	00	0000	0000
	SYM	RINIT	1310	13	0000	00	0000	0000
	SYM	DELB	1800	14	0000	00	0000	0000
	SYM	DELR	1810	15	0000	00	0000	0000
	SYM	TEMP	1320	16	0000	00	0000	0000
	SYM	TERM	1520	17	0000	00	0000	0000
	SYM	C	1720	18	0000	00	0000	0000
	SYM	FRAC	1730	19	0000	00	0000	0000
	SYM	QUOT	1740	20	0000	00	0000	0000
	SYM	W	1750	21	0000	00	0000	0000
PRNTM	STO	EXXT		22	0000	24	0003	0006
	LOD		EDDCL	23	0006	69	0009	0012
	LOD	INOXA		24	0009	69	0062	0015
RESST	RAA	8001	RESST	25	0015	80	8001	0021
	LOD	EIGHT		26	0021	69	0024	0027
	R88	8001	STUUF	27	0027	83	8001	0033
STUUF	LOD	Z		28	0033	69	3200	0053
	STO	1985		29	0053	24	5985	0038
	LOD	G		30	0038	69	3240	0043
	STO	1986		31	0043	24	5986	0039
	LOD	FLUX		32	0039	69	3220	0023
	STO	1987		33	0023	24	5987	0040
	8XA	0001		34	0040	51	0001	0046
	AX8	0004		35	0046	52	0004	0002
	NZA	MDRRG	PONNM	36	0002	40	0005	0056
PONNM	PCH	1977	EXXT	37	0056	71	1977	0003
MDRRG	NZR	STUUF	CARRO	38	0005	42	0033	0059
CARRU	PCH	1977		39	0059	71	1977	0077
	LOD	RE88T	EDDCL	40	0077	69	0021	0012
EODEA	STO	AAA1		41	0050	24	0103	0106
	STL	AAA14		42	0106	20	0011	0014
	RAU	AAA16		43	0014	60	0017	0071
	FAM	AAA14		44	0071	37	0011	0037
	STU	AAA2		45	0037	21	0042	0045
	LOD	AAA3		46	0045	69	0040	0001
AAA8	STO	AAA4	AAA8	47	0001	24	0004	0007
	RAU	AAA2		48	0007	60	0042	0047
	F88	AAA5		49	0047	33	0100	0127
	8MI	AAA6		50	0127	46	0030	0031
	STU	AAA2		51	0031	21	0042	0095
	RAU	AAA4		52	0095	60	0004	0109
	FMP	AAA7		53	0109	39	0112	0162
AAA6	STU	AAA4	AAA6	54	0162	21	0004	0007
	RAU	AAA2		55	0030	60	0042	0097
	F88	AAA3		56	0097	33	0048	0025
	8MI	AAA28		57	0025	46	0028	0029
	STU	AAA2		58	0029	21	0042	0145
	RAU	AAA4		59	0145	60	0004	0159
	FMP	AAA9		60	0159	39	0212	0262
AAA28	STU	AAA4	AAA6	61	0262	21	0004	0030
	RAU	AAA2		62	0030	60	0042	0147
	F88	AAA10		63	0147	33	0150	0177
	8MI	AAA11		64	0177	46	0080	0081
	STU	AAA2		65	0081	21	0042	0195
	RAU	AAA4		66	0195	60	0004	0209
	FMP	AAA12		67	0209	39	0312	0362
AAA11	STU	AAA4	AAA28	68	0362	21	0004	0028
	RAU	AAA2		69	0080	60	0042	0197
	LOD		AAA17	70	0197	69	0200	0153
	FMP	AAA4		71	0200	39	0004	0054
	STU	AAA13		72	0054	21	0008	0061
	RAU	AAA14		73	0061	60	0011	0065
	8MI	AAA15		74	0065	46	0018	0019
AAA15	RAL	AAA13	AAA1	75	0019	65	0008	0103
	RAU	AAA3		76	0018	60	0048	0203
	FOV	AAA13		77	0203	34	0708	0058
	RAL	8003	AAA1	78	0058	65	8003	0103
AAA17	STO	AAA18		79	0153	24	0156	0259
	RAU	AAA3		80	0259	60	0048	0253
	FAD	AAA2		81	0253	32	0042	0069
	STU	AAA19		82	0069	21	0074	0227
	LOD	AAA27		83	0227	69	0130	0083
	STO	AAA20		84	0083	24	0036	0089
	STO	AAA21		85	0089	24	0092	0245
	RAU	AAA2		86	0245	60	0042	0247
	FMP	AAA2		87	0247	39	0042	0142
AAA22	STU	AAA23	AAA22	88	0142	21	0096	0049
	FOV	AAA21		89	0049	34	0092	0192
	STU	AAA24		90	0192	21	0146	0099
	FAD	AAA19		91	0099	32	0074	0051
	STU	AAA19		92	0051	21	0074	0277
	RAU	AAA24		93	0277	60	0146	0101
	FDV	AAA19		94	0101	34	0074	0124
	F88	AAA25		95	0124	33	0327	0103
AAA26	8MI	AAA19	AAA26	96	0303	46	0206	0057
	RAU	AAA20	AAA18	97	0206	60	0074	0156
	FAD	AAA3		98	0057	60	0036	0041
	STU	AAA20		99	0041	32	0048	0075
	FMP	AAA21		100	0075	21	0036	0139
	STU	AAA21		101	0139	39	0092	0242
	RAU	AAA23		102	0242	21	0092	0295
	FMP	AAA23		103	0295	60	0096	0151
	STU	AAA23	AAA22	104	0151	39	0042	0292
AAA3	10	0000		105	0292	21	0096	0049
AAA5	50	0000	0051	106	0048	10	0000	0051
AAA7	14	8410	0053	107	0100	50	0000	0051
AAA9	27	1830	0051	108	0112	14	8410	0053
AAA10	20	0000	0050	109	0212	27	1830	0051
AAA12	12	2140	0051	110	0150	20	0000	0050
AAA16	00	0000	0000	111	0312	12	2140	0051
AAA25	70	0000	0047	112	0017	00	0000	0000
AAA27	20	0000	0051	113	0327	70	0000	0047
EODCL	STO	ZZZ1		114	0130	20	0000	0051
				115	0012	24	0115	0068

LOD	ZZZ10		116	006R	69	0121	0174
STD	1977		117	0174	24	1977	0180
STD	1978		118	0180	24	1978	0131
STD	1979		119	0131	24	1979	0032
STD	1980		120	0032	24	1980	0133
STD	1981		121	0133	24	1981	0034
STD	1982		122	0034	24	1982	0035
STD	1983		123	0035	24	1983	0086
STD	1984		124	0086	24	1984	0115
OD	0000	ZZZ1	125	0121	00	0000	0000
ZZZ10	0000	0000	126	0250	24	0353	0256
TEMPP	EGSIT		127	0256	60	3200	0055
RAU	Z	A	128	0255	39	52R0	0230
FMP	R	B	129	0230	21	00R4	00R7
STU	RZEE		130	0087	32	0090	0067
FAD	HMORO		131	0067	46	0020	0171
SMI	STO	GO	132	0020	69	0073	0026
LOD	ZERO		133	0026	24	7320	0353
STD	TEMP	C EGSIT	134	0171	65	00R4	0189
RAL	RZEE		135	0189	69	0342	0050
LOD		E00EA	136	0342	20	7320	0353
STL	TEMP	C EGSIT	137	0300	24	0403	0306
STO	EXIT		138	0306	60	7320	0325
RAU	TEMP	C	139	0125	39	5260	0010
FMP	H	C	140	0010	21	7520	0403
STU	TERM	C EXIT	141	0350	24	0453	0356
STO	EXIT		142	0356	69	0073	0076
LOU	ZERO		143	0076	88	8001	0082
RAC	8001		144	0082	24	00R5	00R8
STO	ERMOR		145	0088	69	0062	0165
LOD	INDXA		146	0165	80	8001	0221
RAA	8001	READY	147	0221	69	0224	0377
LOD	INOXC		148	0377	58	8001	0183
AXC	8001		149	0183	69	0073	0126
LOD	ZERO		150	0126	24	0079	0132
STO	ACCUM	DOONE	151	0132	60	7520	0175
RAU	TERM	C	152	0175	32	0079	0105
FAD	ACCUM		153	0105	21	0079	0182
STU	ACCUM		154	0182	69	0062	0215
LOD	INDXA		155	0215	59	8001	0271
SXC	8001		156	0271	40	0274	0225
MZC	REPET	DIDIT	157	0274	49	0225	0132
BMC	DIDIT	DOONE	158	0225	60	0079	0233
RAU	ACCUM		159	0233	33	3220	0297
F8B	FLOX	A	160	0297	21	3240	0093
STU	G	A A	161	0093	39	3240	0140
FMP	G	A A	162	0140	34	3750	0400
FOV	W	A	163	0400	32	00R5	0111
FAD	ERROR		164	0111	21	00R5	0138
STU	ERROR		165	0138	59	0001	0044
SXC	0001		166	0044	51	0001	0450
SXA	0001		167	0450	40	0221	0453
MZA	READY	EXIT	168	0500	24	0503	0406
STO	EXET		169	0406	69	0309	0012
LOD		E00CL	170	0309	69	0412	0265
LOD	INDXB		171	0265	82	8001	0321
RAB	8001	RESIT	172	0321	69	0024	0427
LOD	EIGHT		173	0427	81	8001	0283
R8A	8001	FILL	174	0283	69	5270	0123
LOD	88E8T	B	175	0123	24	19R8	018R
STO	1985	A	176	018R	69	5290	0143
LOD	88E8T	B	177	0143	24	39R6	0239
STO	1986	A	178	0239	53	0001	0345
8XR	0001		179	0345	50	0002	0201
AXA	0002		180	0201	42	0104	0155
MZR	NEXTR	WHOP	181	0104	40	02R3	010R
NZA	FILL	CARDZ	182	010R	71	1977	0477
PCH	1977		183	0477	69	0321	0012
LOD	RE8IT	E00CL	184	0155	71	1977	0527
PCH	1977		185	0527	69	02R0	0012
LOD		E00CL	186	0280	69	0333	0136
LOD	ERMIN		187	0136	24	19R4	0137
STO	1984		188	0137	71	1977	0503
PCH	1977	EXET	189	0550	24	0553	0456
STO	TIME		190	0456	69	5260	0013
LOD	B	B	191	0013	24	5270	0173
STO	88E8T	B	192	0173	69	52R0	03R3
LOD	R	B	193	03R3	24	5290	0193
STO	88E8T	B	194	0193	69	00R5	023R
LOD	ERROR		195	023R	24	0333	0553
STO	ERMIN	TIME	196	1999	69	0412	0315
LOD	INDXB	LOADY	197	0315	82	8001	0371
RAB	8001		198	0371	69	5300	0403
LOD	8INIT	B	199	0603	24	5260	0063
STO	B	B	200	0063	24	5270	0223
STO	88E8T	B	201	0223	69	5310	0113
LOD	RINIT	B	202	0113	24	52R0	0433
STO	R	B	203	0433	24	5290	0243
STU	88E8T		204	0243	53	0001	0149
8XR	0001	SETUP	205	0149	42	0371	0653
MZB	LOADY		206	0653	60	0062	0117
RAU	INDXA		207	0117	80	8001	0273
RAA	8001		208	0273	69	0412	0365
LOD	INDXB		209	0365	82	8001	0421
RAB	8001		210	0421	19	0001	0094
MPY	8001		211	0094	20	0224	0577
STL	INDXC		212	0577	88	8001	04R3
RAC	8001	CALCA	213	04R3	69	01R6	0250
LOD		TURMM	214	01R6	69	02R9	0300
LOD			215	0289	59	0001	0395
8XC	0001		216	0395	51	0001	0251
8XA	0001	CALCR	217	0251	40	04R3	0205
MZA	CALCA		218	0205	69	0062	0415
LOD	INDXA		219	0415	80	8001	0471
RAA	8001		220	0471	53	0001	0627
8XR	0001	FILUP	221	0627	42	04R3	0101
NZR	CALCA	ERR	222	0181	69	0134	0350
LOD		PRIME	223	0134	69	01R7	0550
LOD		PRINT	224	0187	69	0190	0500
LOD		PRNTM	225	0190	69	0293	0000
LOD	INDXB		226	0293	69	0412	0465
RAB	8001		227	0465	82	8001	0521
LOD	INDXC		228	0521	69	0224	0677
RAC	8001	LOOPS	229	0677	8R	8001	0533
LOD	ZERO		230	0533	69	0073	0176

	STD	INDXF			231	0176	24	0144	0232
	RAU	BBEST	B		232	0232	60	5270	0275
	FAD	DELB	B	SUBB1	233	0275	32	5800	0727
SUBR1	STU	B	B		234	0727	21	5260	0163
	LDD	B007			235	0163	69	8007	0119
	STD	CTEMP			236	0119	24	0022	0325
	LDD	B006			237	0325	69	8006	0231
	STD	BTEMP			238	0231	24	0184	0237
	LDD	INDXA			239	0237	69	0062	0515
	RAA	B001		SUBB2	240	0515	60	8001	0571
SUBB2	LDD			TURMM	241	0571	69	0324	0300
	BXC	0001			242	0324	59	0001	0330
	SXA	0001			243	0330	51	0001	0236
	NZA	SUBB2		SUBB3	244	0236	40	0571	0240
SUBB3	LDD			ERR	245	0240	69	0343	0350
	RAU	ERWIN			246	0343	60	0333	0287
	FRR	ERRDR			247	0287	33	0085	0161
	RMI	BADDR		GOODR	248	0161	46	0064	0565
GODDR	LDD	BTEMP			249	0565	69	0184	0337
	RAA	B001			250	0337	82	8001	0393
	LDD	CTEMP			251	0393	69	0022	0375
	RAC	B001			252	0375	88	8001	0281
	RAU	BBEST	B		253	0281	60	5270	0425
	FRR	B	B		254	0425	33	5260	0387
	RMI	RPLUS		BWINS	255	0387	46	0290	0091
BPLUS	LDD			PRIME	256	0290	69	0443	0550
	LDD	FPONE			257	0443	69	0196	0199
	STD	INDXF			258	0199	24	0129	0282
	STD	INDXD			259	0282	24	0135	0288
	RAU	BBEST	B		260	0288	60	5270	0475
	FAD	DELB	B	SUBB1	261	0475	32	5800	0727
	LDD			PRIME	262	0091	69	0144	0550
	LDD	ZERO			263	0144	69	0073	0226
	STD	INDXF			264	0226	24	0129	0332
	STD	INDXD			265	0332	69	0196	0249
	RAU	BBEST	B		266	0249	24	0135	0338
	FRR	DELB	B	BURB1	267	0338	60	5270	0525
	LDD	BTEMP	B		268	0525	33	5800	0727
BADDR	RAA	B001			269	0064	69	0184	0437
	RAA	INDXF			270	0437	82	8001	0493
	NZU	LDDPR		LETUP	271	0493	60	0129	0583
LETUP	LDD	BTEMP			272	0583	44	0487	0388
	RAA	B001			273	0388	69	0184	0537
	RAU	BBEST	B		274	0537	82	8001	0543
	FRR	B	B		275	0543	60	5270	0575
	BMI	MDREB		LDDPR	276	0575	33	5260	0587
MDREB	LDD	BTEMP			277	0587	46	0144	0487
	RAA	B001			278	0340	69	0184	0637
	LDD	CTEMP			279	0637	82	8001	0593
	RAC	B001			280	0593	69	0022	0625
	RAU	BBEST	B		281	0625	88	8001	0331
	FRR	DELB	B	SUBB1	282	0331	60	5270	0675
	LDD	ZERO			283	0675	33	5800	0727
LDDPR	STD	INDXF			284	0487	69	0073	0276
	LDD	FDUR			285	0276	24	0129	0382
	STD	INDXZ			286	0382	69	0185	0438
	LDD	INDXD			287	0438	24	0144	0394
	STD	INDXW			288	0194	69	0135	0488
	LDD	BBEST	R		289	0488	24	0191	0244
	STD	B	B		290	0244	69	5270	0323
	STD	BINIT	B		291	0323	24	5260	0213
	RAU	BBEST	B		292	0213	24	5300	0703
	FAD	DELB	B	SUBR1	293	0703	60	5290	0445
	STU	R	B		294	0445	32	5810	0687
SUBR1	LDD	CTEMP			295	0687	21	5280	0633
	RAC	B001			296	0633	69	0022	0725
	LDD	BTEMP			297	0725	88	8001	0381
	RAA	B001			298	0381	69	0184	0737
	LDD	INDXA			299	0737	82	8001	0643
	RAA	B001		SUBR2	300	0643	69	0062	0615
SUBR2	LDD			TEMP	301	0615	80	8001	0621
	LDD			TURMM	302	0621	69	0374	0250
	BXC	0001			303	0374	69	0777	0300
	SXA	0001			304	0777	59	0001	0683
	NZA	SUBR2		RDU	305	0683	51	0001	0339
RDU	RAU	RREBT	B		306	0339	40	0621	0693
	FRR	R	B		307	0693	60	5290	0495
	NZU	SUBR3		NEXT	308	0495	33	5280	0107
SUBR3	LDD			ERR	309	0107	44	0211	0462
	RAU	ERWIN			310	0211	69	0114	0350
	FRR	ERRDR			311	0114	60	0333	0787
	NZU	BTAY		PLAY	312	0787	33	0085	0261
PLAY	RAU	INDXZ			313	0261	44	0665	0016
	FRR	FPONE			314	0016	60	0141	0545
	STU	INDXZ			315	0545	33	0196	0373
	NZU	STAY		PLYMR	316	0373	21	0141	0294
STAY	BMI	BADDR		GODDR	317	0294	44	0665	0098
PLYMR	LDD	INDXW			318	0665	46	0118	0169
	STD	INDXD		NEXT	319	0098	69	0191	0344
	LDD	BTEMP			320	0344	24	0135	0462
GOODR	LDD				321	0169	69	0184	0837
	RAA	B001			322	0837	82	8001	0743
	LDD	CTEMP			323	0743	69	0022	0775
	RAC	B001			324	0775	88	8001	0431
	RAU	RREBT	B		325	0431	60	5290	0595
	FRR	R	B		326	0595	33	5280	0157
	BMI	RPLUS		BWINS	327	0157	46	0060	0311
RPLUS	LDD			PRIME	328	0060	69	0263	0550
	LDD	FPONE			329	0263	69	0196	0299
	STD	INDXF			330	0299	24	0129	0432
	STD	INDXD			331	0432	24	0135	0538
	RAU	RREBT	B		332	0538	60	5290	0645
	FAD	DELB	B	SUBR1	333	0645	32	5810	0687
	LDD			PRIME	334	0311	69	0164	0550
	LDD	ZERO			335	0164	69	0073	0326
	STD	INDXF			336	0326	24	0129	0482
	LDD	FPONE			337	0482	69	0196	0349
	STD	INDXD			338	0349	24	0135	0588
	RAU	RREBT	B		339	0588	60	5290	0695
	FRR	DELB	B	SUBR1	340	0695	33	5810	0687
BADDR	LDD	FDUR			341	0118	69	0185	0638
	STD	INDXZ			342	0638	24	0141	0394
	RAU	INDXF			343	0394	60	0129	0733
	NZU	FIXUP		TEBTR	344	0733	44	0887	0688
TEBTR	LDD	BTEMP			345	0688	69	0184	0937

	RAB	8001		346	0937	82	8001	U793
	RAU	RREBT	B	347	0793	60	5290	0745
	F3R	R	B	348	0745	33	5280	0207
	BMI	MOREC		349	0207	46	0110	0887
	LDO	BTMP		350	0110	69	0184	0987
WDRER	RA8	8001		351	0987	82	8001	0843
	LDO	CTMP		352	0843	69	0022	0825
	RAC	8001		353	0825	88	8001	0481
	RAU	RREBT	B	354	0481	60	5290	0795
	F8B	DELR	B	355	0795	33	5810	0687
FIXUP	RAU	RREBT	B	356	0887	60	5290	0687
NEXT	LDO	RREBT	B	357	0462	69	5290	0993
	STD	RINIT	B	358	0893	84	5310	0313
	STB	0001		359	0313	53	0001	0219
	NZR	AGAIN		360	0219	42	0072	0423
AGAIN	RAU	CTMP		361	0072	60	0022	0827
	SUP	INOXA		362	0827	11	0062	0167
	STU	CTMP		363	0167	21	0022	0875
	RAU	BTMP		364	0875	60	0184	0389
	SUP	ONE		365	0389	11	0392	0347
	STU	BTMP		366	0347	21	0184	1037
	LDO	CTMP		367	1037	69	0022	0925
	RAC	8001		368	0925	88	8001	0531
	LDO	BTMP		369	0531	69	0184	1087
	RAB	8001		370	1087	82	8001	0533
ENUFF	LDO			371	0423	69	0376	0500
	LDO	8000		372	0376	69	8000	0532
	RAU	8001		373	0532	60	8001	0439
	BMI	OEVEA		374	0439	46	0442	0943
PLU8B	RAU	INOXA		375	0943	60	0135	0489
	NZU	TIREO		376	0489	44	0993	0444
TIREU	LDO	INOXA		377	0993	69	0412	0715
	RAB	8001		378	0715	82	8001	0671
	LDO	INOXA		379	0671	69	0224	0877
	RAC	8001		380	0877	88	8001	0783
	LDO	ZERO		381	0783	69	0073	0426
	STD	INOXA		382	0426	24	0135	0533
TIGHT	LDO	INOXA		383	0444	69	0412	0765
	RAB	8001		384	0765	82	8001	0721
RETTN	RAU	OELB	B	385	0721	60	5800	0255
	FOY	TEM		386	0255	34	0158	0208
	STU	DELB	B	387	0208	21	5800	0753
	RAU	DELR	B	388	0753	60	5810	0815
	FOY	TEM		389	0815	34	0158	0258
	STU	DELR	B	390	0258	21	5810	0363
	STB	0001		391	0363	53	0001	0269
	NZB	RETTN		392	0269	42	0721	0473
QUAAD	RAB	8001		393	0473	82	0001	0179
	RAU	DELR	B	394	0179	60	5810	0865
	F8B	ONEHD		395	0865	33	0168	0845
	BMI	OEVEA		396	0845	46	0442	0993
DEVEA	LDO			397	0442	69	0895	0012
	LDO	INOXA		398	0895	69	0062	0915
	RAB	8001		399	0915	80	8001	0771
REBET	LDO	EIGHT		400	0771	69	0024	0927
	RAB	8001		401	0927	83	8001	0833
STUFF	LDO	Z	A	402	0833	69	3200	0803
	STD	1985	B	403	0803	24	5985	0738
	LDO	C	A	404	0738	69	3240	1043
	STD	1986	B	405	1043	24	5986	0539
	LDO	FLUX	A	406	0539	69	3220	0523
	STD	1987	B	407	0523	24	5987	0390
	STX	0001		408	0390	51	0001	0246
	AX8	0004		409	0246	52	0004	0052
	NZA	MOREC		410	0052	40	0305	0506
MOREC	NZR	STUFF		411	0305	42	0833	0359
CARD3	PCH	1977		412	0359	71	1977	0977
	LDO	REBET		413	0977	69	0771	0012
FINIB	RAB	8001		414	0506	82	0001	0518
	RAU	OELR	B	415	0512	60	5810	0965
	F8B	ONEHO		416	0965	33	0168	0945
	BMI	END		417	0945	46	0148	0399
SOMOR	PCH	1977		418	0399	71	1977	0043
ENO	PCH	1977		419	0148	71	1977	8000
		8000			0073	00	0000	0000
					0196	10	0000	0051
					0185	40	0000	0051
					0158	10	0000	0052
					0090	10	0000	0053
					0392	00	0000	0001
					0024	00	0000	0008

## APPENDIX C

Description and Explanation of the IBM-650  
Computer Program Used for Fitting Empirically  
Experimental Data with an Even Fourier Series

The computer code was written to fit an even Fourier series to the experimentally determined surface temperature traces during a transient burst. The program was written in SOAP II and floating point form. The object program is listed and the logic diagram is shown in this appendix.

The data were fit empirically by a finite number of terms of the even trigonometric series.

$$\theta(t) = \sum_{i=1}^P B_i \cos \frac{2\pi i t}{a} ,$$

(C-1)

where

$$B_0 = 2/a \int_0^a y(t) dt$$

and  $B_1 = 1/a \int_0^a y(t) \cos \frac{2\pi i t}{a} dt .$

The integrations were carried out numerically by means of Simpson's rule thus requiring an odd number of data points.

The program input consisted of the experimental data and their respective times, the period, the time increment between data points and a specification of the number of terms. These data were read into the machine on one-word load cards. Each one-word load card contained a particular constant or piece of data and its specific storage location. Table C-1 lists the input data needed for this program. Storage locations limit the product of the number of terms and the number of data points to



less than \$50. The number of terms and the number of data points are each limited to less than 50.

Table C-1. Input data required for use of the IBM-650 program which fits empirically experimental data with a finite number of terms of an even Fourier series.

Symbol	Expanation	Storage Location
ZERO	0.00	0083
FPONE	1.00	0034
FPTWO	2.00	0108
FPTRE	3.00	0207
FPFOR	4.00	0008
PI	3.14159	0261
INDX2	Index Number 2 (0000000002)	0160
INDXJ	Number of Terms (00000000xx)	1001
INDXK	Number of Data Points (00000000xx)	1002
A	Period of Cosine Terms	1003
H	Time Increment Between Data Points	1004
T <sub>i</sub>	Time of i <sup>th</sup> data point	(1100 + i)
Y <sub>i</sub>	Experimental data at i <sup>th</sup> point	(1150 + i)

The machine punched out a card having an eight word capacity, each work consisting of 10 digits and a sign. The first output consisted of the time, the calculated value and the residual between the calculated values and the experimental data for the last data point in word locations 1, 2 and 3, respectively. The same information for the next to last data point was punched out in columns 5, 6 and 7 of the same card. The same information for the two previous data points was punched out on the next card. The above procedure was continued until the time, residuals and calculated values were punched for each data point.  $B_1$  was then stored in word location 1,  $B_2$  in word location two, etc. until all of the  $B$ 's



had been stored and punched. If more than 8 B's were calculated the first 8 were stored and a card punched. Additional B's were punched in succeeding cards with the lower number B's starting on the left of each card. Finally the summation of the square of the residual at each data point was punched out in word location 8 of a final card.



## OBJECT PROGRAM-APPENDIX C

	BLR	1000	1999	1	0000	00	0000	0000
	SYN	ERROR	1050	2	0000	00	0000	0000
	BLR	0977	0985	3	0000	00	0000	0000
	SYN	T	1100	4	0000	00	0000	0000
	SYN	Y	1150	5	0000	00	0000	0000
	SYN	8	1200	6	0000	00	0000	0000
	SYN	STA	1250	7	0000	00	0000	0000
	SYN	PHI	1300	8	0000	00	0000	0000
	SYN	FLUX	1350	9	0000	00	0000	0000
	SYN	COSBT	1400	10	0000	00	0000	0000
	SYN	START	1000	11	0000	00	0000	0000
	SYN	INDXJ	1001	12	0000	00	0000	0000
	SYN	INOXK	1002	13	0000	00	0000	0000
	SYN	A	1003	14	0000	00	0000	0000
	SYN	H	1004	15	0000	00	0000	0000
E00CR	STO	EXIT		16	0000	24	0003	0006
	8MI	NEGAT	REDUC	17	0006	46	0009	0010
NEGAT	FAO	TWOPI		18	0009	32	0012	0039
	8MI	NEGAT		19	0039	46	0009	0043
	F8B	ONEPI	COSIO	20	0043	33	0046	0023
REDUC	F8B	TWOPI		21	0010	33	0012	0089
	8MI		REDUC	22	0089	46	0042	0010
	FAO	ONEPI	COSIU	23	0042	32	0046	0023
COSIO	STU	THETA		24	0023	21	0028	0031
	RSU	FPONE		25	0031	61	0034	0139
	STU	TERMM		26	0139	21	0044	0047
	STU	FUNKT		27	0047	21	0002	0005
	STL	ENN	NEGST	28	0005	20	0059	0062
E00SR	STO	EXIT		29	0050	24	0003	0056
	8MI	NEGAV	REODU	30	0056	46	0109	0060
NEGAV	FAO	TWOPI		31	0109	32	0012	0189
	8MI	NEGAV		32	0189	46	0109	0093
	F8B	ONEPI	SINET	33	0093	33	0046	0073
REDUD	F8B	TWOPI		34	0060	33	0012	0239
	8MI		REDUD	35	0239	46	0092	0060
	FAO	ONEPI	SINET	36	0092	32	0046	0073
SINET	STU	THETA		37	0073	21	0028	0001
	R8U	8003		38	0081	61	8003	0289
	STU	TERMM		39	0289	21	0044	0097
	STU	FUNKT		40	0097	21	0002	0055
	LOO	FPONE		41	0055	69	0034	0037
	STO	ENN	NEGST	42	0037	24	0059	0062
NEGST	RAU	ENN		43	0062	60	0059	0013
	FAO	FPONE		44	0013	32	0034	0011
	STU	NPONE		45	0011	21	0016	0019
	FAO	FPONE		46	0019	32	0034	0061
	STU	ENN		47	0061	21	0059	0112
	RSU	TERMM		48	0112	61	0044	0049
	FMP	THETA		49	0049	39	0028	0078
	FMP	THETA		50	0078	39	0028	0128
	FOV	NPONE		51	0128	34	0016	0060
	FOV	ENN		52	0060	34	0059	0159
	STU	TERMM		53	0159	21	0044	0147
	RAM	FUNKT		54	0147	67	0002	0007
	STL	FMAG		55	0007	20	0111	0014
	RAM	TERMM		56	0014	67	0044	0099
	RAU	8002		57	0099	60	8002	0057
	FOV	FMAG		58	0057	34	0111	0161
	F8B	SIZEB		59	0161	33	0064	0041
	8MI	ENUFF		60	0041	46	0094	0045
	RAU	FUNKT		61	0045	60	0002	0107
	FAO	TERMM		62	0107	32	0044	0021
	STU	FUNKT	NEGST	63	0021	21	0002	0062
	RAU	FUNKT	EXIT	64	0094	60	0002	0003
ENUFF	10	0000	0043	65	0064	10	0000	0043
SIZEB	62	8318	5351	66	0012	62	8318	5351
TWOPI	31	4159	2751	67	0046	31	4159	2751
ONEPI	10	0000	0051	68	0034	10	0000	0051
FPONE	STO	EXITC		69	0100	24	0053	0106
COS	RAU	STA	A	70	0106	60	3250	0105
	FMP	T	B	71	0105	39	5100	0150
	LOD			72	0150	69	0103	0000
	STU	COSBT	EXITC	73	0103	21	7400	0053
INTGT	STO	EGSIT		74	0200	24	0153	0156
	RA8	0001		75	0156	82	0001	0162
	RAU	PHI	B	76	0162	60	5300	0155
	STU	ACCUM	LOP33	77	0155	21	0110	0063
LOP33	AX8	0001		78	0063	52	0001	0069
	RAU	PHI	B	79	0069	60	5300	0205
	FMP	PPFOR		80	0205	39	0008	0058
	FAO	ACCUM		81	0058	32	0110	0087
	STU	ACCUM		82	0087	21	0110	0113
	AX8	0001		83	0113	52	0001	0119
	RAU	PHI	B	84	0119	60	5300	0255
	FMP	PTWO		85	0255	39	0108	0158
	FAO	ACCUM		86	0158	32	0110	0137
	STU	ACCUM		87	0137	21	0110	0163
	RAU	8006		88	0163	60	8006	0071
	SUP	INDXK		89	0071	11	1002	0157
	AUP	INOX2		90	0157	10	0160	0015
	NZU	LOP33	G0111	91	0015	44	0063	0020
G0111	AX8	0001		92	0020	52	0001	0026
	RAU	PHI	B	93	0026	60	5300	0308
	FMP	PPFOR		94	0308	39	0008	0208
	FAO	ACCUM		95	0208	32	0110	0187
	STU	ACCUM		96	0187	21	0110	0243
	AX8	0001		97	0243	52	0001	0169
	RAU	PHI	B	98	0169	60	5300	0355
	FAO	ACCUM		99	0355	32	0110	0237
	FMP	H		100	0237	39	1004	0004
	FOV	PTRE	EGBIT	101	0004	34	0207	0153
E00CL	STO	ZZZ1		102	0250	24	0203	0206
	LOD	ZZZ10		103	0206	69	0209	0212
	STO	0977		104	0212	24	0977	0130
	STO	0978		105	0030	24	0978	0131
	STO	0979		106	0131	24	0979	0032
	STO	0980		107	0032	24	0980	0033
	STO	0981		108	0033	24	0981	0084
	STO	0982		109	0084	24	0982	0035
	STO	0983		110	0035	24	0983	0036
	STO	0984	ZZZ1	111	0036	24	0984	0203
ZZZ10	OO	0000	0000	112	0209	00	0000	0000
START	RAU	INDXK		113	1000	60	1002	0257
	WPU	INDXJ		114	0257	19	1001	0022
	STL	INDXC		115	0022	20	0027	0080

	LDD ZERO		INPUT	116	0080	69	0083	0086
	RAA 8001			117	0086	80	8001	0142
	STD M	LOOP1		118	0142	24	0095	0048
LDDP1	AXA 0001			119	0048	50	0001	0054
	RAU N		INPUT	120	0054	60	0095	0149
	FAD FPONE			121	0149	32	0034	0211
	BTU N			122	0211	21	0095	0098
	FMP FPTWO		INPUT	123	0098	39	0108	0258
	FMP PI		INPUT	124	0258	39	0261	0311
	FDV A		INPUT	125	0311	34	1003	0253
	STU HTA	A		126	0253	21	3250	0303
	RAU 8005			127	0303	60	8005	0361
	SUP INDXJ			128	0361	11	1001	0405
	NZU LOOP1	CONT1		129	0405	44	0048	0210
CONT1	LDD INDXJ			130	0210	69	1001	0104
	RAA 8001			131	0104	80	8001	0260
	LDD INDXK			132	0260	69	1002	0455
	RAB 8001			133	0455	82	8001	0411
	LDD INDXC			134	0411	69	0027	0130
	RAC 8001	LOOP2		135	0130	88	8001	0136
LOOP2	LDD 0001		SUBROUTINE	136	0136	69	0339	0100
	SXC 0001			137	0339	53	0001	0145
	NZB LOOP2	MORET		138	0145	59	0001	0001
MORET	SXA 0001			139	0001	42	0136	0505
	NZA CONT2	CDNT3		140	0505	51	0001	0461
CONT2	LDD INDXK			141	0461	40	0114	0065
	AXB 8001	LOOP2		142	0114	69	1002	0555
CONT3	RAA 0000			143	0555	52	8001	0136
	LDD INDXK			144	0065	80	0000	0121
	AXB 8001	LODP3		145	0121	69	1002	0605
LODP3	LDD Y			146	0605	52	8001	0511
	STD PHI	B		147	0511	69	5150	0353
	SXB 0001			148	0353	24	5300	0403
	NZB LOOP3	CONT4		149	0403	53	0001	0259
CONT4	LDD 0001		SUBROUTINE	150	0259	42	0511	0263
	FMP FPTWO	INTGT		151	0263	69	0116	0200
	FDV A			152	0116	39	0108	0308
	BTU HZERO	CONT5		153	0308	34	1003	0453
CONT5	RAA 0000			154	0453	21	0358	0561
	RAB 0000			155	0561	80	0000	0017
	RAC 0000	CON55		156	0017	82	0000	0123
CON55	LDD INDXC			157	0123	88	0000	0029
	RAC 8001			158	0029	69	0027	0180
	LDD INDXJ			159	0180	88	8001	0186
	RAA 8001	LOPPP		160	0186	69	1001	0154
LOPPP	LDD INDXK			161	0154	80	8001	0310
	RAB 8001	LOOP4		162	0310	69	1002	0655
LODP4	RAU Y			163	0655	82	8001	0611
	FMP COBBT	B		164	0611	60	5150	0705
	STD PHI	CR		165	0705	39	7400	0300
	SXB 0001			166	0300	21	5300	0503
	SXC 0001			167	0503	53	0001	0309
	NZR LOOP4	CDNT6		168	0309	59	0001	0115
CONT6	LDD 0001	INTDT		169	0115	42	0611	0219
	FMP FPFOR			170	0219	69	0072	0200
	FDV A			171	0072	39	0008	0408
	STU B	A		172	0408	34	1003	0553
	SXA 0001			173	0553	21	3200	0603
	NZA LOPPPP	CONT7		174	0603	51	0001	0359
CONT7	RAA 0000			175	0359	40	0310	0313
	RAB 0000			176	0313	80	0000	0269
	RAC 0000			177	0269	82	0000	0025
	LDD INDXK			178	0025	69	1002	0755
	AXB 8001			179	0755	52	8001	0661
	LDD INDXJ			180	0661	69	1001	0204
	AXA 8001			181	0204	50	8001	0360
	RAC 0000	CONT77		182	0360	88	0000	0166
	LDD INDXC			183	0166	69	0027	0230
	AXC 8001			184	0230	58	8001	0236
	LDD INDXJ			185	0236	69	1001	0254
	RAA 8001			186	0254	80	0001	0410
	LDD ZERO			187	0410	69	0083	0286
	STD HOLA	LOOP5		188	0286	24	0389	0192
LOOP5	RAU B			189	0192	60	3200	0805
	FMP COBBT	A		190	0805	39	7400	0350
	FAD HOLD	C		191	0350	32	0389	0165
	BTU HOLD			192	0165	21	0389	0242
	SXA 0001			193	0242	51	0001	0148
	LDD INDXK			194	0148	69	1002	0855
	SXC 8001			195	0855	59	8001	0711
	NZC	CONT8		196	0711	48	0164	0215
	BWC CONT8	LOOP5		197	0164	49	0215	0192
CONT8	RAU HOLD			198	0215	60	0389	0143
	FAD HZERO			199	0143	32	0358	0085
	BTU FLUX			200	0085	21	5350	0653
	F8B Y	B		201	0653	33	5150	0077
	BTU ERROR	B		202	0077	21	5050	0703
	SXB 0001			203	0703	53	0001	0409
	SXC 0001			204	0409	59	0001	0265
	NZB COM77	PRINT		205	0265	42	0166	0319
PRINT	LDD INDXK			206	0319	69	1002	0905
	AXB 8001	LOOP7		207	0905	52	8001	0761
LOOP7	LDD 0008	LOOP6		208	0761	69	0214	0250
LOOP6	RSA 0008		SUBROUTINE	209	0214	81	0008	0070
	LDD T			210	0070	69	5100	0753
	STD 0985	B		211	0753	24	2985	0038
	LDD FLUX	A		212	0038	69	5350	0803
	STD 0986	B		213	0803	24	2986	0439
	LDD ERROR	B		214	0439	69	5050	0853
	STD 0987	A		215	0853	24	2987	0040
	AXA 0004			216	0040	50	0004	0096
	SXB 0001			217	0096	53	0001	0052
	NZB	FINIS		218	0052	42	0955	0256
	NZA LOOP6	CONT9		219	0256	40	0070	0459
	PCH 0977	LOOP7		220	0459	71	0977	0761
	PCH 0977			221	0761	71	0977	0127
	R8B 0007			222	0127	83	0007	0133
	LDD 0007			223	0133	69	0336	0250
	LDD HZERO	EOOCL		224	0250	69	0358	0811
	STD 0977			225	0811	24	0977	0280
	RAA 0001	LOOP8		226	0280	80	0001	0386
LOOP8	LDD B			227	0386	69	5200	0903
	STD 0985	A		228	0903	24	4985	0088
	AXA 0001	B		229	0088	50	0001	0144
	AXB 0001			230	0144	52	0001	0400

	RAU	8006	
	BU	INDEX	
	NZU		FINAL
	NZB	LOOPB	MOBT
MOBT	PCH	0977	
	LDD		EOOCL
	RBB	0007	LOOPB
FINAL	LDD	B	A
	MTD	0985	B
	PCM	0977	
	LDD	INDEX	
	XAP	8001	
	LDD	ZERO	
	STD	SOMME	LOPPU
LOPPU	RAU	ERROR	B
	FMP	ERROR	B
	AD	SOMME	
	STU	SOMME	
	SXB	0001	
	NZB	LOPPU	NDONE
NOONE	LDD		EOOCL
	LDD	SOMME	
	STD	0984	
	PCH	0977	8000

231	0400	60	8005	0307
232	0307	11	1001	0306
233	0306	44	0509	0460
234	0509	42	0386	0363
235	0363	71	0977	0177
236	0177	69	0330	0250
237	0330	83	0007	0386
238	0460	69	3200	0953
239	0953	24	4985	0138
240	0138	71	0977	0227
241	0227	69	1002	0356
242	0356	82	8001	0262
243	0262	69	0083	0436
244	0436	24	0489	0292
245	0292	60	5050	0406
246	0406	39	5050	0450
247	0450	32	0489	0315
248	0315	21	0489	0342
249	0342	53	0001	0198
250	0198	42	0292	0102
251	0102	69	0456	0250
252	0456	69	0489	0392
253	0392	24	0984	0287
254	0287	71	0977	8000
	0083	00	0000	0000
	0034	10	0000	0051
	0108	20	0000	0051
	0207	30	0000	0051
	0008	40	0000	0051
	0160	00	0000	0002
	0261	31	4159	2751

## APPENDIX D

Description and Explanation of the IBM-650  
Computer Program Used to Calculate Temperature  
Distributions.

The computer program was written to calculate the temperature distribution in a unit cell of a nuclear reactor system given the heat generation rate and fuel element surface temperature as a function of time. The temperature rise over the initial temperature is given by

$$\theta_f(x,t) = \sum_{i=1}^p B_i Z_i^{\frac{1}{2}} \cos(\beta_i t + \varphi_i) - \sum_{n=1,3,5,\dots}^{\infty} \frac{\cos(\frac{n\pi x}{2L}) e^{-\frac{n^2 \pi^2 \alpha}{4L^2} t}}{(L^2 / n\pi\alpha) (\sin \frac{n\pi}{2})}$$

$$+ \left\{ \sum_{i=1}^p \frac{B_i \left( \frac{n^2 \pi^2 \alpha}{4L^2} \right)}{\frac{n^2 \pi^2 \alpha}{16L^2} + \beta_i^2} + \sum_{j=1}^s \frac{q_{\infty} \alpha A_j \cosh \kappa L}{k \left( \frac{n^2 \pi^2 \alpha}{4L^2} + \lambda_j \right) \left( \frac{n^2 \pi^2 \alpha}{4L^2} + \alpha \kappa^2 \right)} \right\} \quad (D-1)$$

$$+ \sum_{j=1}^s \frac{q_{\infty} \alpha A_j e^{\lambda_j t}}{k(\alpha \kappa^2 - \lambda_j)} \left\{ \frac{\cosh(\sqrt{\frac{\lambda_j}{\alpha}} x) \cosh \kappa x}{\cosh(\sqrt{\frac{\lambda_j}{\alpha}} L)} - \cosh \kappa x \right\}$$

in the fuel and by

$$\theta_m(x,t) = \sum_{i=1}^p B_i Z_i^{\frac{1}{2}} \cos(\beta_i t + \varphi_i) + \sum_{n=1,3,5,\dots}^{\infty} \frac{\cos(\frac{n\pi x}{2L}) e^{-\frac{n^2 \pi^2 \alpha}{4L^2} t}}{(L^2 / n\pi\alpha) (\sin \frac{n\pi}{2})}$$



$$\begin{aligned}
 & \times \left\{ \sum_{i=1}^p \frac{B_i \left( \frac{n^2 \pi^2 \alpha}{4L^2} \right)}{\frac{n^2 \pi^2 \alpha}{16L^4} + \beta_i} - \sum_{j=1}^s \frac{F \propto A_j}{k \left( \frac{n^2 \pi^2 \alpha}{4L^2} + \lambda_j \right)} \right\} \\
 & + \sum_{j=1}^s \frac{F \propto A_j e^{\rho_j t}}{k (-\lambda_j)} \left\{ \frac{\cosh \sqrt{\frac{\lambda_j}{\alpha}} x}{\cosh \sqrt{\frac{\lambda_j}{\alpha}} L} - 1 \right\}
 \end{aligned} \tag{D-2}$$

in the moderator. The moderator equation is obtained from the fuel temperature distribution by setting  $q_{\infty}$  equal to  $\underline{F}$  and  $\underline{\kappa}$  equal to zero.

The equivalence between elements of the algebraic equations and the symbolic logic of the computer program is shown in Table D-1.

Table D-1. Definition of symbolic terms of the IBM-650 computer program for calculating temperature distributions.

$$\begin{aligned}
 A1_i &= B_i Z_i(x) \cos \beta_i t \\
 A3P_j &= q_{\infty} \propto A_j e^{\lambda_j t} / k (\alpha \kappa^2 - \lambda_j) \\
 A3SUM_j &= \frac{\cosh \kappa L \cosh \sqrt{\frac{\lambda_j}{\alpha}} x}{\cosh \sqrt{\frac{\lambda_j}{\alpha}} L} - \cosh \kappa x \\
 A3_j &= (A3P_j) (A3SUM_j) \\
 CSHLL_j &= \cosh \sqrt{\frac{\lambda_j}{\alpha}} L \\
 CSHLX_j &= \cosh \sqrt{\frac{\lambda_j}{\alpha}} x \\
 COSLL_j &= \cos \sqrt{\frac{\lambda_j}{\alpha}} L \\
 COSLX_j &= \cos \sqrt{\frac{\lambda_j}{\alpha}} x
 \end{aligned}$$

Table D-1 cont.

$$\text{ARG1}_n = n\pi \quad 2L$$

$$\text{ARG2}_n = n^2 \pi^2 \alpha \quad 4L^2$$

$$\text{A2ST1}_i = B_i \left( \frac{n^2 \pi^2 \alpha}{4L^2} \right) / \left( \frac{n^4 \pi^4 \alpha^2}{16L^2} + \beta_i^2 \right)$$

$$\text{A2ST1}_j = q_{\infty} \alpha \quad A_j \cosh \kappa L / k \left( \frac{n^2 \pi^2 \alpha}{4L^2} + \lambda_j \right) \left( \frac{n^2 \pi^2 \alpha}{4L^2} + \alpha \kappa^2 \right)$$

$$\text{A2DDT}_n = \frac{\cos \frac{n\pi x}{2L} e^{-\frac{n^2 \pi^2 \alpha}{4L^2} t}}{\left( \frac{L^2}{n\pi \alpha} \right) \sin \frac{n\pi}{2}}$$

$$\text{A2SUM}_n = \left( \sum_{i=1}^p \text{A2ST1}_i + \sum_{j=1}^s \text{A2ST1}_j \right)_n$$

$$\text{TERM}_n = (\text{A2DDT}_n) (\text{A2SUM}_n)$$

Table D-2. Input Data Required for Use of the  
IBM-650 Computer Program Used to  
Calculate Temperature Distributions.

Symbol	Explanation	Storage Location
ZERO	0.00	0264
ONE	1.00	0662
TWO	2.00	0520
PI	3.14159	0018
FIFTY	50.00	0361
CRIT	0.0001	0788
ALPHA	Thermal Diffusivity	0278

Table D-2 cont.

Symbol	Explanation	Storage Location
KAPPA	Reciprocal of Thermal Neutron Diffusion Length in Fuel	0436
Q <sub>00</sub>	Normalization Factor for Heat Generation	0324
KAY	Thermal Conductivity	0581
L	Half-Thickness of Region	0186
INDXM	No. of Terms, Surface Temperature Fit (00000000xx)	0076
NOLAM	No. of Terms, Heat Generation Fit (00000000xx)	0456
AYEJ <sub>j</sub>	Amplitude Parameter, Heat Generation Fit, A <sub>j</sub>	(0200 + j)
LAMDA <sub>j</sub>	Exponential Parameter, Heat Generation Fit, j	(0220 + j)
AMMM <sub>i</sub>	Amplitude Parameter, Surface Temperature Fit, B <sub>i</sub>	(0100 + i)
BTAA <sub>i</sub>	Period Parameter Surface Temperature Fit, B <sub>i</sub>	(0120 + i)

The output from this program is punched out on one card having an eight word capacity, one word consisting of 10 digits and a sign. The form of the output is shown in Table D-3.

Table D-3. Output Form for IBM-650 Computer  
Program Used to Calculate Temperature  
Distribution

WORD 1	WORD 2	WORD 3	WORD 4	WORD 5	WORD 6	WORD 7	WORD 8
$\theta(x, t)$	$\sum_{i=1}^p A1_i$	$\sum_{n=1,3,5}^{\infty} (\text{Term})_n$	$\sum_{j=1}^s A3_j$	x	t	--	--



## OBJECT PROGRAM-APPENDIX D

	HLR 0200	0W60	1	0000	00	0000	0000	-1
	HLR 1800	1800	2	0000	00	0000	0000	-1
	SYN ARTAN	1800	3	0000	00	0000	0000	-1
	SYN STAHT	1999	4	0000	00	0000	0000	-1
	SYN AYEJ	0200	5	0000	00	0000	0000	-1
	SYN LAMDA	0280	6	0000	00	0000	0000	-1
	SYN A3	0240	7	0000	00	0000	0000	-1
	HLR 1951	1960	8	0000	00	0000	0000	-1
	HLR 1977	1984	9	0000	00	0000	0000	-1
	HLR 0100	0160	10	0000	00	0000	0000	-1
	SYN AMUH	0100	11	0000	00	0000	0000	-1
	SYN HTAA	0120	12	0000	00	0000	0000	-1
	SYN ALPHA	027H	13	0000	00	0000	0000	-1
	SYN KAPPA	0436	14	0000	00	0000	0000	-1
	SYN L	0186	15	0000	00	0000	0000	-1
	SYN QOO	0324	16	0000	00	0000	0000	-1
	SYN KAY	05H1	17	0000	00	0000	0000	-1
	SYN INOXM	0076	18	0000	00	0000	0000	-1
	SYN NOLAM	0456	19	0000	00	0000	0000	-1
	SYN A1	0140	20	0000	00	0000	0000	-1
PHISH	STO ABCD2		21	0000	24	0003	0006	-1
	RAU FCL		22	0006	60	0009	0013	-1
	FMP FCX		23	0013	39	0016	0024	-1
	STU DENN1		24	0066	21	0020	0023	-1
	RAU FSL		25	0023	60	0026	0031	-1
	FMP FSX		26	0031	39	0034	0044	-1
	FAD DENN1		27	0084	32	0020	0047	-1
	STU DN		28	0047	21	0002	0005	-1
	RAU FSL		29	0005	60	0026	0081	-1
	FMP FCX		30	0081	39	0016	0166	-1
	STU NUMM2		31	0166	21	0070	0073	-1
	RAU FCL		32	0073	60	0009	0063	-1
	FMP FSX		33	0063	39	0034	0184	-1
	FSR NUMM2		34	0184	33	0070	0097	-1
	FDV DN		35	0097	34	0002	0052	-1
	LOO		36	0052	69	0055	1800	-1
	STU THETO	ARTAN	37	0055	21	0010	0163	-1
	RAU DN		38	0163	60	0002	0007	-1
	HMI THETO	ABCD2	39	0007	46	0060	0003	-1
	FAD PI		40	0060	60	0010	0015	-1
	STU THETO	ABCD2	41	0015	32	0018	0045	-1
	STO AAA1		42	0045	21	0010	0003	-1
EOOEA	STU AAA14		43	0050	24	0053	0056	-1
	RAU AAA16		44	0056	31	0310	0263	-1
	FAM AAA14		45	0263	60	0266	0021	-1
	STU AAA2		46	0021	37	0310	0037	-1
	LOO AAA3		47	0037	31	0042	0095	-1
	STU AAA4	AAAAH	48	0095	69	0040	0001	-1
AAAAH	STU AAA4		49	0001	24	0004	0057	-1
	RAU AAA2		50	0057	60	0042	0127	-1
	FSR AAA5		51	0197	33	0300	0027	-1
	HMI AAA6		52	0027	46	0030	0141	-1
	STU AAA2		53	0181	21	0042	0195	-1
	RAU AAA4		54	0195	60	0004	0059	-1
	FMP AAA7		55	0059	39	0012	0062	-1
AAAA6	STU AAA4	AAAAH	56	0062	21	0004	0057	-1
	RAU AAA2		57	0030	60	0042	0297	-1
	FSR AAA3		58	0297	33	0048	0025	-1
	HMI AAA28		59	0025	46	0028	0029	-1
	STU AAA2		60	0029	21	0042	0295	-1
	RAU AAA4		61	0295	60	0004	0309	-1
	FMP AAA9		62	0309	39	0162	0262	-1
AAAA2H	STU AAA4	AAAA6	63	0262	21	0004	0070	-1
	RAU AAA4		64	0070	60	0042	0347	-1
	FSR AAA10		65	0347	33	0350	0077	-1
	HMI AAA11		66	0077	46	0080	0281	-1
	STU AAA2		67	0281	21	0042	0345	-1
	RAU AAA4		68	0345	60	0004	0359	-1
	FMP AAA12		69	0359	39	0312	0362	-1
	STU AAA4	AAAA2H	70	0362	21	0004	0388	-1
AAAA11	RAU AAA2		71	0388	60	0042	0397	-1
	LOO	AAAA1?	72	0397	69	0400	0303	-1
	FMP AAA4		73	0400	39	0004	0054	-1
	STU AAA13		74	0054	21	0008	0011	-1
	RAU AAA14		75	0011	60	0310	0065	-1
	HMI AAA15		76	0065	46	0048	0019	-1
	RAU AAA13	AAAA1	77	0019	60	0008	0033	-1
AAAA15	RAU AAA3		78	0068	60	0048	0353	-1
	FOV AAA13	AAAA1	79	0353	34	0008	0053	-1
AAAA17	STU AAA18		80	0303	24	0306	0403	-1
	RAU AAA3		81	0409	60	0048	0043	-1
	FAD AAA2		82	0403	32	0042	0069	-1
	STU AAA19		83	0069	21	0024	0177	-1
	LOO AAA27		84	0177	69	0180	0033	-1
	STU AAA20		85	0033	24	0036	0039	-1
	STU AAA21		86	0039	24	0092	0395	-1
	RAU AAA2		87	0395	60	0042	0447	-1
	FMP AAA2		88	0447	39	0042	0192	-1
AAAA22	STU AAA23	AAAA22	89	0192	21	0046	0049	-1
	FOV AAA21		90	0049	34	0092	0292	-1
	STU AAA24		91	0292	21	0096	0099	-1
	FAD AAA19		92	0099	32	0024	0051	-1
	STU AAA19		93	0051	21	0024	0277	-1
	RAU AAA24		94	0277	60	0096	0301	-1
	FOV AAA19		95	0301	34	0024	0074	-1
	FSR AAA25		96	0074	33	0327	0453	-1
	HMI	AAAA26	97	0453	46	0356	0307	-1
AAAA26	RAU AAA19	AAAA1H	98	0356	60	0024	0306	-1
	RAU AAA20		99	0307	60	0036	0041	-1
	FAD AAA20		100	0041	32	0048	0075	-1
	STU AAA20		101	0075	21	0036	0089	-1
	FMP AAA21		102	0089	39	0092	0342	-1
	STU AAA21		103	0342	21	0092	0445	-1
	RAU AAA23		104	0445	60	0046	0351	-1
	FMP AAA2		105	0351	39	0042	0392	-1
	STU AAA23	AAAA22	106	0392	21	0046	0049	-1
AAAA3	STU		107	0049	10	0000	0031	-1
AAAA5	STU		108	0000	50	0000	0051	-1
AAAA7	STU		109	0051	14	0410	0053	-1
AAAA9	STU		110	0053	27	1830	0051	-1
AAAA10	STU		111	0051	20	0000	0050	-1
AAAA12	STU		112	0050	12	2140	0051	-1
AAAA16	STU		113	0051	00	0000	0000	-1
AAAA25	STU		114	0000	70	0000	0047	-1
AAAA27	STU		115	0047	20	0000	0051	-1

ZMXSH	STU	ARCD1			
	RAU	ARGGX			
	LDD		CUSHX		
	STU	CHAAAX			
	RAU	ARGGX			
	LDD		EODCR		
	STU	CSAAX			
	RAU	ARGGX			
	LDD		SINHX		
	STU	SHAAX			
	RAU	ARGGX			
	LDD		EODSH		
	STU	SNAAX			
	RAU	ARGGL			
	LDD		COSH		
	STU	CHAAL			
	RAU	ARGGL			
	LDD		EODCH		
	STU	CSAAL			
	RAU	ARGGL			
	LDD		SINHX		
	STU	BHAAL			
	RAU	ARGGL			
	LDD		EODSH		
	STU	SMAAL			
	RAU	CHAAL			
	FMP	CBAAL			
	STU	FCL			
	FMP	CHAAL			
	FMP	CSAAL			
	STU	DEIIN			
	RAU	SMAAL			
	FMP	SMAAL			
	STU	FSL			
	FMP	SMAAL			
	FMP	SMAAL			
	FAD	DEIIN			
	STU	DENNMM			
	RAU	CHAAAX			
	FMP	CSAAX			
	STU	FCX			
	FMP	BOOJ			
	STU	NUIIM			
	RAU	SMAAX			
	FMP	SMAAX			
	STU	FSX			
	FMP	BOOJ			
	FAD	NUIIM			
	FOV	DENNMM			
	LDD	ABCD1	EODAU		
	STU	NEXTC			
	STU	ARG			
COSH	LDD		EODEA		
	STU	EARGP			
	RSU	ARG			
	LDD		EODEA		
	FAD	EARGP			
	FOV	TWO	NEXTC		
SINHX	STU	NEXTS			
	STU	ARG			
	RSU	ARG			
	LDD		EODEA		
	STU	EARGM			
	RAU	ARG			
	LDD		EODEA		
	FBB	EARGM			
	FOV	TWO	NEXTS		
EODCR	STU	EXIT			
	BMI	NEGAT	NEIUC		
NEGAT	FAD	TWOPI			
	BMI	NEGAT			
	FBB	ONEPI	COSIO		
REDUC	FBB	TWOPI			
	BMI		REDUC		
	FAD	ONEPI	COSIO		
	STU	THETA			
	RSU	FPONE			
	STU	TERMM			
	STU	FUNKT			
	STL	ENN	NEGST		
EODSR	STU	EXIT			
	BMI	NEGAV			
NEGAV	FAD	TWOPI	REDUU		
	BMI	NEGAV			
	FBB	ONEPI	SINET		
REDUO	FBB	TWOPI			
	BMI		REDUU		
	FAD	ONEPI	SINET		
	STU	THETA			
	RSU	BOOJ			
	STU	TERMM			
	STU	FUNKT			
	LDD	FPONE			
	STU	ENN	NEGST		
	RAU	ENN			
	FAD	FPONE			
	STU	NPONE			
	FAD	FPONE			
	STU	ENN			
	RSU	TERMM			
	FMP	THETA			
	FMP	THETA			
	FOV	NPONE			
	FOV	ENN			
	STU	TERMM			
	RAM	FUNKT			
	STL	FMAG			
	RAM	TERMM			
	RAU	BOOJ			
	FOV	FMAG			
	FBB	SIZEB			
	BMI	ENUFF			
	RAU	FUNKT			
	FAD	TERMM			
	STU	FUNKT	NEGST		
	RAU	FUNKT	EXIT		
ENUFF		10	0000	0043	
SIZEB		62	8318	5351	
TWOPI		31	4159	2751	
ONEPI		10	0000	0051	
FPONE					
EODAU	STU	8EXT			

116	0450	24	0503	0406
117	0406	60	0459	0313
118	0313	60	0316	0169
119	0316	21	0170	0173
120	0173	60	0459	0363
121	0363	60	0366	0269
122	0366	21	0270	0273
123	0273	60	0459	0413
124	0413	60	0416	0319
125	0416	21	0320	0323
126	0323	60	0459	0463
127	0463	60	0466	0369
128	0466	21	0370	0373
129	0373	60	0176	0331
130	0373	60	0284	0169
131	0284	21	0038	0091
132	0091	60	0176	0381
133	0381	60	0334	0269
134	0334	21	0088	0191
135	0191	60	0176	0431
136	0431	60	0384	0319
137	0384	21	0188	0291
138	0291	60	0176	0481
139	0481	60	0434	0369
140	0434	21	0288	0441
141	0441	60	0038	0043
142	0043	39	0088	0338
143	0338	21	0009	0412
144	0412	39	0038	0388
145	0388	39	0088	0438
146	0438	21	0442	0495
147	0495	60	0288	0093
148	0093	39	0188	0488
149	0488	21	0026	0079
150	0079	39	0288	0538
151	0538	39	0188	0588
152	0588	32	0442	0419
153	0419	21	0174	0377
154	0377	60	0170	0175
155	0175	39	0270	0420
156	0420	21	0016	0469
157	0469	39	8003	0423
158	0423	21	0078	0531
159	0531	60	0370	0275
160	0275	39	0320	0470
161	0470	60	0034	0087
162	0087	39	8003	0391
163	0391	32	0078	0305
164	0305	34	0174	0274
165	0274	69	0503	0506
166	0169	24	0022	0325
167	0325	21	0280	0083
168	0083	60	0086	0050
169	0086	21	0040	0193
170	0193	61	0280	0035
171	0035	60	0638	0050
172	0638	32	0040	0017
173	0017	34	0520	0022
174	0319	24	0072	0375
175	0375	21	0280	0183
176	0183	61	0280	0085
177	0085	60	0688	0050
178	0688	21	0492	0545
179	0545	60	0280	0005
180	0185	60	0738	0050
181	0738	33	0492	0519
182	0519	34	0520	0072
183	0269	24	0172	0425
184	0425	46	0178	0179
185	0178	32	0631	0357
186	0357	46	0178	0061
187	0061	33	0014	0441
188	0179	33	0631	0407
189	0407	46	0360	0179
190	0360	32	0014	0441
191	0441	21	0196	0199
192	0199	61	0302	0457
193	0457	21	0462	0165
194	0165	21	0570	0473
195	0473	20	0427	0530
196	0530	24	0172	0475
197	0475	46	0328	0279
198	0328	32	0631	0507
199	0507	46	0328	0161
200	0161	33	0014	0491
201	0279	33	0631	0557
202	0557	46	0410	0279
203	0410	32	0014	0491
204	0491	21	0196	0299
205	0299	61	8003	0697
206	0697	21	0462	0265
207	0265	21	0570	0523
208	0523	60	0302	0355
209	0355	24	0427	0330
210	0330	60	0427	0681
211	0681	32	0302	0329
212	0329	21	0484	0187
213	0187	32	0302	0379
214	0379	30	0427	0380
215	0380	61	0462	0067
216	0067	39	0196	0296
217	0296	39	0196	0346
218	0346	34	0484	0534
219	0534	34	0427	0477
220	0477	21	0462	0315
221	0315	67	0570	0525
222	0525	60	0429	0032
223	0032	67	0462	0167
224	0167	60	8002	0575
225	0575	34	0429	0479
226	0479	33	0082	0509
227	0509	46	0512	0513
228	0513	60	0570	0625
229	0625	32	0462	0169
230	0169	21	0570	0330
231	0330	60	0570	0172
232	0082	10	0000	0043
233	0631	62	8318	5351
234	0014	31	4159	2751
235	0302	10	0000	0051
236	0506	24	0559	0562



	RMI	SERR		237	0562	46	0365	0514
	NZE		BE XT	238	0516	45	0620	0559
	STU	SA		239	0620	21	0374	0527
	FAD	S10		240	0527	32	0430	0657
	FMP	SHAF	BB	241	0657	39	0460	0510
SR	STU	SSAV	SAH	242	0510	21	0064	0267
BAR	RAU	SA		243	0267	60	0374	0529
	FOV	SSAV		244	0529	34	0064	0164
	FAU	SSAV		245	0164	32	0064	0541
	FMP	SHAF		246	0541	39	0460	0560
	FSR	SSAV		247	0560	33	0064	0591
	NZU		BR	248	0591	44	0595	0396
	RMI		BR	249	0595	46	0098	0396
	FAD	SSAV		250	0098	32	0064	0641
	STU	SSAV	BAH	251	0641	21	0064	0267
SR	RAU	SSAV	BE XT	252	0396	60	0064	0559
BERR	HLT	0000	BE XT	253	0365	01	0000	0559
SHAF	S10	0000	0050	254	0460	50	0000	0060
		10	0051	255	0430	10	0000	0051
START	RCO	1951		256	1999	70	1951	0401
	LOO	1951		257	0401	69	1951	0304
	STO	X		258	0304	24	0707	0610
	LOO	1952		259	0610	69	1952	0405
	STO	T		260	0405	24	0058	0261
	LOO	ZERO		261	0261	69	0264	0317
	STO	HOLD		262	0317	24	0670	0573
	LOO	INDXW		263	0573	69	0076	0579
	RAU	8001		264	0579	82	8001	0285
	LOO	ZERO		265	0285	69	0264	0367
	STO	HOLD	LOPP1	266	0367	24	0670	0623
LOPP1	RAU	STAA	B	267	0623	60	4120	0675
	FOV	ALPHA		268	0675	34	0278	0378
	FOV	TWO		269	0378	34	0520	0720
	LOO		E00AU	270	0720	69	0673	0506
	STU	HQRTT		271	0673	21	0428	0731
	FMP	X		272	0731	39	0707	0757
	STU	ARGGX		273	0757	21	0459	0612
	RAU	SQRTT		274	0612	60	0428	0283
	FMP	L		275	0283	39	0186	0286
	STU	ARGGL		276	0286	21	0176	0629
	LOO		ZMXSB	277	0629	69	0142	0450
	STU	ZMX		278	0142	21	0336	0289
	LOO		PHIRB	279	0289	69	0542	0000
	RAU	HTAA	B	280	0542	60	4120	0725
	FMP	T		281	0725	39	0058	0300
	FAU	THETO		282	0308	32	0010	0287
	LOO		E00CR	283	0287	69	0090	0269
	FMP	ZMX		284	0090	39	0336	0386
	FMP	AMMM	R	285	0386	39	4100	0500
	STU	A1	B	286	0500	21	4140	0293
	SXR	0001		287	0293	53	0001	0349
CONT1	NZS	LOPP1	CONT1	288	0349	42	0623	0553
	LOO	NOLAM		289	0553	69	0456	0609
LOOP9	RAU	8001	LODP9	290	0609	69	8001	0415
	RAU	ALPHA		291	0415	60	0278	0333
	FMP	KAPPA		292	0333	39	0436	0486
	FMP	KAPPA		293	0486	39	0436	0536
	STU	ALKAP		294	0536	21	0190	0343
	FSR	LAWOA	B	295	0343	33	4220	0497
	STU	DIFF		296	0497	21	0352	0455
	RAU	LAWOA	B	297	0455	60	4220	0775
	FMP	T		298	0775	39	0058	0358
	LOO		E00EA	299	0358	69	0311	0050
	STU	ELAMT		300	0311	21	0566	0569
	RAU	ELAMT		301	0569	60	0566	0071
	FMP	Q00		302	0071	39	0324	0424
	FMP	AYEJ	B	303	0424	39	4200	0550
	FMP	ALPHA		304	0550	39	0278	0478
	FOV	KAY		305	0478	34	0581	0781
	FOV	DIFF		306	0781	34	0352	0402
	STU	A3P		307	0402	21	0556	0659
	RAU	KAPPA		308	0659	60	0436	0691
	FMP	X		309	0691	39	0707	0807
	LOO		CUSHX	310	0807	69	0660	0169
	STU	CSHXX		311	0660	21	0314	0417
	RAU	KAPPA		312	0417	60	0436	0741
	FMP	L		313	0741	39	0186	0586
	LOO		COSH X	314	0586	69	0339	0169
	STU	CSHKL		315	0339	21	0044	0547
	RAU	LAMDA	B	316	0547	60	4220	0825
NEG	RMI	NEG	POS	317	0825	46	0528	0679
	RSU	LAWOA	S	318	0528	61	4220	0875
	FOV	ALPHA		319	0875	34	0278	0578
	LOO		E00AU	320	0578	69	0831	0506
	STU	SQRLA		321	0831	21	0636	0389
	FMP	X		322	0389	39	0707	0857
	LOO		E00CH	323	0857	69	0710	0269
	STU	CSLX		324	0710	21	0364	0467
	RAU	SQRLA		325	0467	60	0636	0791
	FMP	L		326	0791	39	0186	0686
	LOO		E00CH	327	0686	69	0439	0269
	STU	COSLL		328	0439	21	0094	0597
	RAU	COSLX		329	0597	60	0364	0619
	FOV	COSLL		330	0619	34	0094	0194
	FMP	CSHKL		331	0194	39	0044	0294
	FSR	CSHKL		332	0294	33	0314	0841
	FMP	A3P		333	0841	39	0556	0606
	STU	A3	B	334	0606	21	4240	0393
	SXR	0001		335	0393	53	0001	0399
POS	HZR	LODP9	CONT3	336	0399	42	0415	0603
	FOV	ALPHA		337	0679	34	0278	0628
	LOO		E00AU	338	0628	69	0831	0506
	STU	SQRLA		339	0831	21	0636	0489
	FMP	X		340	0489	39	0707	0907
	LOO		COSH X	341	0907	69	0760	0169
	STU	CSHLX		342	0760	21	0414	0517
	RAU	SQRLA		343	0517	60	0636	0891
	FMP	L		344	0891	39	0186	0736
	LOO		COSH X	345	0736	69	0539	0169
	STU	CSHLL		346	0539	21	0344	0647
	RAU	CSHLX		347	0647	60	0414	0669
	FOV	CSHLL		348	0669	34	0344	0394
	FMP	CSHKL		349	0394	39	0044	0444
	FSR	CSHKL		350	0444	33	0314	0941
	FMP	A3P		351	0941	39	0556	0656
	STU	A3	B	352	0656	21	4240	0443
	SXR	0001		353	0443	53	0001	0449
CONT3	NZS	LODP9	CONT3	354	0449	42	0415	0603
	RAA	0001		355	0603	80	0001	0709
	RAU	ONE		356	0709	60	0662	0567
	RSL	8003		357	0567	66	0003	0925
	STL	N		358	0925	20	0729	0282

LODP3	RAU ZERO		359	0282	60	0264	0719
	STU HOLO	LUOP3	360	0719	21	0670	0723
	RAU N		361	0723	60	0729	0383
	FAO TWO		362	0383	32	0520	0697
	STU N		363	0697	21	0729	0332
	FMP PI		364	0332	39	0018	0168
	FOV TWO		365	0168	34	0520	0770
	FDV L		366	0770	34	0186	0784
	STU ARG1		367	0784	21	0290	0423
	FMP ARG1		368	0493	39	0290	0340
	FMP ALPHA		369	0340	39	0278	0478
	STU ARG2		370	0678	21	0382	0335
	RAU ZERO		371	0335	60	0264	0769
	STU A24		372	0769	21	0474	0577
LOP3	LDD MDLAW	LOP5	373	0577	69	0456	0759
	RAU 8001		374	0759	82	0001	0465
	RAU ARG2		375	0465	60	0382	0337
	FAD LAMOA		376	0337	32	0220	0747
	STU A2841		377	0747	21	0452	0505
	RAU ARG2		378	0505	60	0382	0387
	FAO ALKAP		379	0387	32	0190	0617
	STU A2842		380	0617	21	0272	0975
	RAU C8HKL		381	0975	60	0044	0499
	FMP ALPHA		382	0499	39	0278	0728
	FMP QOU		383	0728	39	0324	0524
	FMP AYEJ		384	0524	39	0200	0600
	FOV KAY		385	0600	34	0581	0931
	FOV A2841		386	0931	34	0452	0502
	FOV A2842		387	0502	34	0272	0322
	FAD A24		388	0322	32	0474	0451
	STU A24		389	0451	21	0474	0627
CONT9	8XB 0001	CONT9	390	0627	53	0001	0433
	NZB LOP5		391	0433	42	0465	0437
	RAU ZERO		392	0437	60	0264	0819
	STU SETT		393	0819	24	0372	1025
	LOO INOXM		394	1025	69	0076	0772
LOPP2	RAU 8001	LUPP2	395	0772	82	0001	0385
	RAU ARG2		396	0385	60	0382	0487
	FMP ARG2		397	0487	39	0382	0432
	STU ARG80		398	0432	21	0836	0589
	RAU STAA		399	0589	60	0120	1075
	FMP STAA		400	1075	39	0120	0820
	FAO ARG80		401	0820	32	0836	0563
	STU OENDM		402	0563	21	0268	0171
	RAU AMMM		403	0171	60	0100	0555
	FMP ARG2		404	0555	39	0382	0482
	FOV OENDM		405	0482	34	0268	0318
	FAO SETT		406	0318	32	0372	0519
	STU SETT		407	0519	21	0372	1125
	8XR 0001		408	1125	53	0001	0981
CONT4	NZB LOPP2	CONT4	409	0981	42	0385	0435
	FAO A24		410	0435	32	0474	0501
	STU A28UM		411	0501	21	0706	0809
	RAU ARG2		412	0809	60	0382	0537
	FMP T		413	0537	39	0058	0408
	F8B FIFTY		414	0408	33	0361	0587
ST0	RAU GD	RTO	415	0587	46	0390	0921
	LOO ZERO		416	0921	69	0264	0667
	STU TERM		417	0667	24	0870	0773
	RAU TERM		418	0773	60	0870	1175
	FAO HOLO		419	1175	32	0670	0797
	STU HOLO		420	0797	21	0670	0823
	NZU		421	0823	44	0677	0778
	RAU HOLO	CONT5	422	0677	60	0670	1225
	F8B TERM	MOREC	423	1225	33	0970	0847
	RAU ARG2		424	0847	61	0382	0637
GO	FMP T		425	0637	39	0058	0458
	LDD		426	0458	69	0411	0050
	STU EAG2T	E00EA	427	0411	21	0616	0859
	RAU ARG1		428	0859	60	0290	0645
	FMP X		429	0645	39	0707	0957
	LDD	E00CR	430	0957	69	0810	0269
	STU COS1X		431	0810	21	0464	0717
	RAU L		432	0717	60	0186	1041
	FMP L		433	1041	39	0186	1088
	FOV ALPHA		434	0886	34	0278	0828
	FOV N		435	0828	34	0729	0829
	FOV PI		436	0829	34	0018	0368
	STU A201V		437	0368	21	0422	1275
	RAU EAG2T		438	1275	60	0616	0271
	FMP COS1X		439	0271	39	0464	0514
	FOV A201V		440	0514	34	0422	0472
	STU A200T		441	0472	21	0276	0879
	FMP A28UM		442	0879	39	0706	0756
	STU TERM		443	0756	21	0870	0847
MOREC	UMA SUB	MOREC	444	0847	41	0650	0551
SUB	RAU 0001	AOO	445	0650	60	0001	0806
	RAU HOLO		446	0806	60	0670	1325
	F8R TERM		447	1325	33	0870	0897
	STU HOLO		448	0897	21	0670	0873
	RAU TERM		449	0873	60	0870	1375
	FOV HOLO		450	1375	34	0670	0920
	RAM 8003		451	0920	67	0003	0727
	RAU 8002		452	0727	60	0002	0485
	F8B CRIT		453	0485	33	0788	0515
	RAU CONT5	LOOP3	454	0515	46	0778	0723
	RAU 0001		455	0551	81	0001	1007
ABO	RAU HOLO		456	1007	60	0670	1425
	FAO TERM		457	1425	32	0870	0947
	STU HOLO		458	0947	21	0670	0923
	RAU TERM		459	0923	60	0870	1475
	FOV HOLO		460	1475	34	0670	0970
	RAM 8003		461	0970	67	0003	0777
	RAU 8002		462	0777	60	0002	0535
	F8R CRIT		463	0535	33	0788	0565
CONT5	RAU CONT5	LDOP3	464	0565	46	0778	0723
	LDD INOXM		465	0778	69	0076	0829
	RAU 8001		466	0829	82	0001	0585
	RAU ZERO		467	0585	60	0264	0919
	STU CELL	LOP	468	0919	21	0574	0827
	FAO CELL		469	0827	60	0410	0695
LOP	STU CELL		470	0695	32	0574	0601
	8XB 0001		471	0601	21	0574	0877
	NZB LOP		472	0877	53	0001	0483
	LDD MDLAW	GOODN1	473	0483	42	0827	0687
	RAU 8001		474	0687	69	0456	0859
	RAU ZERO		475	0859	82	0001	0615
	STU CELL3		476	0615	60	0264	0969
LOP2	RAU A3	LOP2	477	0969	21	0624	0927
	FAD CELL3		478	0927	60	0420	0745
			479	0745	32	0624	0651

	STU	CELL3		480	0651	21	0624	0777
	SXR	0001		481	0977	53	0001	0533
GOON2	NZR	LOP2	GOON4	482	0533	42	0727	0737
	RSU	HOLD		483	0737	61	0670	1525
	FAD	CELL		484	1525	32	0574	0701
	FAD	CELL3		485	0701	32	0624	0751
FINIS	STU	ANSWR	FINIS	486	0751	21	0856	0909
	LDD	ANSWR		487	0909	69	0856	0959
	STD	1977		488	0959	24	1977	0480
	LDD	CELL		489	0480	69	0574	1027
	STD	1978		490	1027	24	1978	1031
	LDD	HOLD		491	1031	69	0670	0773
	STD	1979		492	0973	24	1979	0532
	LDD	CELL3		493	0532	69	0624	1077
	STD	1980		494	1077	24	1980	0583
	LDD	X		495	0583	69	0707	0860
	STD	1981		496	0860	24	1981	0584
	LDD	T		497	0584	69	0058	0461
	STD	1982		498	0461	24	1982	0635
	PCH	1977	START	499	0635	71	1977	1909
ONE	10	0000	0051	500	0662	10	0000	0051
TWO	20	0000	0051	501	0520	20	0000	0051
PI	31	4159	2751	502	0018	31	4159	2751
FIFTV	50	0000	0052	503	0361	50	0000	0052
ZERO	00	0000	0000	504	0264	00	0000	0000
CRIT	10	0000	0047	505	0788	10	0000	0047
ARTAN	STD	EXIT	EXIT	5	1800	24	1800	1806
	NZE	EXIT		6	1806	45	1810	1803
	SMI	MINUS		7	1810	46	1813	1814
	STU	ARTAO		8	1814	21	1818	1821
	LDD	FPONE		9	1821	69	1824	1827
	STD	ENNNN	SURTH	10	1827	24	1830	1833
	STD	AYE		11	1833	24	1836	1839
MINUS	RSU	8003		12	1839	66	0003	1871
	STL	ARTAO		13	1871	20	1818	1822
	RSU	FPONE		14	1822	61	1824	1829
	STD	ENNNN		15	1829	24	1830	1833
	STU	AYE	SUSTH	16	1833	21	1836	1839
SUBTR	RAU	ARTAO		17	1839	60	1818	1823
	F88	FPONE		18	1823	33	1824	1801
	NZE	DIFFE		19	1801	45	1804	1805
	LDD	PIOV4		20	1805	69	1808	1811
	STD	FUNCT	MULTA	21	1811	24	1864	1817
DIFFE	SMI	SMALL		22	1804	46	1807	1858
	F88	FPONE		23	1858	33	1824	1851
	RMI	NEGAT	POSIT	24	1851	46	1854	1855
NEGAT	LDD	PIOV4		25	1854	69	1808	1861
	STD	FUNCT		26	1861	24	1864	1867
	RAU	ARTAO		27	1867	60	1818	1873
	FAD	FPONE		28	1873	32	1824	1802
	STU	TURRN		29	1802	21	1856	1809
	F88	FPTWO		30	1809	33	1812	1889
	FDV	TURRN	COMBI	31	1889	34	1856	1857
SMALL	FAD	ARTAO		32	1807	32	1818	1845
	SMI	ARTAO	NEGAT	33	1845	46	1848	1854
	F88	LO8ND		34	1848	60	1818	1854
	SMI	TINEY		35	1874	33	1877	1853
	RAU	ARTAO		36	1853	46	1859	1860
	STL	FUNCT	COMBI	37	1860	60	1818	1825
POSIT	STD	PIOV2		38	1825	20	1864	1857
	STD	FUNCT		39	1855	69	1862	1815
	F88	UP8ND		40	1815	24	1864	1868
	SMI	FPONE	MULTA	41	1868	33	1872	1849
	RSU	FPONE		42	1849	46	1852	1817
	FDV	ARTAO	COMBI	43	1852	61	1824	1879
COMBI	STU	TURRN		44	1879	34	1818	1857
	STD	TURRN		45	1857	21	1856	1843
	FMP	TURRN		46	1863	24	1816	1819
	STU	ARGUE	FIGUR	47	1819	39	1856	1865
FIGUR	RAU	TURRN		48	1865	21	1820	1875
	FAD	FUNCT		49	1875	60	1816	1826
	STU	FUNCT		50	1826	32	1864	1841
	RAU	ENNNN		51	1841	21	1864	1869
	FAD	FPTWO		52	1869	60	1830	1835
	STU	ENNNN		53	1835	32	1812	1840
	RSU	TURRN		54	1840	21	1830	1834
	FMP	ARGUE		55	1834	61	1856	1866
	STU	TURRN		56	1866	39	1820	1870
	FDV	ENNNN		57	1870	21	1856	1876
	STU	TURRN		58	1876	34	1830	1880
	RAM	FUNCT		59	1880	21	1816	1828
	STL	FMAGG		60	1828	67	1864	1878
	RAU	TURRN		61	1878	20	1884	1837
	RAU	8002		62	1837	67	1816	1831
	FOV	FMAGG		63	1831	60	8002	1890
	F88	SIZE8		64	1890	34	1884	1885
	SMI	MULTA	FIGUR	65	1885	33	1838	1881
TINEY	RAU	ARTAO	MULTA	66	1881	46	1817	1875
MULTA	RAU	AYE		67	1859	60	1818	1817
	FMP	FUNCT	EXIT	68	1817	60	1836	1891
FPONE	10	0000	0051	69	1891	39	1864	1803
FPTWO	20	0000	0051	70	1824	10	0000	0051
SIZE8	10	0000	0043	71	1812	20	0000	0051
PIOV2	15	7079	6351	72	1838	10	0000	0043
PIOV4	78	5398	1650	73	1862	15	7079	6351
UPRNU	10	0000	0060	74	1808	78	5398	1650
LOBNU	10	0000	0040	75	1872	10	0000	0060
					1877	10	0000	0040

## APPENDIX E

Description and Explanation of the IBM-650  
Computer Program Used to Calculate Surface  
Heat Flow.

The computer program was written to calculate the heat flow out of the fuel and into the moderator. The heat flow out of the fuel surface is given by

$$\begin{aligned}
 (q/A)_f(t) = & -k_f \left\{ \sum_{i=1}^p \sqrt{\frac{\beta_i}{2\alpha}} B_i (D_i \cos \beta_i t + E_i \sin \beta_i t) \right. \\
 & + \sum_{n=1,3,5,\dots}^{\infty} \frac{\left(\frac{n\pi}{2L}\right) e^{-\frac{n^2 \pi^2 \alpha}{4L^2} t}}{\frac{L^2}{n\pi\alpha}} \left( \sum_{i=1}^p \frac{B_i \left(\frac{n^2 \pi^2 \alpha}{4L^2}\right)}{\frac{n^4 \pi^4 \alpha^2}{16L^4} + \beta_i^2} \right. \\
 & \left. + \sum_{j=1}^s \frac{q_{\infty} \alpha A_j \cosh \kappa L}{k_m \left(\frac{n^2 \pi^2 \alpha}{4L^2} + \lambda_j\right) \left(\frac{n^2 \pi^2 \alpha}{4L^2} + \alpha \kappa^2\right)} \right) \\
 & \left. + \sum_{j=1}^s \frac{q_{\infty} - A_j e^{\lambda_j t}}{k_f (\alpha \kappa^2 - \lambda_j)} \left[ \frac{\sqrt{\frac{\lambda_j}{\alpha}} \cosh(\kappa L) \sinh\left(\sqrt{\frac{\lambda_j}{\alpha}} L\right)}{\cosh\left(\sqrt{\frac{\lambda_j}{\alpha}} L\right)} - \kappa \sinh \kappa L \right] \right\}
 \end{aligned} \quad (E-1)$$

and the heat flow into the moderator is given by

$$\begin{aligned}
 (q/A)_m(t) = & \rho k_m \left\{ \sum_{i=1}^p \sqrt{\frac{\beta_i}{2\alpha}} B_i (D_i \cos \beta_i t + E_i \sin \beta_i t) \right. \\
 & + \sum_{n=1,3,5,\dots}^{\infty} \frac{\left(\frac{n\pi}{2L}\right) e^{-\frac{n^2 \pi^2 \alpha}{4L^2} t}}{\frac{L^2}{n\pi\alpha}} \left( \sum_{i=1}^p \frac{B_i \left(\frac{n^2 \pi^2 \alpha}{4L^2}\right)}{\frac{n^4 \pi^4 \alpha^2}{16L^4} + \beta_i^2} + \sum_{j=1}^s \frac{q_{\infty} \alpha A_j \cosh \kappa L}{k_m \left(\frac{n^2 \pi^2 \alpha}{4L^2} + \lambda_j\right) \left(\frac{n^2 \pi^2 \alpha}{4L^2} + \alpha \kappa^2\right)} \right)
 \end{aligned}$$

$$- \sum_{j=1}^s \frac{\alpha F A_j}{k_m \lambda_j} \left( \frac{\sqrt{\frac{\lambda_j}{\alpha}} \sinh \sqrt{\frac{\lambda_j}{\alpha}} L}{\cosh \sqrt{\frac{\lambda_j}{\alpha}} L} \right),$$

$$\text{where } D_1 = \frac{\cosh \gamma_1 L \sinh \gamma_1 L - \cos \gamma_1 L \sin \gamma_1 L}{\cos^2 \gamma_1 L \cosh^2 \gamma_1 L + \sin^2 \gamma_1 L \sinh^2 \gamma_1 L}, \quad (E-2)$$

$$E_1 = \frac{\cosh \gamma_1 L \sinh \gamma_1 L + \cos \gamma_1 L \sin \gamma_1 L}{\cos^2 \gamma_1 L \cosh^2 \gamma_1 L + \sin^2 \gamma_1 L \sinh^2 \gamma_1 L}$$

$$\text{and } \gamma_1 = \sqrt{\frac{\beta_1}{2\alpha}}.$$

The equivalence between elements of the algebraic equation and the symbolic logic of the computer program is shown in Table E-1.

Table E-1. Definition of symbolic terms of the IBM-650 computer program for calculating surface heat flow.

$$\gamma_1 = \sqrt{\frac{\beta_1}{2\alpha}}$$

$$ZMX1_1 = \frac{\cosh \gamma_1 L \sinh \gamma_1 L - \cos \gamma_1 L \sin \gamma_1 L}{\cos^2 \gamma_1 L \cosh^2 \gamma_1 L + \sin^2 \gamma_1 L \sinh^2 \gamma_1 L} = D_1$$

$$A1_1 = \gamma_1 A_1 (ZMX1_1 \cos \beta_1 t - ZMX2_1 \sin \beta_1 t)$$

$$A3P_j = \frac{q_\infty \alpha A_j e^{\lambda_j t}}{k(\alpha \kappa^2 - \lambda_j)}$$

$$A3SUM_j = \frac{\sqrt{\frac{\lambda_j}{\alpha}} \cosh \kappa L \sinh \sqrt{\frac{\lambda_j}{\alpha}} L}{\cosh \sqrt{\frac{\lambda_j}{\alpha}} L} - \kappa \sinh \kappa L$$

$$ZMX2_1 = \frac{\cos \gamma_1 L \sin \gamma_1 L + \cosh \gamma_1 L \sinh \gamma_1 L}{\cos^2 \gamma_1 L \cosh^2 \gamma_1 L + \sin^2 \gamma_1 L \sinh^2 \gamma_1 L} = E_1$$

Table E-1 cont.

$$A3_j = (A3P_j) (A3SUM_j)$$

$$CSHLL_j = \cosh \sqrt{\frac{\lambda_j}{\alpha}} L$$

$$COSLL_j = \cos \sqrt{\frac{\lambda_j}{\alpha}} L$$

$$ARG1_n = n\pi/2L$$

$$ARG2_n = n^2 \pi^2 \alpha / 4L^2$$

$$A2ST1_i = B_i \left( \frac{n^2 \pi^2 \alpha}{4L^2} \right) / \left( \frac{n^4 \pi^4 \alpha^2}{16L^2} + \beta_i^2 \right)$$

$$A2ST1_j = q_\infty \alpha A_j \cosh \kappa L / k \left( \frac{n^2 \pi^2 \alpha}{4L^2} + \lambda_j \right) \left( \frac{n^2 \pi^2 \alpha}{4L^2} + \alpha \kappa^2 \right)$$

$$A2DDT_n = \frac{\frac{n\pi}{2L} e^{-\frac{n^2 \pi^2 \pi}{4L^2} t}}{L^2 / n\pi\alpha}$$

$$A2SUM_n = \sum_{i=1}^p A2ST1_i + \sum_{j=1}^s A2ST1_j$$

$$TERM_n = (A2DDT_n) (A2SUM_n)$$

The input data consists of the heat generation and surface temperature parameters, appropriate material constants, half-thickness of the region and numerical constants. Table E-2 lists input data required for the program.



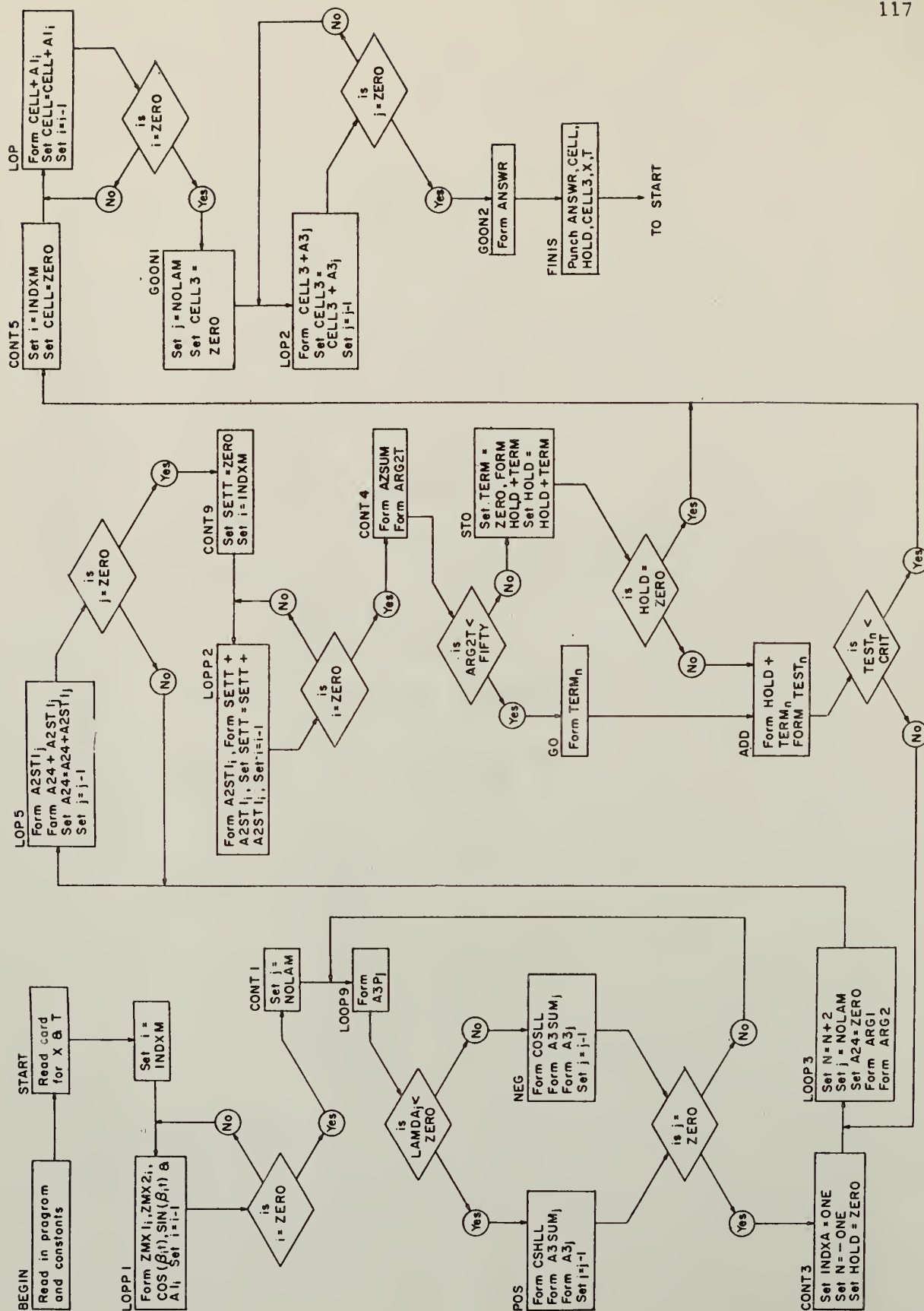
Table E-2. Input Data Required for Use of the IBM-650 Computer Program Used to Calculate Surface Heat Flow Rates.

Symbol	Explanation	Storage Location
ZERO	0.00	0164
ONE	1.00	0656
TWO	2.00	0820
P <sub>i</sub>	3.14159	0779
FIFTY	50.00	0461
CRIT	0.0001	0388
ALPHA	Thermal Diffusivity	0278
KAPPA	Reciprocal of Thermal Neutron Diffusion Length in Fuel	0436
Q00	Normalization Factor for Heat Generation	0324
KAY	Thermal Conductivity	0581
L	Half-thickness of Region	0186
INDXM	No. of Terms, Surface Temperature Fit (00000000xx)	0076
NOLAM	No. of Terms, Heat Generation Fit (00000000xx)	0456
AYEJ <sub>j</sub>	Amplitude Parameter, Heat Generation Fit	(0200 + j)
LAMDA <sub>j</sub>	Exponential Parameter, Heat Generation Fit	(0020 + j)
AMMM <sub>j</sub>	Amplitude Parameter, Surface Temperature Fit	(0100 + j)
BTAA <sub>j</sub>	Period Parameter, Surface Temperature Fit	(0120 + j)

The output from this program is punched out on one card having an eight word capacity, one word consisting of 10 digits and a sign. The form of the output is shown in Table E-3.

Table E-3. Output form for IBM-650 Computer Program Used to Calculate Surface Heat Flow Rates.

WORD 1	WORD 2	WORD 3	WORD 4	WORD 5	WORD 6	WORD 7	WORD 8
(q/A)	$\sum_{i=1}^P A1_i$	$\sum_{n=1,3,5}^{\infty} (\text{Term})_n$	$\sum_{j=1}^S A3_j$	--	t	--	--



LOGIC DIAGRAM-APPENDIX E

## OBJECT PROGRAM-APPENDIX E

	BLR	0200	0260	1	0000	00	0000	0000
	BLR	1800	1899	2	0000	00	0000	0000
	SYN	ARTAN	1800	3	0000	00	0000	0000
	SYN	START	1999	4	0000	00	0000	0000
	SYN	AYEJ	0200	5	0000	00	0000	0000
	SYN	LAMDA	0220	6	0000	00	0000	0000
	SYN	A3	0240	7	0000	00	0000	0000
	HLR	1951	1960	8	0000	00	0000	0000
	HLR	1977	19H4	9	0000	00	0000	0000
	SLR	0100	0160	10	0000	00	0000	0000
	SYN	AMMM	0100	11	0000	00	0000	0000
	SYN	STAA	0120	12	0000	00	0000	0000
	SYN	ALPHA	027H	13	0000	00	0000	0000
	SYN	KAPPA	0436	14	0000	00	0000	0000
	SYN	L	0186	15	0000	00	0000	0000
	SYN	QOO	0324	16	0000	00	0000	0000
	SYN	KAY	05H1	17	0000	00	0000	0000
	SYN	INOXM	0076	18	0000	00	0000	0000
	SYN	NOLAM	0456	19	0000	00	0000	0000
	SYN	A1	0140	20	0000	00	0000	0000
E00EA	STO	AAA1		21	0000	24	0003	0006
	STU	AAA14		22	0006	21	0010	0013
	RAU	AAA16		23	0013	60	0016	0021
	FAM	AAA14		24	0021	37	0010	0037
	STU	AAA2		25	0037	21	0042	0045
	LDD	AAA3		26	0045	69	0048	0051
AAA8	STD	AAA4	AAA8	27	0001	24	0004	0007
	RAU	AAA2		28	0007	60	0042	0047
	F88	AAA5		29	0047	33	0050	0077
	SMI	AAA6		30	0027	46	0030	0031
	STU	AAA2		31	0031	21	0042	0095
	RAU	AAA4		32	0095	60	0004	0009
	FMP	AAA7		33	0009	39	0012	0062
AAA6	STU	AAA4	AAA8	34	0062	21	0004	0007
	RAU	AAA2		35	0030	60	0042	0077
	F88	AAA3		36	0097	33	0048	0075
	SMI	AAA28		37	0025	46	0028	0029
	STU	AAA2		38	0029	21	0042	0195
	RAU	AAA4		39	0195	60	0004	0059
	FMP	AAA9		40	0059	39	0162	0262
AAA28	STU	AAA4	AAA6	41	0262	21	0004	0030
	RAU	AAA2		42	0028	60	0042	0197
	F88	AAA10		43	0197	33	0300	0077
	SMI	AAA11		44	0077	46	0080	0081
	STU	AAA2		45	0081	21	0042	0295
	RAU	AAA4		46	0295	60	0004	0309
	FMP	AAA12		47	0309	39	0312	0362
AAA11	STU	AAA4	AAA28	48	0362	21	0004	0028
	RAU	AAA2		49	0080	60	0042	0297
	LDD		AAA17	50	0297	69	0350	0053
	FMP	AAA4		51	0350	39	0004	0054
	STU	AAA13		52	0054	21	0008	0011
	RAU	AAA14		53	0011	60	0010	0015
	SMI	AAA15		54	0015	46	0018	0019
AAA15	RAU	AAA13	AAA1	55	0019	60	0008	0003
	RAU	AAA3		56	0018	60	0048	0303
AAA17	STO	AAA13	AAA1	57	0303	34	0008	0003
	STU	AAA18		58	0053	24	0056	0359
	RAU	AAA3		59	0359	60	0048	0353
	FAO	AAA4		60	0353	32	0042	0069
	STU	AAA19		61	0069	21	0024	0177
	LDD	AAA27		62	0177	69	0180	0033
	STO	AAA20		63	0033	34	0036	0039
	STO	AAA21		64	0039	24	0092	0345
	RAU	AAA2		65	0345	60	0042	0347
	FMP	AAA2		66	0347	39	0042	0192
AAA22	STU	AAA23	AAA28	67	0192	21	0046	0049
	FDV	AAA21		68	0049	34	0092	0292
	STU	AAA24		69	0292	21	0096	0099
	FAO	AAA19		70	0099	32	0024	0051
	STU	AAA19		71	0051	21	0024	0277
	RAU	AAA24		72	0277	60	0096	0301
	FDV	AAA19		73	0301	34	0024	0074
	F88	AAA25		74	0074	33	0327	0403
	SMI		AAA26	75	0403	46	0306	0057
AAA26	RAU	AAA19	AAA18	76	0306	60	0024	0056
	RAU	AAA20		77	0057	60	0036	0041
	FAD	AAA3		78	0041	32	0048	0075
	STU	AAA20		79	0075	21	0036	0089
	FMP	AAA21		80	0089	39	0092	0342
	STU	AAA21		81	0342	21	0092	0395
	RAU	AAA23		82	0395	60	0046	0351
	FMP	AAA2		83	0351	39	0042	0392
	STU	AAA23	AAA28	84	0392	21	0046	0049
AAA3	10	0000	0051	85	0048	10	0000	0051
AAA5	50	0000	0051	86	0050	50	0000	0051
AAA7	14	R410	0053	87	0012	14	R410	0053
AAA9	27	1R30	0051	88	0162	27	1R30	0051
AAA10	20	0000	0050	89	0300	20	0000	0050
AAA12	12	2140	0051	90	0112	12	2140	0051
AAA16	00	0000	0000	91	0016	00	0000	0000
AAA25	70	0000	0047	92	0327	70	0000	0047
AAA27	20	0000	0051	93	0180	20	0000	0051
ZMXSH	STO	ABCO1		94	0400	24	0453	0356
	RAU	ARGGL		95	0356	60	0409	0063
	LDD		COSH X	96	0063	69	0066	0169
	STU	CHAAL		97	0066	21	0020	0023
	RAU	ARGGL		98	0023	60	0409	0163
	LDD		E00CH	99	0163	69	0166	0269
	STU	CSAAL		100	0166	21	0070	0073
	RAU	ARGGL		101	0073	60	0409	0263
	LOO		SINH X	102	0263	69	0266	0319
	STU	SHAAL		103	0266	21	0170	0173
	RAU	ARGGL		104	0173	60	0409	0313
	LDD		E008R	105	0313	69	0316	0369
	STU	SNAAL		106	0316	21	0270	0273
	RAU	CHAAL		107	0273	60	0020	0175
	FMP	CSAAL		108	0175	39	0070	0320
	STU	FCL		109	0320	21	0174	0377
	FMP	CHAAL		110	0377	39	0020	0370
	FMP	CSAAL		111	0370	39	0070	0420
	STU	DEJIN		112	0420	21	0274	0427
	RAU	SNAAL		113	0427	60	0270	0275
	FMP	SNAAL		114	0275	39	0170	0470
	STU	FSL		115	0470	21	0374	0477

	RAU	C8AAL	116	0477	60	0070	0325
	FMP	SHAAL	117	0325	39	0170	0520
	STU	C8SHL	118	0520	21	0424	0527
	RAU	C8AAL	119	0527	60	0070	0375
	FMP	SHAAL	120	0375	39	0270	0570
	STU	C8SHL	121	0570	21	0474	0577
	RAU	C8AAL	122	0577	60	0020	0425
	FMP	SHAAL	123	0425	39	0170	0620
	STU	C8SHL	124	0620	21	0524	0627
	RAU	F8L	125	0627	60	0374	0079
	FMP	8003	126	0079	39	8003	0083
	STU	D2	127	0083	21	0038	0091
	RAU	FCL	128	0091	60	0174	0179
	FMP	8003	129	0179	39	8003	0103
	FAD	D2	130	0183	32	0038	0065
	STU	DENN2	131	0065	21	0670	0323
	RAU	CH8HL	132	0323	60	0524	0279
	F88	C8SHL	133	0279	33	0474	0401
	FDV	DENN2	134	0401	34	0670	0720
	STU	ZMX1	135	0720	21	0574	0677
	RAU	C8SHL	136	0677	60	0474	0329
	FAD	CH8HL	137	0329	32	0524	0451
	FDV	DENN2	138	0451	34	0670	0770
	STU	ZMX2	139	0770	21	0624	0453
CO8HX	STO	NEXTC	140	0169	24	0022	0475
	STU	ARG	141	0475	21	0240	0283
	LDD		142	0283	69	0086	0000
	STU	EARGP	143	0086	21	0040	0043
	RSU	ARG	144	0043	61	0280	0035
	LDD		145	0035	69	0086	0000
	FAD	EARGP	146	0086	32	0040	0017
	FDV	TWO	147	0017	34	0820	0022
BINHX	STO	NEXT8	148	0319	24	0072	0525
	STU	ARG	149	0525	21	0280	0333
	RSU	ARG	150	0333	61	0280	0085
	LDD		151	0085	69	0188	0000
	STU	EARGM	152	0188	21	0442	0445
	RAU	ARG	153	0445	60	0280	0185
	LDD		154	0185	69	0288	0000
	F88	EARGM	155	0288	33	0442	0419
	FDV	TWO	156	0419	34	0820	0072
E00CR	STO	EXIT	157	0269	24	0172	0575
	SMI	NEGAT	158	0575	46	0078	0379
NEGAT	FAD	TWOPI	159	0078	32	0181	0307
	BMI	NEGAT	160	0307	46	0078	0061
	F88	ONEPI	161	0061	33	0014	0191
REDUC	F88	TWOPI	162	0379	33	0181	0357
	BMI		163	0357	46	0060	0379
	FAD	ONEPI	164	0060	32	0014	0191
	STU	THETA	165	0191	21	0196	0199
	RSU	FPONE	166	0199	61	0002	0407
	STU	TERMM	167	0407	21	0412	0165
	STU	FUNKT	168	0165	21	0870	0373
	STL	ENN	169	0373	20	0727	0330
	STO	EXIT	170	0369	24	0172	0625
E00SR	SMI	NEGAV	171	0625	46	0178	0424
NEGAV	FAD	TWOPI	172	0178	32	0181	0457
	BMI	NEGAV	173	0457	46	0178	0161
	F88	ONEPI	174	0161	33	0014	0291
	F88	TWOPI	175	0429	33	0181	0507
	SMI		176	0507	46	0310	0429
	FAD	ONEPI	177	0310	32	0014	0291
	STU	THETA	178	0291	21	0196	0209
	RSU	8003	179	0299	61	8003	0557
	STU	TERMM	180	0557	21	0412	0265
	STU	FUNKT	181	0265	21	0870	0423
	LDD	FPONE	182	0423	69	0002	0005
	STO	ENN	183	0005	24	0727	0330
NEG8T	RAU	ENN	184	0330	60	0727	0201
	FAD	FPONE	185	0201	32	0002	0479
	STU	NPONE	186	0479	21	0034	0087
	FAD	FPONE	187	0087	32	0002	0529
	STU	ENN	188	0529	21	0727	0380
	RSU	TERMM	189	0380	61	0412	0067
	FMP	THETA	190	0067	39	0196	0296
	FMP	THETA	191	0296	39	0196	0346
	FDV	NPONE	192	0346	34	0034	0084
	FDV	ENN	193	0084	34	0727	0777
	STU	TERMM	194	0777	21	0412	0315
	RAM	FUNKT	195	0315	67	0870	0675
	STL	FMAG	196	0675	20	0579	0032
	RAM	TERMM	197	0032	67	0412	0167
	RAU	8002	198	0167	60	8002	0725
	FDV	FMAG	199	0725	34	0579	0629
	F88	SIZE2	200	0629	33	0082	0459
	RM1	ENUFF	201	0459	46	0462	0363
	RAU	FUNKT	202	0363	60	0870	0775
	FAD	TERMM	203	0775	32	0412	0189
	STU	FUNKT	204	0189	21	0870	0330
	RAU	FUNKT	205	0462	60	0870	0172
ENUFF			206	0082	10	0000	0043
SIZE8	10	0000	207	0181	62	8318	5351
TWOPI	62	8318	208	0014	31	4159	2751
ONEPI	31	4159	209	0002	10	0000	0051
FPONE	10	0000	210	0450	24	0503	0404
E00AU	STO	SEXT	211	0406	46	0509	0360
	BMI	BERK	212	0360	45	0064	0503
	NZE		213	0064	21	0068	0071
	STU	SA	214	0071	32	0674	0501
	FAD	S10	215	0501	39	0304	0384
SR	FMP	SHAF	216	0384	21	0058	0261
SR	STU	SSAV	217	0261	60	0068	0473
	RAU	SA	218	0473	34	0058	0308
	FDV	SSAV	219	0308	32	0058	0285
	FAD	SSAV	220	0285	39	0304	0404
	FMP	SHAF	221	0404	33	0058	0335
	F88	SSAV	222	0335	44	0289	0090
	NZU		223	0289	46	0492	0090
	SMI		224	0492	32	0058	0385
	FAD	SSAV	225	0385	21	0058	0261
	STU	SSAV	226	0090	60	0058	0503
	RAU	SSAV	227	0509	01	0000	0503
SR	HLT	0000	228	0304	50	0000	0050
SERR	50	0000	229	0674	10	0000	0051
SHAF	10	0000	230	1999	70	1951	0551
S10							
STAKT	RCU	1951					

	LDD	1952		231	0551	69	1952	0055
	STU	T		232	0055	24	0350	0311
	LDD	ZERO		233	0311	69	0164	0267
	STU	HOLD		234	0267	24	0920	0523
	LDD	INDXW		235	0523	69	0076	0679
	RAU	H001		236	0679	62	0001	0435
	LDD	ZERO		237	0435	69	0164	0317
	STU	HOLD		238	0317	24	0920	0573
LOPP1	RAU	HTAA	R	239	0573	60	4120	0325
	FOV	ALPHA		240	0825	34	0278	0328
	FOV	TWO		241	0328	34	0820	0970
	LDD			242	0970	69	0623	0450
	STU	SQRRY		243	0623	21	0378	0331
	FMP	L		244	0331	39	0186	0286
	STU	ARGGL		245	0286	21	0409	0512
	LDD			246	0512	69	0365	0400
	RAU	HTAA	B	247	0365	60	4120	0875
	FMP	T		248	0875	39	0358	0408
	STU	PHEEE		249	0408	21	0562	0415
	LDD			250	0415	69	0160	0269
	FMP	ZMX1		251	0160	39	0574	0724
	STU	A11		252	0724	21	0428	0381
	RAU	PHEEE		253	0381	60	0562	0367
	LDD			254	0367	69	1020	0369
	FMP	ZMX2		255	1020	39	0624	0774
	STU	A12		256	0774	21	0478	0431
	RAU	A11		257	0431	60	0428	0383
	F8R	A12		258	0383	33	0478	0305
	FMP	AMMM	R	259	0305	39	4100	0500
	FMP	SQRRY		260	0500	39	0378	0528
	STU	A1	B	261	0528	21	4140	0093
	8X8	0001		262	0093	53	0001	0349
CONT1	NZ8	LOPP1	CONT1	263	0349	42	0573	0553
	LDD	NOLAM		264	0553	69	0456	0559
LDOP9	RA8	H001	LOOP9	265	0559	82	8001	0465
	RAU	ALPHA		266	0465	60	0278	0433
	FMP	KAPPA		267	0433	39	0436	0336
	FMP	KAPPA		268	0336	39	0436	0386
	STU	ALKAP		269	0386	21	0190	0193
	F8R	LAMDA	B	270	0193	33	4220	0397
	STU	DIFF		271	0397	21	0052	0355
	RAU	LAMDA	B	272	0355	60	4220	0925
	FMP	T		273	0925	39	0358	0458
	LDD			274	0458	69	0361	0000
	STU	ELAMT		275	0361	21	0366	0469
	RAU	ELAMT		276	0469	60	0366	0171
	FMP	QOO		277	0171	39	0324	0824
	FMP	AYEJ	B	278	0824	39	4200	0550
	FMP	ALPHA		279	0550	39	0278	0578
	FOV	KAY		280	0578	34	0581	0481
	FOV	DIFF		281	0481	34	0052	0302
	STU	A3P		282	0302	21	0506	0609
	RAU	KAPPA		283	0609	60	0436	0341
	FMP	L		284	0341	39	0186	0486
	LDD			285	0486	69	0339	0319
	STU	SNHKL		286	0339	21	0044	0447
	FMP	KAPPA		287	0447	39	0436	0536
	STU	KSHKL		288	0536	21	0290	0293
	RAU	KAPPA		289	0293	60	0436	0391
	FMP	L		290	0391	39	0186	0586
	LDD			291	0586	69	0389	0169
	STU	CSHKL		292	0389	21	0094	0497
	RAU	LAMDA	B	293	0497	60	4220	0975
NEG	RM1	NEG	POS	294	0975	46	0628	0729
	RSU	LAMDA	B	295	0628	61	4220	1025
	FOV	ALPHA		296	1025	34	0278	0678
	LDD			297	0678	69	0531	0450
	STU	SQRLA		298	0531	21	0636	0439
	FMP	L		299	0439	39	0186	0686
	LDD			300	0686	69	0489	0369
	STU	SINLL		301	0489	21	0194	0547
	RAU	SQRLA		302	0547	60	0636	0441
	FMP	L		303	0441	39	0186	0736
	LDD			304	0736	69	0539	0269
	STU	COSLL		305	0539	21	0294	0597
	RSU	SINLL		306	0597	61	0194	0399
	FMP	SQRLA		307	0399	39	0636	0786
	FOV	COSLL		308	0786	34	0294	0344
	FMP	CSHKL		309	0344	39	0094	0394
	F8R	KSHKL		310	0394	33	0290	0417
	FMP	A3P		311	0417	39	0506	0556
	STU	A3	B	312	0556	21	4240	0343
	8X8	0001		313	0343	53	0001	0449
POS	NZ8	LOOP9	CONT3	314	0449	42	0465	0603
	FOV	ALPHA		315	0603	34	0278	0728
	LDD			316	0728	69	0631	0450
	STU	SQRLA		317	0631	21	0636	0589
	FMP	L		318	0589	39	0186	0836
	LDD			319	0836	69	0639	0319
	STU	SNHLL		320	0639	21	0444	0647
	RAU	SQRLA		321	0647	60	0636	0491
	FMP	L		322	0491	39	0186	0886
	LDD			323	0886	69	0689	0169
	STU	CSHLL		324	0689	21	0494	0699
	FOV	CSHLL		325	0699	60	0444	0499
	FMP	CSHKL		326	0499	34	0494	0544
	FMP	SQRLA		327	0544	39	0094	0594
	F8R	KSHKL		328	0594	39	0636	0936
	FMP	A3P		329	0936	33	0290	0467
	STU	A3	B	330	0467	39	0506	0606
	8X8	0001		331	0606	21	4240	0353
CONT3	NZ8	LOOP9	CONT3	332	0353	53	0001	0549
	RAU	ONE		333	0549	42	0465	0603
	STL	8003		334	0603	60	0656	0411
	RAU	ZERO		335	0411	66	8003	0519
	STU	HOLD		336	0519	20	0673	0026
LOOP3	RAU	N	LOOP3	337	0026	60	0164	0569
	FAD	TWO		338	0569	21	0920	0723
	STU	N		339	0723	60	0673	0827
	FMP	PI		340	0827	32	0820	0747
	FOV	TWO		341	0747	21	0673	0176
	FOV	L		342	0176	39	0779	0829
	STU	ARG1		343	0829	34	0820	1070
				344	1070	34	0186	0986
				345	0986	21	0340	0443



	FMP	ANG1		346	0443	39	0340	0390
	FMP	ALPHA		347	0390	39	0270	0770
	STU	ARG2		348	0778	21	0182	0485
	RAU	ZERO		349	0485	60	0164	0619
	STU	A24		350	0619	21	0174	0877
	LOD	NOLAM		351	0877	69	0456	0655
	RAR	H001		352	0659	82	0001	0515
LOP5	RAU	ARG2		353	0515	60	0182	0337
	FAD	LAMDA	H	354	0187	32	4220	0777
	STU	A2841		355	0777	21	0352	0405
	RAU	ARG2		356	0405	60	0182	0287
	FAD	ALKAP		357	0287	32	0190	0517
	STU	A2842		358	0517	21	0272	1075
	RAU	C8HKL		359	1075	60	0094	0599
	FMP	ALPHA		360	0599	39	0278	0828
	FMP	Q00		361	0828	39	0324	0924
	FMP	AYEJ	H	362	0924	39	4200	0600
	FOV	KAY		363	0600	34	0581	0681
	FOV	A2841		364	0681	34	0352	0402
	FOV	A2842		365	0402	34	0272	0322
	FAD	A24		366	0322	32	0874	0601
	STU	A24		367	0601	21	0674	0927
	8X8	0001		368	0927	53	0001	0483
CONT9	NZR	LOP5		369	0483	42	0515	0337
	RAU	ZERO		370	0337	60	0164	0619
	STO	SETT		371	0669	24	0372	1125
	LOD	INDXM		372	1125	69	0076	0879
LOPP2	RAR	H001	LOPP2	373	0879	82	0001	0535
	RAU	ARG2		374	0535	60	0182	0387
	FMP	ARG2		375	0387	39	0182	0287
	STU	ARG80		376	0287	21	1036	0739
	RAU	8TAA	8	377	0739	60	4120	1175
	FMP	8TAA	8	378	1175	39	4120	1120
	FAD	ARG90		379	1120	32	1036	0413
	STU	DENOM		380	0413	21	0268	0271
	RAU	AMMM	8	381	0271	60	4100	0455
	FMP	ARG2		382	0455	39	0182	0332
	FOV	DENOM		383	0332	34	0268	0318
	FAD	SETT		384	0318	32	0372	0649
	STU	SETT		385	0649	21	0372	1225
	8X8	0001		386	1225	53	0001	0731
CONT4	NZR	LOPP2	CONT4	387	0731	42	0535	0585
	FAD	A24		388	0585	32	0674	0651
	STU	A28UM		389	0651	21	0706	0709
	RAU	ARG2		390	0709	60	0182	0437
	FMP	T		391	0437	39	0358	0508
	FBR	FIFTY		392	0508	33	0461	0487
STO	SMI	GO	STO	393	0487	46	0440	0541
	LOD	ZERO		394	0541	69	0164	0567
	STO	TERM		395	0567	24	1170	0773
	RAU	TERM		396	0773	60	1170	1275
	FAD	HOLD		397	1275	32	0920	0847
	STU	HOLD		398	0847	21	0920	0823
	NZU			399	0823	44	0977	0878
	RAU	HOLD	CONT5	400	0977	60	0920	1325
	FBR	TERM	ADD	401	1325	33	1170	0897
GO	RBU	ARG2		402	0440	61	0182	0537
	FMP	T		403	0537	39	0358	0558
	LOD		EOOE A	404	0558	69	0511	0000
	STU	EAG2T		405	0511	21	0416	0719
	RAU	L		406	0719	60	0186	0591
	FMP	L		407	0591	39	0186	1086
	FOV	ALPHA		408	1086	34	0278	0928
	FOV	N		409	0928	34	0673	0873
	FOV	PI		410	0873	34	0779	0929
	STU	A20IV		411	0929	21	0184	0587
	RAU	EAG2T		412	0587	60	0416	0321
	FMP	ARG1		413	0321	39	0340	0490
	FOV	A20IV		414	0490	34	0184	0284
	STU	A200T		415	0284	21	0338	0641
	FMP	A28UM		416	0641	39	0706	0756
	STU	TERM	ADD	417	0756	21	1170	0807
ADD	RAU	HOLD		418	0807	60	0920	1375
	FAD	TERM		419	1375	32	1170	0947
	STU	HOLD		420	0947	21	0920	0923
	RAU	TERM		421	0923	60	1170	1425
	FOV	HOLD		422	1425	34	0920	1220
	RAM	H003		423	1220	67	8003	1027
	RAU	H002		424	1027	60	8002	0635
	FBR	CRIT		425	0635	33	0388	0565
CONT5	HMI	CONT5	LOUP3	426	0565	46	0878	0723
	LOD	INDXM		427	0878	69	0076	0979
	RAR	H001		428	0979	82	0001	0685
	RAU	ZERO		429	0685	60	0164	0769
	STU	CELL	LOP	430	0769	21	0974	1077
LOP	RAU	A1	R	431	1077	60	4140	0445
	FAD	CELL		432	0445	32	0374	0701
	STU	CELL		433	0701	21	0974	1127
	8X8	0001		434	1127	53	0001	0533
	NZR	LOP	GOON1	435	0533	42	1077	0637
GOON1	LOD	NOLAM		436	0637	69	0456	0759
	RAR	H001		437	0759	82	0001	0615
	RAU	ZERO		438	0615	60	0164	0819
	STU	CELL3	LOP2	439	0819	21	1024	1177
LOP2	RAU	A3	H	440	1177	60	4240	0545
	FAD	CELL3		441	0545	32	1024	0751
	STU	CELL3		442	0751	21	1024	1227
	8X8	0001		443	1227	53	0001	0583
	NZR	LOP2	GOON4	444	0583	42	1177	0617
GOON2	RAU	HOLD		445	0617	60	0920	1475
	FAD	CELL		446	1475	32	0974	0801
	FAD	CELL3		447	0801	32	1024	0811
	FMP	KAY		448	0811	39	0581	0781
	RBL	H003		449	0781	66	8003	0789
	STL	ANSWR	FINIS	450	0789	20	0493	0394
	LOD	ANSWR		451	0394	69	0493	0446
FINIS	STO	1977		452	0446	24	1977	0430
	LOD	CELL		453	0430	69	0974	1277
	STO	1978		454	1277	24	1978	0931
	LOD	HOLD		455	0931	69	0920	0973
	STO	1979		456	0973	24	1979	0382
	LOD	CELL3		457	0382	69	1024	1327
	STO	1980		458	1327	24	1980	0633
	LOD	X		459	0633	69	1136	0839
	STO	1981		460	0839	24	1981	0334





AN INVESTIGATION OF NUCLEAR EXCURSIONS TO  
DETERMINE THE SELF-SHUTDOWN EFFECTS IN  
THERMAL, HETEROGENEOUS, HIGHLY ENRICHED  
LIQUID-MODERATED REACTORS

by

JOHN ROBERT FAGAN

B.S., University of Nebraska, 1957

---

AN ABSTRACT OF  
A MASTER'S THESIS

submitted in partial fulfillment of the  
requirements for the degree

MASTER OF SCIENCE

Department of Nuclear Engineering

KANSAS STATE UNIVERSITY

Manhattan, Kansas

1962

The safe operation of nuclear reactors is imperative if there is to be increased engineering application of these systems. Transient reactor experiments, such as the SPERT tests, have demonstrated that thermal, heterogeneous, liquid-moderated reactor systems will safely shut themselves down following step and ramp insertions of limited amounts of excess reactivity. It is important that a model based on the nuclear, thermodynamic and hydrodynamic properties of the reactor system be developed to explain this phenomena so that it can be used in the design of new systems.

Equations for the fine structure of the temperature distribution in a unit cell of a heterogeneous reactor during a transient burst were derived based on the known power and fuel surface temperature distributions. A model based on recognized shutdown effects was developed to calculate the excess reactivity during a transient using the temperature distributions to define the deposition of energy. The calculated excess reactivities show this model to be satisfactory. The effect on reactivity due to steam formation required one empirical parameter which can probably be removed when a greater knowledge of transient boiling is available.

[illegible]